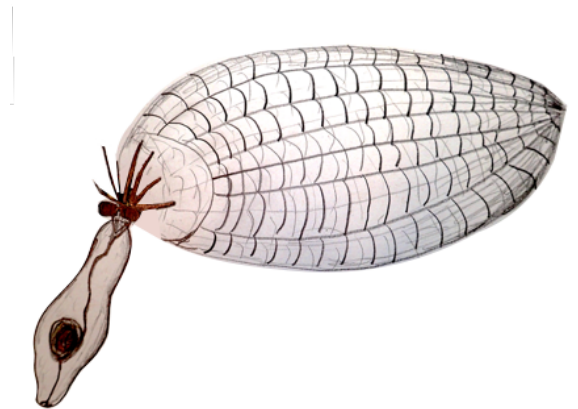# Distribution, eddy association and biogeochemical importance of the pelagic polychaete *Poeobius* sp. in the tropical Atlantic

## Master Thesis in Biological Oceanography

submitted by

**Svenja Christiansen**

(6100)



Kiel

31st October 2016

Examined by:

Prof. Dr. Thorsten Reusch

Supervised by:

Dr. Henk-Jan T. Hoving & Dr. Rainer Kiko

GEOMAR
Helmholtz Centre for Ocean Research Kiel [1]

C|A|U
Christian-Albrechts-Universität zu Kiel [2]

# Declaration of authorship

Hiermit erkläre ich, dass ich die vorliegende Arbeit selbstständig geschrieben habe und keine anderen als die ausgewiesenen Quellen zur Hilfe genommen habe. Diese Masterarbeit wurde in keinem anderen Prüfungsverfahren eingereicht. Die gedruckte Version entspricht der auf einem elektronischen Datenträger gespeicherten. Mit einer Veröffentlichung in der Bibliothek des GEOMAR und in der Zentralbibliothek der Christian-Albrechts-Universität bin ich einverstanden.

Hereby I certify that this Master thesis is my own work and no other than the declared references were used. This thesis has not been in any other examination procedure. The printed version is consistent to the version provided on a digital data carrier.

Kiel, 31.10.2016

# Zusammenfassung

Die Verbreitung und Rolle von gelatinösem Zooplankton im ausgedehnten Lebensraum des pelagischen Ozeans ist weitgehend unbekannt und es werden immer noch neue Arten und neue ökologische Zusammenhänge entdeckt. Gelatinöses Zooplankton wird auf Grund seiner empfindlichen Struktur während des Fanges mit Netzen oft beschädigt, daher wurde diese sehr vielfältige Gruppe lange unterschätzt. Erst die Entwicklung von Unterwasserkameras machte die quantitative Erfassung dieser Organismen möglich. Im Jahr 2015 wurden während eines Einsatzes einer geschleppten Videokamera (PELAGIOS) im tropischen Atlantik hohe Abundanzen eines holopelagischen Polychaeten der Gattung *Poeobius* in einem mesoskaligen Eddy entdeckt. Außerdem wurden in diesem Wirbel sehr geringe Partikelkonzentrationen festgestellt. Bisher ist nur eine Art dieser Gattung, *Poeobius meseres*, im pazifischen Ozean bekannt. Dort wurde eine Abhängigkeit zwischen hoher Polychaetendichte und abnehmenden Partikelkonzentrationen beschrieben. Mehrere Veröffentlichungen betonen die Wichtigkeit des Meso- und Makrozooplanktons in der Remineralisation von Partikeln in den oberen 100 m der Wassersäule, aber es ist wenig darüber bekannt, welchen Einfluss gelatinöse Partikelfresser auf den Partikelfluss in mesoskaligen Eddies haben. Nach der ersten Beobachtung von *Poeobius* sp. im tropischen Atlantik in dem PELAGIOS Video wurde der Polychaet auch auf Bildern des Underwater Vision Profilers (UVP5) identifiziert. Der UVP5 ist eine hoch auflösende Kamera, welche sowohl Partikel als auch Meso- und Makrozooplankton quantitativ aufnimmt.

In dieser Arbeit nutze ich UVP5- und Umweltdaten von 13 Forschungsfahrten im tropischen Atlantik mit über 1.8 Millionen Bildern, um die horizontale und vertikale Verbreitung von *Poeobius* sp. zu charakterisieren. Ich teste die Hypothese, dass *Poeobius* sp. Eddy-assoziiert ist und untersuche die möglichen Auswirkungen hoher Abundanzen auf die Biogeochemie von Eddies. Insgesamt wurden 481 Individuen zwischen 5°S und 20°N und 16°W bis 46°W beobachtet, mit einer Mindesttiefe von 22 m und einer maximalen Tiefe von fast 1000 m. Ein Vergleich von verschiedenen Eddytypen sowie Stationen außerhalb von Eddies zeigte eine erhöhte Abundanz und eine eingeschränkte Tiefenverteilung von *Poeobius* sp. in antizyklonischen mode-water Eddies ('anticyclonic mode-water eddies', ACMEs). Die Ergebnisse dieser Arbeit suggerieren, dass Eddies, insbesondere ACMEs, einen Mechanismus für die Vermehrung und die Verbreitung von sonst seltenem Zooplankton darstellen können. Diese können wiederum die Umweltbedingungen im Eddy beeinflussen: Zum Beispiel konnten hohe *Poeobius* sp. Abundanzen mit sehr geringen

Partikelkonzentrationen und Partikelflüssen in den unmittelbar darunter befindlichen Schichten in Verbindung gebracht werden. Der Partikelfresser *Poeobius* sp. könnte durch ausgedehnte Schleimnetze einen wesentlichen Teil des vertikalen Partikelflusses aufnehmen. Insbesondere in mesoskaligen Eddies könnten diese Prozesse eine wichtige Rolle in der Entwicklung von Partikelflüssen spielen. Diese Ergebnisse sollten bei der Diskussion und Modellierung der Ökologie und Biogeochemie von Eddies berücksichtigt werden. Sie betonen die Wichtigkeit optischer Methoden für die Erfassung von ökologischen Zusammenhängen im pelagischen Ozean.

# Abstract

The distribution and ecological function of gelatinous zooplankton in the vast habitat of the pelagic oceans is mostly unknown and new species and their roles in the ecosystem are still being discovered. Nets undersample and destroy this highly diverse group of organisms, thus, the use of underwater optical systems is the most appropriate way to observe them. In 2015, the deployment of the towed pelagic *in situ* video camera system (PELAGIOS) revealed high abundances of a holopelagic polychaete of the genus *Poeobius* in a mesoscale eddy in the tropical Atlantic, where it co-occurred with very low particle concentrations. Its sister species, the flux-feeder *Poeobius meseres*, is only known from the Pacific Ocean. A negative correlation of the polychaete with particle concentrations was described there. Several publications emphasize the role of mesozooplankton in remineralisation, but little is known about the impact of gelatinous particle-feeders on the flux in mesoscale eddies. After the discovery of *Poeobius* sp. in the Atlantic by PELAGIOS, it was also identified on images of the Underwater Vision Profiler 5 (UVP5), a high-resolution camera that quantitatively records both particle concentrations and mesozooplankton. Here I use UVP5 and environmental data, including more than 1.8 million images from 13 cruises, to identify the horizontal and vertical distribution of *Poeobius* sp. in the tropical Atlantic Ocean. I test the hypothesis that *Poeobius* sp. is associated with mesoscale eddies and investigate its biogeochemical role in these features. In total, 481 individuals were observed between 5°S and 20°N and between 16°W to 46°W with the shallowest observation at around 22 m and the deepest at around 1000 m depth. A comparison between non-eddy stations and three different eddy types revealed elevated abundances and a restricted depth distribution of *Poeobius* sp. especially in anticyclonic mode water eddies (ACMEs), confirming the hypothesis of eddy association. The results from this thesis suggest that mesoscale eddies, especially ACMEs, may serve as an aggregation and dispersal mechanism for *Poeobius* sp. and possibly other low-oxygen tolerant zooplankton species. These in turn influence the environment of the eddy: High *Poeobius* sp. abundances could be related to  strongly reduced particle concentrations and fluxes in the layers directly below the polychaetes. It is shown that the worms take up almost the entire vertical particle flux by feeding with their mucus nets. *Poeobius* sp. may play a significant role in the development of particle fluxes, and thus the biological carbon pump, in ageing mesoscale eddies. These results should be considered when discussing or modelling mesoscale eddy ecology and biogeochemistry.

# Contents

# 1 Introduction

The pelagic ocean is the largest and least explored ecosystem on earth (Ramirez-Llodra *et al.* 2010). Its communities include planktonic organisms that no one has ever seen until the use of underwater camera systems. One example is the polychaete *Poeobius* sp., which was not known from the Atlantic until recently. This study explores its distribution in the tropical Atlantic and its potential impact on biogeochemical processes in mesoscale eddies.

## 1.1 Biogeochemistry in the upper ocean

Anthropogenic greenhouse gas emissions, such as $CO_2$, have lead to global climate change with significant consequences for ocean ecosystems, such as ocean warming, deoxygenation and acidification. This makes the understanding of processes that remove $CO_2$ from the atmosphere necessary. The ocean is an important buffering system for the climate. It is the biggest carbon store on earth with 38000 GT C; in contrast the atmosphere only holds 762 GT (Bollmann *et al.* 2010). Large amounts of $CO_2$ are fixed at the oceans surface by phytoplankton and thus get introduced into the marine food web. Although most of this surface production never leaves the upper 100 m due to fast remineralisation (Martin *et al.* 1987), a still considerable amount (2.47 GT $y^{-1}$ in total for the Atlantic Ocean alone; Antia *et al.* 2001) is transported into deeper layers in the form of small to large particles (diatom frustules, leftovers of small crustaceans, marine snow, fecal pellets and other detritus) and thus represents an important way of carbon sequestration and one major process of the biological carbon pump (Longhurst and Harrison 1989; Karakaş *et al.* 2009; Durkin *et al.* 2015). The actual carbon export to the deep ocean depends on the dynamics and types of planktonic processes in the water column.

## 1.2 Zooplankton and its role in the biological carbon pump

The oceanic ecosystem is inhabited by a large diversity of heterotrophic organisms ranging from protists to large nekton predators. Among these, zooplankton make up 51% (Gasol *et al.* 1997) of open ocean biomass. Within this extremely diverse group, organisms show wide ranges of sizes, morphology, behaviour and distribution. Zooplankton is a key link between primary production and higher trophic levels in the marine food web by feeding on phytoplankton and being fed upon by larger animals (Banse 1995).

Zooplankton is known to contribute to the biological carbon pump by producing fast-sinking particles (fecal pellets and dead bodies (Wilson *et al.* 2013)) and by performing diel vertical migrations (DVM), *i.e.* feeding at the surface at night and excreting at depth during the day (Turner 2015). On the other hand, sinking particles are also utilised by many of these animals. There are two basic feeding modes for particle-feeding zooplankton: Filter feeding, which is well described for salps (*e.g.* (Hamner *et al.* 1975) and copepods (Kiørboe 2000), and flux-feeding, which is known for example from pteropods, polychaete larvae and adult polychaetes (Hamner *et al.* 1975; Jackson 1993; Uttal and Buck 1996; Stemmann *et al.* 2004; Jackson and Checkley 2011; Turner 2015). Flux-feeders deploy net-like mucus structures on which they collect sinking particles (Gilmer 1974; Hamner *et al.* 1975). Jackson (1993) distinguishes clearly between filter-feeding and flux-feeding as two different modes, as the former is dependent on particle size and concentration, whereas the latter is independent from particle size, but dependent on particle flux (*i.e.* the amount of sinking particles per unit time). Iversen (2010) point out the importance of flux-feeding zooplankton for the degradation of particles off Cape Blanc and indicate flux-feeding to be an important process of carbon removal from sinking organic matter in that region: The authors calculated that zooplankton flux feeding was responsible for about 90% of the degradation of particles in particle size classes larger than 1 mm in the upper ocean. Jackson (1993) calculated the influence of pteropods on particle flux by formulating the cross-sectional impact of these animals' mucus web on falling particles and found a median loss of 26% flux by two species alone in the upper 100 m of five different regions of the Atlantic Ocean .

## 1.3   The flux-feeder *Poeobius* sp.

In the eastern Pacific Ocean, high abundances of the flux-feeding gelatinous polychaete *Poeobius meseres* (Heath 1930) were found to significantly increase the light transmission, indicating a decrease in particle concentrations, in the respective depth layer (Robison *et al.* 2010). *Poeobius meseres* is a fragile gelatinous worm of up to 2.7 cm length. The holopelagic polychaete of the family Flabelligeridae (Burnette *et al.* 2005) either catches particles by deploying a mucus net or by grasping single particles with its tentacles (Uttal and Buck 1996). It has a very low metabolism (Thuesen and Childress 1993). *Poeobius meseres* has been known in the Pacific Ocean for more than 80 years, and the genus was thought to be endemic to that ocean (McGowan 1960), however we only recently discovered an organism belonging to the same genus in the eastern tropical North Atlantic (ETNA) when using underwater imaging systems.

## 1.4   Sampling bias and the need for optical methods

Zooplankton research has been focussed on hard-bodied, robust animals, especially crustaceans (Robison 2004; Quéré *et al.* 2005), for a long time. The implementation of optical methods like underwater photography and video led to the discovery that the fragile gelatinous zooplankton (including *e.g.* medusae, ctenophores, salps, siphonophores and more) is largely undersampled by conventional plankton nets (Remsen *et al.* 2004; Robison 2004). A time series of ROV video transects revealed the substantial carbon transport to the deep sea by discarded larvacean houses (Robison *et al.* 2005). Biard et al (2016) performed the first global assessment of the distribution and biomass of large rhizarians, including phaeodaria, radiozoa and foraminifera, by analysing the global image database of the Underwater Vision Profiler (UVP5), which records both particles and mesozooplankton. The authors pointed out the high biomass of rhizaria in comparison to the mesozooplankton biomass known from net catch data, especially in tropical and subtropical oceans and in upwelling regions. In 2015, the deployment of a towed video camera system (pelagic *in situ* observation system, PELAGIOS) lead to the discovery of high abundances of the flux-feeding polychaete *Poeobius* sp. in a mesoscale eddy in the tropical Atlantic. These examples show that many aspects of marine zooplankton are still to be investigated, and that the use of optical methods is a key for this. The bias of current biogeochemical models towards crustacean zooplankton (Stemmann *et al.* 2004; Quéré *et al.* 2005) can only be overcome with a better knowledge of fragile zooplankton species distributions and their functions in the ecosystem.

## 1.5   Influence of oceanographic features on zooplankton distribution and particle flux, and the role of mesoscale eddies

The distribution of zooplankton in the three dimensional habitat of the world's oceans is patchy (Davis *et al.* 1992b). It is determined by biological processes (Folt and Burns 1999), but also by small- to large-scale oceanographic processes, for example mixing, upwelling, downwelling and the distribution of water masses (Martin 2003). Features like oceanic fronts (Fernández and Pingree 1996; Stemmann *et al.* 2008; Prants *et al.* 2014), seamounts (*e.g.*, (Boehlert and Genin 1987; Denda and Christiansen 2013) and eddies (Ring 1981; Tsurumi *et al.* 2005; Stemmann *et al.* 2008; Godø *et al.* 2012; Löscher *et al.* 2015; Waite *et al.* 2015; Hauss *et al.* 2016) play an important role in zooplankton aggregation and dispersal.

Mesoscale eddies are prominent features in the ocean. In the eastern tropical North Atlantic  they have recently gained attention due to their strong impacts on physical,

biological and biogeochemical processes in this otherwise oligotrophic region. Physical processes such as upwelling in the core or around the margins of mesoscale eddies (Karstensen *et al.* 2016) lead to increased nutrient input and influence surface primary productivity (Oschlies 2002; Sweeney *et al.* 2003; Godø *et al.* 2012; Stramma *et al.* 2013; Löscher *et al.* 2015) and in the following also to enhanced secondary production (Godø *et al.* 2012; Hauss *et al.* 2016), particle production (Sweeney *et al.* 2003; Waite *et al.* 2015; Fiedler *et al.* 2016; Fischer *et al.* 2016) and oxygen consumption (Karstensen *et al.* 2015; Waite *et al.* 2015; Fiedler *et al.* 2016). Eddies can have different origins: They can spin off coastal boundary currents and, transporting an enclosed water mass across the shelf, propagate into the open ocean (Mackas and Galbraith 2002; Whitney and Robert 2002; Waite *et al.* 2015; Schütte *et al.* 2016a). Also, eddies can be generated in the leeward of islands (leeward eddies; *e.g.* Seki *et al.* 2002). Another possible origin of eddies is the generation through disturbance by internal waves or underlying topography in the open ocean (J. Karstensen, GEOMAR, personal communication), but only little is known about these open ocean eddies. Three types of eddies are discriminated: 1. anticyclones (AC), 2. cyclones (CE) and 3. anticyclonic mode-water eddies (ACME; McGillicuddy *et al.* 2007; Schütte *et al.* 2016a). While 'normal' anticyclones are often less productive than the surrounding water due to downwelling in the eddy core, cyclones and anticyclonic mode-water eddies are known as 'oases in the desert' (Godø *et al.* 2012).

Are eddies also 'oases in the desert' for flux feeding organisms such as *Poeobius* sp.*?* Eddies can be seen as natural mesocosms as they transport an enclosed water mass with different properties than the surrounding waters (Ring 1981). Processes in these isolated features, like for example, the biological pump working at a different pace (Romero *et al.* 2016), provide different conditions for life inside the eddy than outside. Increased particle fluxes (*e.g.*: Fiedler *et al.* 2016) would suggest eddies to be a favourable habitat for particle-feeding organisms. Additionally, low oxygen conditions, as reported from several mesoscale eddies in the study region (Karstensen *et al.* 2015; Hauss *et al.* 2016; Schütte *et al.* 2016c), may exclude predators with a high oxygen demand (Hauss *et al.* 2016). The special properties of eddies have been known for many years (Ring 1981), and some work has been done to describe the impact of gulf stream cold- and warm-core rings on the ecosystem. Examples are also known from the Pacific Ocean: Tsurumi et al (2005) described increased pteropod densities in so-called Haida eddies compared to background conditions in the Alaska Gyre. They relate the higher abundances to more favourable conditions (warmer water than the surrounding sub-polar gyre) but do not go into detail about relations to particle concentrations and possible enhanced food availability. Tsurumi et al (2005) and others (Mackas and Galbraith 2002; Mackas *et al.* 2005) found eddies

of different stage and distance to the coast having a different composition of coastal and oceanic species. This indicates that eddies transport coastal species into the open ocean, but also take up oceanic species on their way. Tsurumi (2005) also found a decreasing ratio of juvenile to adult stages of pteropods with ageing eddies and concluded that these animals develop in the favourable habitats of these eddies. However, only a small number of publications describe the biology of mesoscale eddies in the subtropical and tropical Atlantic.

## 1.6 Scope

The relation of gelatinous fauna to mesoscale eddies and the impact of flux feeders on the biogeochemistry of these features is poorly understood. Due to its outstanding abundance in the tropical Atlantic eddy where it was discovered, I concentrated on *Poeobius* sp. in this thesis. This organism is well identifiable in the large dataset of UVP5 images that is available for the tropical Atlantic. In this thesis, particle and mesozooplankton data from 993 UVP5 profiles (including data from 36 mesoscale eddies) in the tropical Atlantic are analysed on *Poeobius* sp. occurrence and particle concentration. The distribution of *Poeobius* sp. in the tropical Atlantic is examined with regards to water mass dependencies and environmental conditions (*e.g.* temperature, salinity, oxygen, particle concentrations). The eddy-association of the flux-feeder in the tropical Atlantic is determined by comparing abundances at eddy and non-eddy stations. Furthermore, relations between particle concentrations, carbon flux and *Poeobius* sp. abundances are evaluated. Additionally, a short comparison of results from the UVP5 and PELAGIOS is done for an assessment of the advantages and disadvantages of these two optical systems. The following research questions are adressed:

1. What are the horizontal and vertical distribution, as well as the distribution in relation to environmental factors of *Poeobius* sp. in the tropical Atlantic?

> H1: *Poeobius* sp. standing stock is higher at shelf stations than at open ocean stations.

2. Is *Poeobius* sp. associated with mesoscale eddies?

> H1: *Poeobius* sp. standing stocks are higher in mesoscale eddies than at open ocean stations.

3. What is the impact of *Poeobius* sp. on particle concentrations and fluxes when occurring in high abundance?

> H1: Where abundant, *Poeobius sp.* substantially reduces the particle concentration and flux.

## 2 Data and Methods

This study aims to describe the distribution of *Poeobius* sp. in the tropical Atlantic. The polychaete was identified from images of the Underwater Vision Profiler (UVP5). The distribution of *Poeobius* sp. was determined from a dataset of 13 cruises with UVP5 deployments in the tropical Atlantic in the years 2012 to 2015. Particle concentrations and environmental data (temperature, salinity, oxygen concentration) were added to the database. UVP5 deployments were conducted in two different ways:

1. As **vertical cast**: The UVP5 was mounted on the Conductivity, Temperature, Depth (CTD) rosette (Figure 1a). It was deployed vertically from the surface to depths between 100 and more than 5000 m. These profiles were always carried out with the same depth routine: the gear was lowered to 22 m to enable the power-up of the UVP5, was then heaved to the surface again and then the actual profiling started. Down to 100 m the instrument was lowered with 0.5 m/s speed, below 100 m with 1 m/s. Images were recorded during the whole downcast.

2. As **horizontal tow**: The UVP5 was mounted on the pelagic *in situ* system (PELAGIOS; Figure 1b). It was towed at a speed of 1 knot and - recording continuously - lowered to discrete sampling depths between 20 m and 1000 m depth. At these discrete sampling depths, horizontal tows between 10 and 20 minutes were performed. Because the sampling depths and towed distances differed substantially between the casts, they were not used for the quantitative comparison of eddy and non-eddy stations. One horizontal tow was used to describe the change in certain abundances over time and distance, but not over depth. Data from tows at two stations were used for a comparison of UVP5 and PELAGIOS. Images of *Poeobius* sp. that were recorded during horizontal tows were included in the length determinations and for the observation of feeding behaviour (3.2.1 and 2.5.2).

### 2.1 The Underwater Vision Profiler and PELAGIOS

The Underwater Vision Profiler (Picheral *et al.* 2010) consists of a black-and-white CCD (charge-coupled device) camera in a pressure-proof case and two red LED light arrays in a defined distance to the camera. During a cast the instrument takes between 6-11 images per second of the illuminated area between the light arrays. The raw images are directly processed within the UVP5 processor unit: particles between 0.006 cm and 2.679 cm size are measured and values are stored in a data file. Additionally, images of single objects larger than 500 $\mu$m are saved as so-called

vignettes. These can be analysed later and sorted for detritus, phyto- and zooplankton categories, first with an automatic sorting system and then validated by manual sorting. The volume recorded by the UVP5 is defined by the known volume of the illuminated field and the frequency of image acquisition. The instrument provides a quantitative method for the estimation of particle and meso- to macrozooplankton concentrations in the water column.

The pelagic *in situ* observation system (PELAGIOS) is a towed video camera system that was developed under the lead of Dr. Henk-Jan Hoving (GEOMAR). It consists of an HD (high definition) camera and battery packs in pressure proof cases, as well as LED lights that are mounted into an open frame. The field of view of PELAGIOS is unknown, therefore the instrument provides qualitative data. Semi-quantitative comparisons between tows are possible, but no quantitative assessment can be done so far.
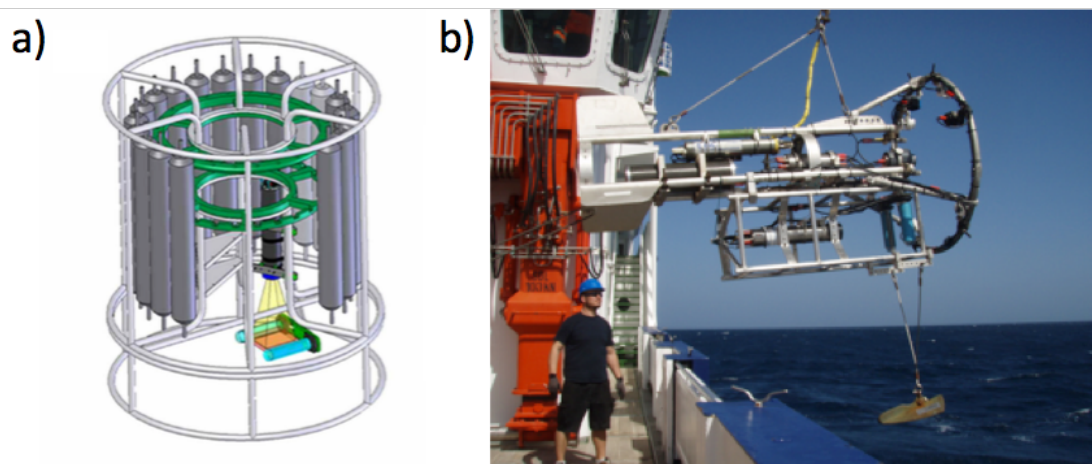


Figure 1: a) The Underwater Vision Profiler (UVP5) mounted in a CTD rosette; image modified from Picheral *et al.* (2010). b) UVP5 mounted onto the towed pelagic *in situ* observation system PELAGIOS.

## 2.2 Study area

From the 993 profiles considered, most data were available from the eastern tropical North Atlantic between 8 - 12 °N and 19 - 23 °W and from the 23°W transect between 14°N and 5°S. Single cruises covered stations on the Mauritanian and Brazilian shelf, on the 11°N transect between 18°W and 50°W and the 13°N and 14°N transect between 18°W and 58°W as well as the region around the Cape Verde archipelago (Figure 2 and Table 1).
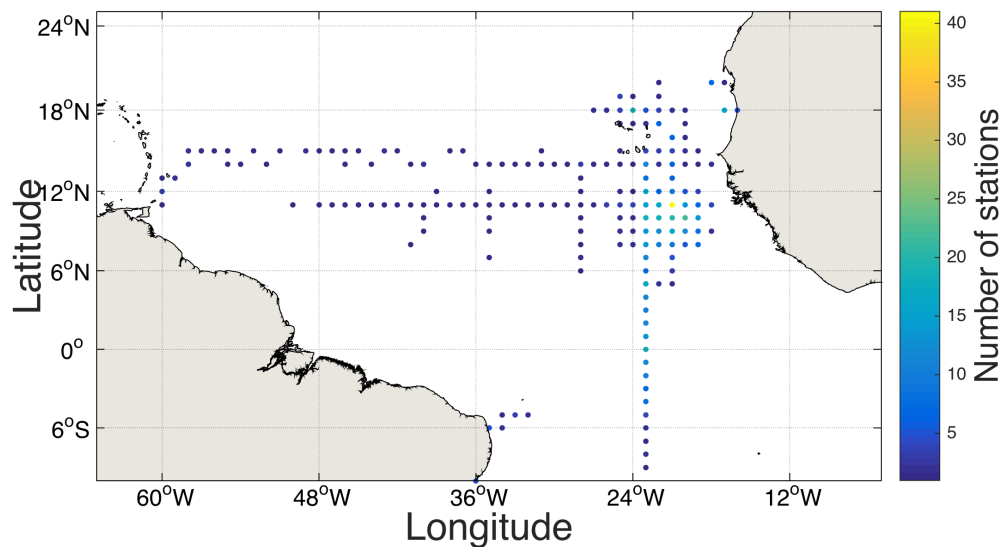
Figure 2: Study area in the tropical Atlantic. Stations are pooled on a 1 degree grid; each dot represents a grid location where UVP5 data were available. The colour of the dots indicates the number of stations at the respective grid location.

Table 1: Overview of the UVP5 profiles and eddies analysed in this thesis. The numbers in brackets indicate the number of horizontal tows; all others are vertical casts.

| Cruise | Cruise area | # UVP5 profiles | Date | Eddy type | # Profiles in eddy | Eddy Location | Eddy recognized on cruise |
|---|---|---|---|---|---|---|---|
| **MSM22** | 5°S - 19°N | 109 | November 2012 | CE | 8 | 18°N 24.5°W | no |
| | 20°W - 27°W | | | ACME | 2 | 18°N 20°W | yes |
| | | | | ACME | 2 | 13°N 21°W | no |
| | | | | AC | 2 | 9°N 23°W | no |
| | | | | CE | 1 | 10°N 23°W | no |
| **MSM23** | 18°S - 18°N | 45 | November/ December 2012 | CE | 1 | 14.5°N 23°W | no |
| | 1°E - 24°W | | | AC | 2 | 13°N 21°W | no |
| **M096** | 11°N - 18°N | 77 | May 2013 | AC | 1 | 14.5°N 42°W | no |
| | 20°W - 60°W | | | AC | 1 | 14.5°N 38°W | no |
| | | | | AC | 1 | 14.5°N 33°W | no |
| | | | | AC | 1 | 14.5°N 31°W | no |
| | | | | CE | 1 | 14.5°N 25°W | no |
| | | | | ACME | 10 | 18°N 25°W | yes |
| **M097** | 8°N - 17.5°N | 180 | June 2013 | CE | 2 | 11°N 22°W | no |
| | 17°W - 24°W | | | AC | 6 | 10°N 21°W | no |
| | | | | CE | 2 | 10°N 19.5°W | no |
| | | | | ACME | 1 | 9°N 21°W | yes |
| | | | | AC | 1 | 8.5°N 20°W | no |
| **ISL00214** | 17°N | 1 | February | / | / | / | / |

| | | | | | | | |
|---|---|---|---|---|---|---|---|
| | 25°W | | 2014 | | | | |
| **ISL00314** | 18.5°N - 19°N 24°W | 3 | March 2014 | ACME | 1 | 19°N 24.3°W | yes |
| **M105** | 7°N - 19°N 17.5°W - 26°W | 143 | March/April 2014 | ACME* | 6 | 19°N 25°W | yes |
| | | | | AC | 2 | 10°N 21°W | no |
| | | | | CE | 1 | 10.5°N 19°W | no |
| | | | | CE | 2 | 8°N 19°W | no |
| | | | | CE | 1 | 11°N 25.5°W | no |
| **M106** | 11.5°S - 18°N 21°W-36°W | 115 | April/May 2014 | AC | 2 | 9°N 23°W | no |
| **M107** | 11°N - 20°N 16°W-23°W | 73 | June 2014 | / | / | / | / |
| **PS88b** | 2°S - 18°N 23°W-24°W | 37 | November 2014 | CE | 2 | 14°N 23°W | no |
| **M116** | 5°N - 18°N 18°W - 58°W | 82 | May 2015 | CE | 1 | 11°N 37°W | no |
| | | | | AC | 1 | 12°N 35°W | no |
| | | | | AC | 1 | 11°N 34°W | no |
| | | | | CE | 1 | 11°N 25°W | no |
| | | | | CE | 1 | 9°N 23°W | no |
| | | | | ACME (E1) | 1 | 8°N 23°W | yes |
| **M119** | 5°S - 18°N 21°W - 24°W | 61 (12) | September 2015 | ACME (E2) | 3 (1) | 8°N 23°W | yes |
| | | | | AC | 1 | 2°N 23°W | no |
| **MSM49** | 12°N - 20°N 20°W - 24°W | 47 (25) | December 2015 | CE | 3 (2) | 17.5°N 24°W | no |
| | | | | CE | 11 (2) | 16°N 21°W | yes |
| **Total** | | 993 (37) | | 36 | 85 (5) | | |

* the same eddy was sampled during cruise ISL00314, the standing stock/abundance and depth distribution data are merged from these two cruises, while animal sizes are presented separately.

## 2.3 Environmental data

Environmental conditions, both biotic and abiotic, may impact the distribution of *Poeobius* sp.. Particle concentration was taken as indicator for biological productivity and as indicator for food availability. Surface particle concentrations were obtained from the UVP5 and calculated as the integrated particle concentration between 20 and 100 m depth. Physical data included temperature, salinity, depth and oxygen concentration and were collected from CTD deployments. Fully calibrated CTD data

were available from all cruises before December 2015. Pre-processed data were used from the cruise MSM49 in December 2015.

CTD and UVP5 data were obtained simultaneously in vertical casts. The only exception for this type of cast was during the cruises ISL00314 and ISL00214, where the UVP5 was deployed as stand-alone instrument and data from the closest (by time and distance) CTD cast at the same station were used. No simultaneous CTD data were available for the transect casts. Environmental conditions of these casts were assessed from the closest CTD profile. The UVP5 has an inbuilt pressure sensor; therefore CTD data and UVP5 data from the same pressures were related with each other. Environmental data were averaged over the same 5 m depth bins that were used for *Poeobius* sp. occurrences (see below).

*Poeobius* sp. distribution is possibly related to water masses, indicated by absolute salinity (SA) and conservative temperature (CT; (IOC 2010). These parameters, and additionally potential density, were computed with version 3.0 of the Gibbs Seawater (GSW) Oceanographic Toolbox that implements the TEOS 10 convention (IOC 2010).

Another physical feature which structures the upper ocean, and which may define the depth distribution of species, is the surface mixed layer. The mixed layer depth was defined as the depth where temperature differed from surface (10 m) conditions by no more than 0.2 °C and density sigma theta by no more than 0.03 as proposed by de Boyer Montegut *et al.* (2004), and was calculated for all profiles. *Poeobius* sp. depths of occurrence were compared with the mixed layer depth for each profile.

Food availability - in case of *Poeobius* sp. in the form of sinking particles - can limit the distribution of a species. Therefore, particle concentrations at which *Poeobius* sp. occurred were determined. These conditions were set into relation with the median particle concentration in non-eddy profiles from vertical casts.

## 2.4   Assignment of profiles to eddy and shelf

In order to investigate the relation of *Poeobius* sp. to mesoscale eddies, all profiles were categorized whether inside or outside an eddy. If inside, the type of eddy was determined. It was differentiated between cyclones (**CE**), anticyclones (**AC**) and anticyclonic mode-water eddies (**ACME**). Several mesoscale eddies had already been identified during the respective cruises (the CE on MSM49 and the ACMEs on MSM22, M96, M97, M105, ISL, M116 and M119, see Table 1). Those profiles which were located in these eddies were assigned to the respective eddy category. The eddy status of the undetermined profiles was provided by Dr. Florian Schütte (GEOMAR). He identified the eddy types by an algorithm that analysed satellite derived sea level

anomaly (SLA) data and evaluated oxygen, temperature and salinity anomalies as described in Schütte *et al.* (2016b). All profiles that were located within 40 km of an eddy core were assigned to the respective eddy type.

Continental shelves are most commonly defined to have water depths of less than 200 m (Spalding *et al.* 2007). Only shelf stations from the West African shelf were included here.

## 2.5 Assessment of *Poeobius* sp. abundance and depth

Polychaetes of the genus *Poeobius* can be identified well on images of the Underwater Vision Profiler (UVP5) as their body plan with its transparent trunk and the (on the black-and-white UVP5 images) dark, spirally gut is very characteristic (Figure 3). However, identification to species level is not possible.

### 2.5.1 Image sorting

UVP5 vignettes were processed after the deployment; they were inverted to black-on-white instead of white-on-black, and, among others, the length (equivalent spherical diameter; ESD) and area of the objects are measured. The resulting data file also contained the depth where the image was taken. The classification of the vignettes into detritus, phyto- and zooplankton categories was done with image recognition algorithms (http://www.zooscan.fr; Gorsky *et al.* 2010) that sort the vignettes into defined categories according to a learning set. Thus predicted profiles were uploaded to Ecotaxa (http://ecotaxa.obs-vlfr.fr/), an online platform that links the classified images into the taxonomic tree. On this platform, the classification was validated, *i.e.* sorted by hand. The information on assignments was extracted as data files. In this thesis I evaluated data from a total of 1822025 vignettes. I validated the vignette classification of the vertical profiles from cruise MSM49 completely and I checked all profiles from the transect casts of MSM49 and M119 and the vertical casts of M116 and M119 on *Poeobius* sp. occurrences, which means that I did not validate any other zooplankton categories there. During this check, I often observed wrong assignments of *Poeobius* sp. into the categories 'Chaetognatha', 'Cnidaria', 'Other_to_check', 'fiber' and 'Eumalostraca'. For all other cruises I only checked those categories.

Information on all profiles was collected in one Matlab database for each cruise. This database contained the complete metadata of each profile (latitude, longitude, time, water depth, sea state, cloud cover, wind), as well as the particle, vignette data and, if

available, CTD data. In the database, concentrations of particles of different size classes and of zooplankton and detritus categories were calculated and stored in

a) 5 m depth bins for the vertical casts and

b) 20 second time bins for transect casts.

### 2.5.2 Size determination

The UVP5 data processing provides size measurements of all particles recorded: equivalent spherical diameter (ESD, mm) and equivalent spherical volume (ESV, mm$^3$) are determined from the minor and major axis of the best fitting ellipse (Picheral *et al.* 2010). More than 10% of the *Poeobius* sp. either had food particles attached or were in an angle unfavourable for length determination, so that the automatic measurements were imprecise. Therefore, additional manual length measurements of all *Poeobius* sp. were conducted in *ImageJ* (http://www.imagej.net) with the linear measuring tool. The length was determined by measuring from the base of the tentacle crown to the posterior end (Figure 3). The quality of the measurements was indicated by assigning quality flags, described in Table 1. Only lengths with quality flag 0 were used in this thesis, although a trend of larger animals being bent more often was observed.

Table 2: Description of quality levels in *Poeobius* sp. measurements.

| Quality flag | Meaning | Description |
| --- | --- | --- |
| 0 | good measurement | *Poeobius* sp. straight and completely on image |
| 1 | low accuracy | *Poeobius* sp. bent or partly not on the image |
| 2 | no measurement possible | *Poeobius* sp. only in parts on the image |



Figure 3: Length determination of *Poeobius* sp., performed in *ImageJ*. *Poeobius* sp. size was measured from the base of the tentacle crown to the posterior end.

To determine the influence of *Poeobius* sp. on particle flux, its feeding behaviour was investigated. Different feeding stages were described, based on the tentacle position

and attached particles. The percentage of feeding animals calculated for eddies with more than 5 individuals, non-eddy observations and all observations.

*Poeobius* sp. could not only be observed on the UVP5 images, but also in PELAGIOS videos. In some of these videos, it was possible to see deployed mucus nets of *Poeobius* sp. In order to detect the potential influence of *Poeobius* sp. flux feeding on particle flux, the size of the mucus net structures was estimated from the measurement of 5 PELAGIOS video frame shots (provided by H.J. Hoving, GEOMAR) taken on MSM49. As objects on the PELAGIOS images are not scaled, the length of *Poeobius* sp. was taken as scale for further measurements in *ImageJ*. The area of the mucus structure was determined by measuring with the polygon tool around the edges of the net (0).

Biomass as a factor accounts for different animal sizes and may represent the impact of a species on the environment better than abundance. Therefore, *Poeobius* sp. individual biomass was calculated from the animal's area. The area was estimated as ellipse from body length and width. A common length-width ratio was calculated from the images of 12 individuals. Biomass ($\mu$g $DW$) was determined from this area, using the coefficients by Lehette *et al.* (2009) for gelatinous zooplankton (specifically siphonophores):

$$DW = 43.17 * Area^{1.02} \qquad\qquad (1)$$

Vertical biomass profiles for two eddies were then calculated from the mean length of the *Poeobius* sp. in the respective feature and the corresponding width from the above described length/width relationship. Biomass per individual was multiplied with the abundance per depth bin.

### 2.5.3 Calculations and binning

*Abundances and standing stock*

Pseudo-replication by having multiple profiles in one location was avoided by pooling:

a) all profiles within 0.01° and sampled within less than 30 days

b) all profiles within the same eddy and sampled within less than 30 days.

All standing stocks presented here were averaged for all profiles of one station. The standing stocks and depths of *Poeobius* sp. in the eddies on M105 and ISL00314 were averaged because it was the same feature on both cruises.

In order to compare profiles with different maximum depths, *i.e.* different scanned volumes, the following approach was used to calculate standing stocks: Only data from profiles that reached depths of more than 550 m were included in the analysis. Then, all vertical profiles were cut off at 600 m for being able to compare eddy and non-eddy stations as some of the eddy profiles did not exceed this depth. *Poeobius* sp. abundance (ind m$^{-3}$) was determined by dividing the count by the profile volume ($V_{tp}$). Standing stocks were calculated by multiplying the abundance with the maximum depth of the profile ($p_{max}$).

$$\text{Standing stock} = \left(\frac{\text{count}}{V_{tp}}\right) * p_{max} \qquad (\,2\,)$$

For presenting the horizontal distribution of *Poeobius* sp., the mean standing stocks found at stations were binned on a 1-degree grid.

*Horizontal tows*

Horizontal tows provide information of particle and zooplankton abundances at discrete sampling depths. They enable a comparison of these abundances over time and distance without depth changes. This was used to investigate the effect of high abundances of *Poeobius* sp. on the particle concentration in the ACME on M119. The discrete sampling depths were identified as those measurements that differed by less than 3 dbar between 20 s time bins. Particle abundance (0.8 - 5 mm), *Poeobius* sp. abundance and the abundance of large aggregates (> 600 $\mu$m) identified from the UVP5 images were plotted over distance at 50 m and 100 m depth. Distance was calculated from time, assuming 1 knot towing speed.

*Other zooplankton*

An assessment of *Poeobius* sp. abundance in relation to other zooplankton in the M116 (E1), M119 (E2) ACMEs and some background profiles was done. Background data included validated profiles of the cruises MSM22, MSM23 and M106. Seven categories of zooplankton were differentiated: copepods (integrating everything copepod-like), phaeodaria, collodaria, other rhizarians, 'other' (containing all other identified zooplankton groups, *e.g.* crustaceans, medusae etc.) and 'to check' (containing all unidentified zooplankton). Integrated abundances of all these categories and of *Poeobius* sp. were plotted as stacked barchart. The percentage of each category within the whole zooplankton was calculated and again illustrated in a stacked barchart.

## 2.6 Assessment of particle concentrations, sizes and flux

The flux-feeder *Poeobius* sp. may have an impact on particle concentrations and sizes and resulting flux when it is abundant. Highest polychaete abundances were found in the ACMEs sampled on cruises M116 and M119, which were both detected at 8°N and 23°W. Data from 8 other cruises were available at this location and used as background information. Particle concentrations (0 to 600 m depth) on the 23°W section were plotted between 7°N and 12°N. Particle density anomaly was derived by interpolating background and eddy data on a 0.5 degree grid using the Matlab function *interp2* with the linear interpolation method and subtracting the gained background density from the eddy densities.

The abundance and integrated volume of particles in different size classes was plotted against size (abundance-size spectrum and volume-size spectrum) as described by Iversen (2010). Depths of particle removal were identified by calculating eddy particle data and median background particle data (profiles within one degree of the eddy profiles position) integrated for three depth layers: 1. The surface: from 12.5 m to the depth, below which the first *Poeobius* sp. occurred, thereby covering the mixed layer. 2. The *Poeobius* sp. layer: between the shallowest and the deepest *Poeobius* sp. occurrence. 3. The layer below the deepest *Poeobius* sp. occurrence: a layer of the same thickness as each of the first two.

Particle fluxes were calculated from the abundance and sizes of particles in single size classes using the coefficients from Tables 1 and 2 of Kriest *et al.* (2002). The relation of particle diameter to particle mass was taken from Table 1. Mass in nmol N was converted to mmol C by using the Redfield ratio (Redfield *et al.* 1963), the relation of diameter to sinking speed was taken from Table 2, assuming a sinking velocity of 2.8 m d$^{-1}$ for a particle of 0.002 cm size (Kriest 2002). Coefficients from Alldredge *et al.* (1998) were used to calculate carbon content from mass:

$$m_{insitu} = c_{insitu} * DSE^{zeta_{insitu}} \qquad (3)$$

$$sink_{k2002} = b_{k2002} * DSE^{eta_{k2002}} \qquad (4)$$

With: $m_{insitu}$ = molar mass (mmol C), $c_{insitu}$ = 273, $zeta_{insitu}$ = 1.62, $sink_{k2002}$ = sinking velocity (m d$^{-1}$), $b_{k2002}$ = 132, DSE = size (cm), and $eta_{k2002}$ = 0.62.

For each size class, the flux (*F*, mg C m$^{-2}$ d$^{-1}$) by a single particle was calculated from the particles sinking velocity ($sink_{k2002}$) and its mass ($m_{in\ situ}$). By multiplying with the atomic mass of carbon (12 g mol$^{-1}$), mmol C was converted to mg C.

$$F = sink\_k2002 * m\_insitu * 1000 * 12 \qquad (5)$$

Individual particle masses and fluxes of each size class were multiplied with the particle abundance in the respective 5 m depth bin. Particle mass and flux were

integrated over size classes between 140 $\mu$m and 2.66 mm in order to obtain the total mass flux in this size range. Smaller particles were excluded in the flux calculation because these are not quantitatively measured with the UVP5. Particles larger than 2.66 mm were not used in order to avoid the inclusion of *Poeobius* sp. in the measurements.

## 2.7 Calculation of *Poeobius* sp. respiration and carbon utilisation

Respiration and carbon utilisation rates were calculated for E1 and E2 in order to relate changes in particle flux to *Poeobius* sp. abundance. Thuesen and Childress (1993) reported respiration rates of 0.068 $\mu$mol g-1 h-1 for *Poeobius meseres*. This value was taken as baseline for the following calculations. Thuesen and Childress (1993) detected no allometric relation so this was omitted here as well. The authors measured respiration at 5°C. *Poeobius* sp. was found at higher temperatures of around 15°C in E1 and E2, therefore a $Q_{10}$ value of 2 (Moloney and Field 1989) was applied, resulting in a doubling of the respiration rate. Multiplication with 24 resulted in the respiration rate per day. Taking into account that *Poeobius* sp. is a gelatinous organism and thus consists to more than 95% of water, body weight (*ww_poeo*) was calculated from the body volume as the weight that the same volume of seawater (with a density of 1.023 g ml$^{-1}$) would have. Body volume (*vol_poeo*) was calculated assuming a body shape of a prolate ellipsoid. The mean length (*length_poeo*) of the animals in E1 and E2 was calculated from the measurements described in 2.5.2 and body width estimated from the mean length and the length/width ratio (*lwr*) as described in the same paragraph.

$$vol_{poeo} = \left(4 * \frac{\pi}{3}\right) * \left(\frac{1}{2} * \frac{length_{poeo}}{lwr}\right) * \left(\frac{1}{2} * length_{poeo}\right) \qquad (6)$$

$$ww_{poeo} = vol_{poeo} * 1.023 \qquad (7)$$

With this body weight, respiration rates per individual and - by multiplying with the abundance in the single depth bins of E1 and E2 - per cubic metre were determined. Integrated community respiration per square metre was obtained by adding up the respiration rates determined for the single depth bins. The respiration rates (*R_poeo*, in $\mu$l O$_2$ d$^{-1}$) were converted into carbon utilisation rates as described by Steinberg *et al.* (1997):

$$C_{util} = R_{poeo} * \left(\frac{12}{22.4}\right) * 0.97 \qquad (8)$$

where 12/22.4 is the weight of C in 1 mol (22.4 L) of $CO_2$ and 0.97 is the respiratory quotient, *i.e.* the relative amount of $CO_2$ produced from $O_2$ taken up by the animal.

## 2.8 Comparison of UVP5 and PELAGIOS counts

The volume recorded by the UVP5 is comparatively small and it also takes images only every few centimetres and possibly misses rare animals. Thus, for assessing the applicability of using the UVP5 for distribution analysis of a rare species, such as *Poeobius* sp., UVP5 counts from horizontal tows were compared with video counts from the pelagic in situ observation system (PELAGIOS) that were obtained in parallel. Counts of *Poeobius* sp. in PELAGIOS transects for each discrete sampling depth were kindly provided by Henk-Jan Hoving. *Poeobius* sp. counts from UVP5 data were obtained by multiplying the abundance (ind m$^{-3}$) at each discrete sampling depth (determined as described in 2.5.3) with the respective volume. Four deployments (each two eddy and eddy reference casts) from cruise MSM49 were compared. A linear regression between the counts of the two instruments was tested. An approximation of the volume recorded by PELAGIOS was calculated from the relationship between the counts.

## 2.9 Statistics

### 2.9.1 Comparisons between eddy and non-eddy stations

Most bins and even most profiles had only 0 or 1 observations, which made the statistical comparison of abundances difficult. In order to compare bin data of *Poeobius* sp. in vertical profiles with environmental conditions only presence/absence data were used. In the horizontal tows, the scanned volume per bin on the single transects was assumed to be comparable as towing speed did not differ. Also the bins were larger than in the vertical casts (20 s bins instead of 5 m (equaling 5 s) bins, *i.e.* fourfold volume), therefore, abundances (ind m$^{-3}$) were calculated and used in the analysis.

All statistical tests were done in the R statistical environment (R Development Core Team, 2011). Because sample sizes were very different and data not normally distributed (tested with the Shapiro-Wilk test (R-function *shapiro.test*, *stats* package)), the following non-parametric statistical tests were applied:

1. The two sample Wilcoxon rank test (also called Mann-Whitney U-test, R-function *wilcox.test*, *stats* package) was used for comparing means of, for example, *Poeobius* sp. abundance between stations and between different eddy types.

2. The Kolomogorov-Smirnov test (R-function *ks.test*, *stats* package) was used for comparing the distribution of data points (*e.g.* depth occurrences) between different eddy types.

The abundance-size and volume-size spectra of particles in E1 and E2 were compared to the background spectra by an ANCOVA (R-funtion *aov*, *stats* package). Two depth layers were compared from each environment. First, the linear regression of the log-log transformed data of the respective layers was calculated and tested for significance. Size was used as independent variable, abundance and volume, respectively, as response variable. The layer description was used as categorical factor. Then the interaction of the categorical factor with the independent variable was determined by applying an ANCOVA to one model with and one model without the interaction of the factors. The two models were compared by an ANOVA (R-function *anova*, *stats* package) and this significance level taken to describe difference in slope. If the interaction was not significant, the model without interaction was concluded to be the most parsimonous model and the significance of the categorical factor determined therein was taken as description of the difference in intercepts. Because the results for the abundance-size and the volume-size ANCOVA were the same, they were summarised in one table for E1 and E2 each.

### 2.9.2 Generalized linear mixed model

In order to include multiple potential factors, which could influence *Poeobius* sp. depth distribution, a generalized linear mixed model (GLMM) was fitted by maximum likelihood (Laplace Approximation), as proposed by Bolker *et al.* (2009) for this type of data. The mean depth of occurrence of each profile with *Poeobius* sp. presence was modelled with the R-function *glmer* (R-package *lme4*) with Gamma error distribution and link = log to account for overdispersion. Sampling method and time were set as random effects. Fixed effects included environmental data from the respective profiles (latitude, longitude, month, surface particle concentration of large, medium and small particles, minimum oxygen concentration). Due to overdispersion, p-values for Wald's t (Bolker *et al.* 2009) were analysed to evaluate the most important factors for *Poeobius* sp. mean depth. Model selection for further identification of important effects was done by stepwise regression (ANOVA): In every step the least significant fixed effect was removed from the model. The $Chi^2$ and p-value for $Chi^2$ from an ANOVA of the model with and without the fixed effect were calculated and the Akaike Information Criterion (AIC) compared between the two model versions. A factor was excluded if this lowered the AIC of the model.

# 3  Results

A database of 993 UVP5 profiles and the corresponding environmental data from large parts of the tropical Atlantic were analysed for *Poeobius* sp. occurrence and horizontal and vertical distribution. *Poeobius* sp. abundance in different types of eddies and its relation to particle abundance, sizes and resulting flux were calculated. The 993 profiles were taken at 719 stations. A total of 36 stations were identified to be located inside a mesoscale eddy.

## 3.1  *Poeobius* sp. distribution and eddy association in the tropical Atlantic

*Poeobius* sp. abundance and distribution was evaluated from non-eddy and eddy stations. The resulting horizontal distribution across the tropical Atlantic and the vertical distribution in the water column are shown in the following chapter. Also, *Poeobius* sp. distribution in relation to water masses (*i.e.* the physical environment) are described and the characteristics of the Atlantic *Poeobius* sp. are pointed out.

### 3.1.1  Horizontal distribution

A total number of 481 *Poeobius* sp. was found in a database of 993 UVP5 profiles in the tropical Atlantic between 16°W to 46° W and 5°S to 20°N. While 197 observations came from non-eddy stations, 284 were observed at eddy stations.

*Non-eddy stations*

*Poeobius* sp. was found at 108 non-eddy stations with vertical casts in the tropical Atlantic. Locations of occurrence ranged between latitudes of 5°S and 20°N and between longitudes of 16°W and 46°W (Figure 4). In the vertical casts, *Poeobius* sp. was observed at roughly every tenth station, numbers ranged between 0 and 3 polychaetes per cast. This resulted in standing stocks of 0 - 123 ind m$^{-2}$ at the grid points and a mean standing stock of about 10 ind m$^{-2}$ in the area covered by vertical casts. Highest standing stocks were observed at 11°N between 31°W and 33°W. However, Most individuals, in the eastern tropical North Atlantic between 8°N - 13°N and 19°W - 23°W, *Poeobius* sp. was observed most frequently. There the sampling coverage was highest. Otherwise *Poeobius* sp. showed no clear distribution pattern in the tropical Atlantic Ocean.
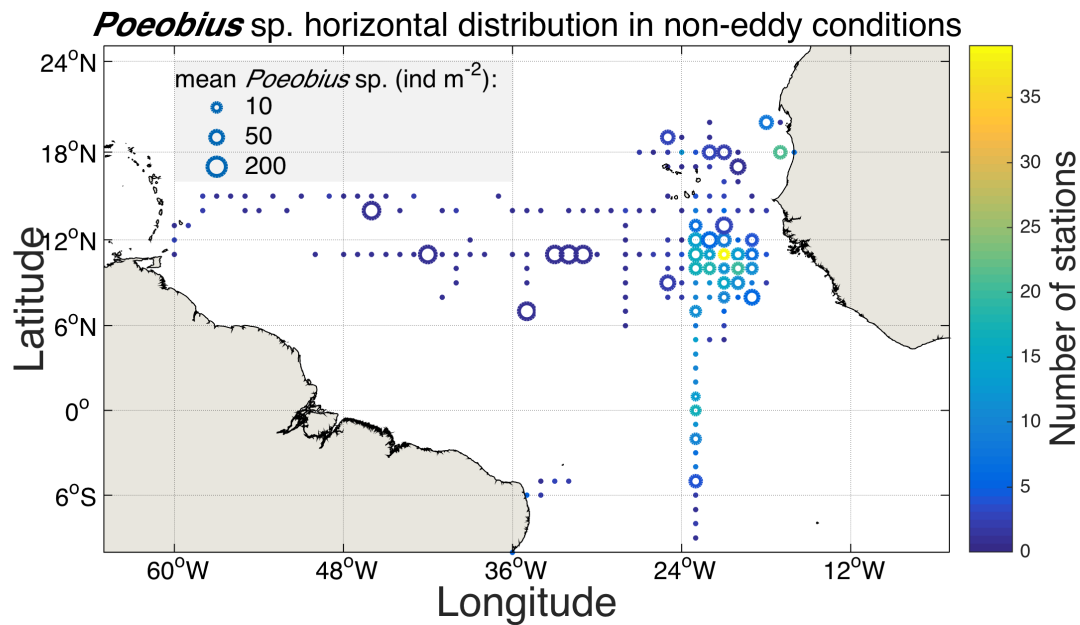
Figure 4: Horizontal distribution map of *Poeobius* sp. at non-eddy stations in the tropical Atlantic Ocean; averaged on a 1 degree grid from vertical UVP5 casts. Dots indicate grid locations where UVP5 data were available, open circles indicate the occurrence of *Poeobius* sp. at this location. The size of the circle represents the mean standing stock (ind m$^{-2}$) of *Poeobius* sp. at the respective grid point and the colour the number of stations. Only data from the upper 600 m are included.

*Eddy stations*

*Poeobius* sp. was observed at 17 out of 36 eddies that were sampled between 2°S and 19°N and 19°W and 41°. Of these eddies, 17 were classified as cyclones (CEs), 13 as anticyclones (ACs) and 6 as anticyclonic modewater eddies (ACME, Figure 5). In CEs and ACs, numbers ranged between 0 and 1 individuals per cast resulting in standing stocks of 0 to 110 ind m$^{-2}$ and a mean standing stock of 30 ind m$^{-2}$ and 10 ind m$^{-2}$, respectively. In ACMEs, *Poeobius* sp. had numbers between 0 and 64 per cast and standing stocks between 0 and 6470 ind m$^{-2}$ with a mean of 1280 ind m$^{-2}$.
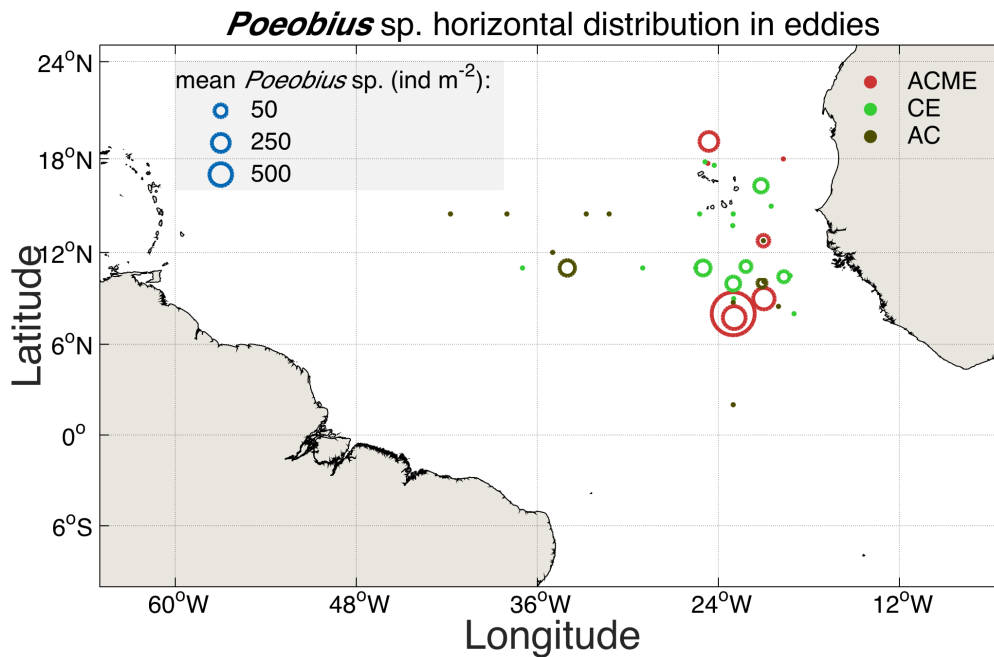
Figure 5: Horizontal distribution map of *Poeobius* sp. in eddies in the tropical Atlantic Ocean from vertical UVP5 casts. Dots indicate eddy locations where UVP5 data were available, open circles indicate the finding of *Poeobius* sp. in that eddy. The size of the circle represents the mean standing stock of *Poeobius* sp. in the respective eddy and the colour the type of eddy. ACME stands for anticyclonic modewater eddy, CE for cyclonic eddy and AC for normal anticyclones. Only data from the upper 600 m are included.

*Shelf conditions*

Most eddies in the eastern tropical North Atlantic form on the West African shelf and propagate westward from there. Increased abundances of a species such as *Poeobius* sp. at shelf stations compared to open ocean stations would indicate eddy transport. Only 26 out of 993 UVP5 profiles were located on the West African shelf. No *Poeobius* sp. was found at any of these shelf stations.

*Comparison between* Poeobius *sp. standing stocks at non-eddy and eddy stations*

A significantly (Mann-Whitney U: $p<0.001$) larger standing stock was found at ACME stations (mean of 1285 ind m$^{-2}$) compared to non-eddy stations (mean of 11 ind m$^{-2}$) in vertical casts. The standing stock was about 100fold larger at these stations. Median standing stock size was 0 ind m$^{-2}$ at non-eddy stations and 330 ind m$^{-2}$ at ACME stations (Figure 6). Mean standing stocks at non-eddy stations and in CEs (mean of 18 ind m$^{-2}$) differed significantly (Mann-Whitney U: $p<0.05$), but the median was 0 in both conditions. There was no difference in abundances between vertical non-eddy casts and anticyclonic eddies (Mann-Whitney U: $p > 0.05$). The largest standing stock was found in the M116 ACME with 6470 ind m$^{-2}$.
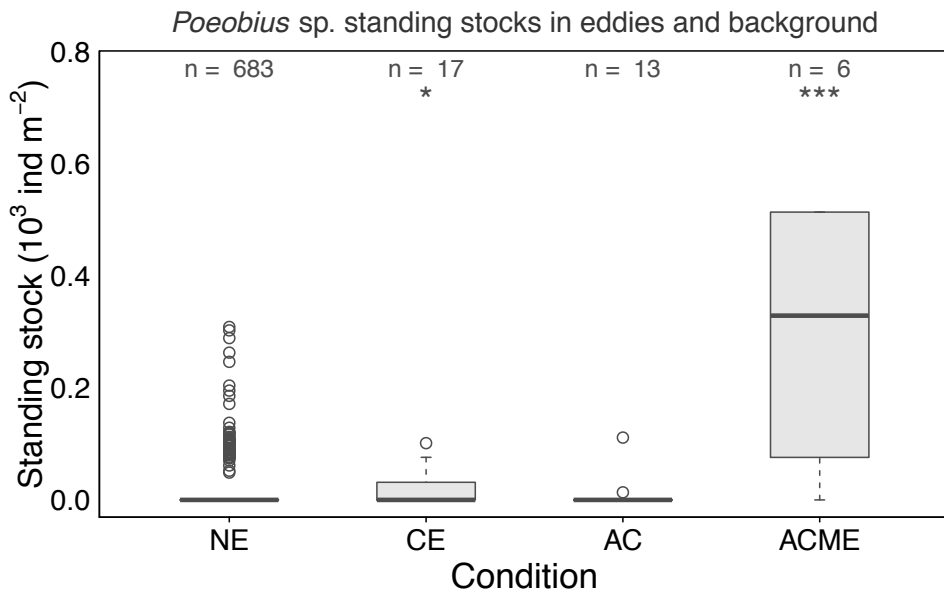
Figure 6: Box plots of *Poeobius* sp. standing stocks (ind m$^{-2}$) at non-eddy stations (NE) and in eddies of different types in UVP5 vertical and transect casts. Only profile data shallower than 600 m were used. One outlier (6470 ind m$^{-2}$) in the ACME standing stocks is not shown, but included in the analysis. Significance level (*Mann-Whitney* U test: *: $p<0.05$, ***: $p<0.001$) from comparing the different eddy type's standing stocks with the stocks at non-eddy stations is shown. n is the number of stations in the respective group.

### 3.1.2 Vertical distribution

*Non-eddy stations*

All *Poeobius* sp. were found shallower than 1000 m depth, with the deepest one living at 997 m and the shallowest at 22.7 m. Occurrences from vertical casts had a median depth of 428 m. In transect casts, non-eddy *Poeobius* sp. were found at a median of 201 m. Almost all depths between the surface and 1000 m depth were represented in the depth distribution of the non-eddy stations. The distribution was bimodal, with one peak between 25 and 75 m and a broader one between 375 and 725 m (Figure 7b).

*Eddy stations*

In the eddies, most animals were observed between 25 and 75 m, only single specimens were observed deeper than 175 m (Figure 7b). The deepest specimen found in an eddy was at around 800 m depth.
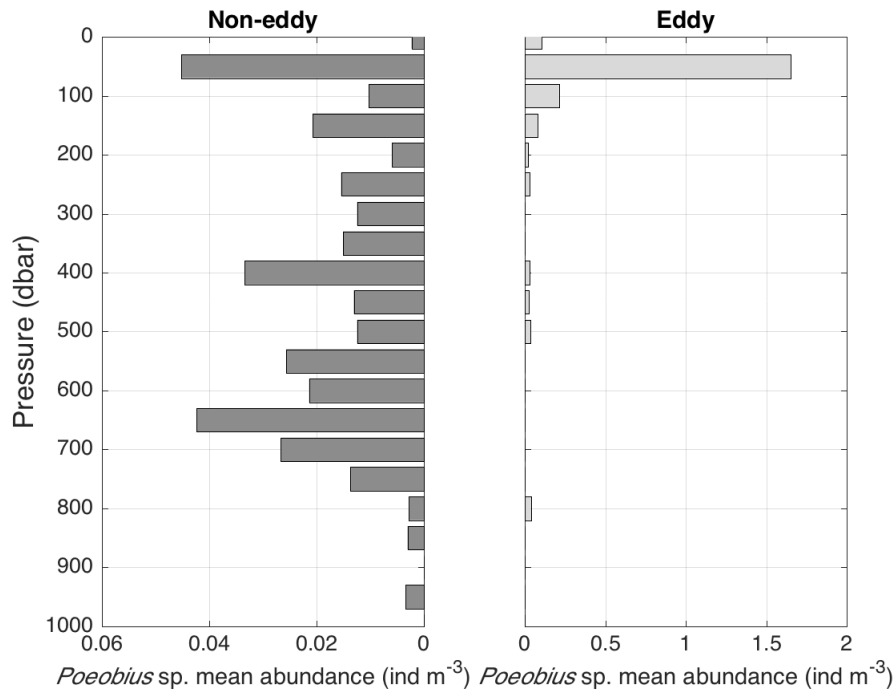
Figure 7: Depth distribution of all recorded *Poeobius* sp. in vertical casts in the tropical Atlantic Ocean. Mean abundance per 50 m depth bin, differentiated between a) non-eddy and b) eddy observations. Note different scaling on abundance axis.

*Impact of environmental factors on* Poeobius *sp. depth distribution*

From the results presented above, the hypothesis arose that eddy conditions impact *Poeobius* sp. depth distribution. In order to verify the importance of eddy conditions in relation to other environmental factors, a generalized linear mixed model (GLMM) was applied. It included different environmental variables that may have an effect on depth distribution, as described in 2.9.2. From the complete model, the variables latitude, longitude, month and surface concentrations of particles of different size could be excluded in the model selection (Chi$^2$: p-value > 0.05 and AIC of full model > AIC of reduced model). The resulting reduced model included only the factor of eddy/non-eddy conditions, minimum oxygen concentration and the interaction of the two variables. *Poeobius* sp. depth was significantly impacted by eddy conditions (Wald's statistic: p-value < 0.01). A trend could be seen in the impact of the minimum oxygen concentration and the interaction of this variable with eddy conditions, but these effects were not significant (Wald's statistic: p-value 0.08 and 0.052, respectively).

Table 3: Factors and results of the generalized linear mixed model (GLMM) after model selection, showing the influence of different environmental factors on *Poeobius* sp. depth. Min Ox stands for minimum oxygen concentration in the profile.

| Random effects | | Variance | | Std. Dev. |
|---|---|---|---|---|
| Method (Intercept) | | 9.411e-11 | | 9.701e-06 |
| Date (Intercept) | | 7.678e-03 | | 8.763e-02 |
| Residual | | 3.795e-01 | | 6.161e-01 |
| Fixed effects | Estimate | Std. Error | t-value | p-value |
| (Intercept) | 5.366387 | 0.169067 | 31.74 | **< 2e-16** |
| Eddy | -1.126395 | 0.406199 | -2.77 | **0.00555** |
| Min Ox | 0.005386 | 0.003048 | 1.77 | 0.07719 |
| Eddy: Min Ox | 0.020916 | 0.010779 | 1.94 | 0.05232 |

Model fit with individual-level variation by the Laplace approximation and a gamma error distribution with link = log using *glmer* implemented in the R package lme4 (R Development Core Team, 2011). Std. dev. and std. Error stand for standard deviation and standard error, respectively. The t-value is the test statistic. Significant p-values are highlighted in bold.

Poeobius *sp. depth distribution at non-eddy and eddy stations*

In order to further analyse the above discovered effect of mesoscale eddies on *Poeobius* sp. abundance, a more detailed comparison between the depth distribution at non-eddy stations and in different eddy types was done. At non-eddy stations in vertical casts, the median depth of *Poeobius* sp. was 217 m (range 32-588 m, Figure 8). The range at which *Poeobius* sp. occurred in CEs and ACs was within that observed for non-eddy stations, but no statistical test was done since only 7 and 2 individuals, respectively, were recorded there. In ACMEs, the depth distribution differed significantly from non-eddy depth distribution (KS: p < 0.001). In this eddy type, the median depth was determined to be around 62 m (range 37-377 m). Only one *Poeobius* sp. was observed below 132 m.
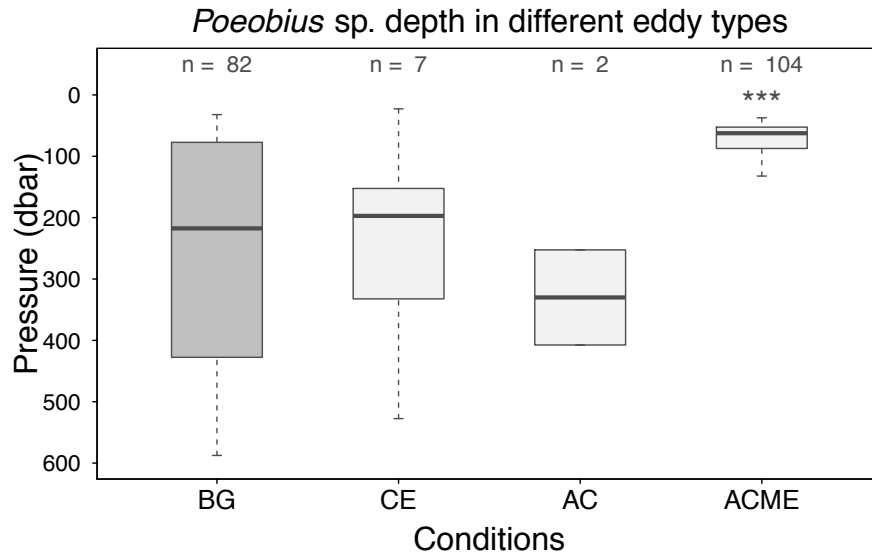
Figure 8: Box plots of *Poeobius* sp. depth distribution at non-eddy stations (NE) and in different eddy types, in vertical UVP5 casts. Only data shallower than 600 m were used. Significance levels (Kolmonogorov-Smirnov test: ***: p<0.001) indicate similarity between the depth distributions in the different eddy types to the depth distribution in non-eddy conditions. n is the number of individuals in the respective conditions.

### 3.1.3 Distribution in relation to environmental factors

Water masses were used to describe the hydrographical environment of *Poeobius* sp. Additionally its occurrence in relation to oxygen concentration as well as to particle concentrations was evaluated.

*Water masses*

The water masses sampled by the UVP5 in this study belonged to the North Atlantic Deep water (NADW), the Antarctic intermediate water (AAIW), the North Atlantic and South Atlantic central waters (NACW and SACW) and the surface water. *Poeobius* sp. mainly occurred in the North Atlantic and South Atlantic central waters of the tropical Atlantic (Figure 9). Only a few specimens were observed in the surface water (at the equator), none inhabited the core of the AAIW, or the NADW with temperatures below 5 °C. An analysis of all occurrences of *Poeobius* sp. showed that no individual occurred within the surface mixed layer.
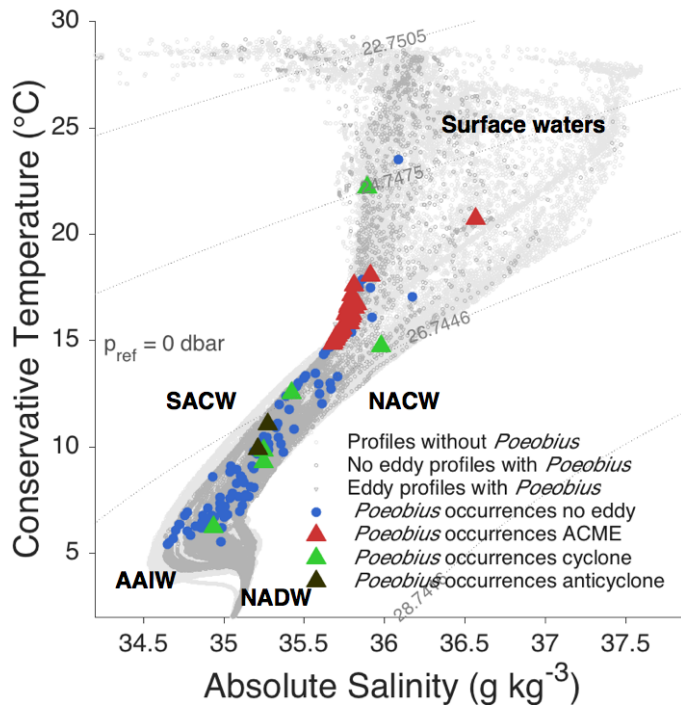
Figure 9: *Poeobius* sp. occurrence in all available profiles from vertical UVP5 casts in temperature and salinity conditions. Eddy observations are marked as triangles with different colours for anticyclonic mode-water eddies (ACME), anticyclones and cyclones. Different water masses are shown: North Atlantic Central Water (NACW), South Atlantic Central Water (SACW), Antarctic Intermediate water (AAIW), North Atlantic Deep Water (NADW) and undifferentiated surface waters.

*Oxygen concentration*

Oxygen concentrations in the tropical Atlantic vary with depth, and vertical profiles differed between eddy (especially ACME) and non-eddy stations. Therefore, *Poeobius* sp. occurrence was analysed in relation to both depth and oxygen concentration, differentiated between non-eddy profiles and profiles of different eddy types. The polychaetes were distributed across most oxygen and depth levels in the non-eddy vertical profiles. More than 50% of the *Poeobius* sp. inhabited waters with oxygen concentrations between 40 and 90 $\mu$mol kg$^{-1}$ (Figure 10). About 13% occurred in oxygen concentrations higher than 90 $\mu$mol kg$^{-1}$, but only one animal was found in concentrations higher than 150 $\mu$mol kg$^{-1}$. In ACMEs, *Poeobius* sp. was found in combination with lower oxygen levels. There, 28% of the animals were observed in oxygen concentrations between 40 and 90 $\mu$mol kg$^{-1}$, whereas 66% occurred below 40 $\mu$mol kg$^{-1}$. The lowest oxygen concentration where *Poeobius* sp. was observed, was 3.77 $\mu$mol kg$^{-1}$ in the ACME encountered on cruise M105. Only a few animals were recorded in CEs and ACs. Their distribution in relation to oxygen concentration and depth was similar to non-eddy profiles (Figure 10).
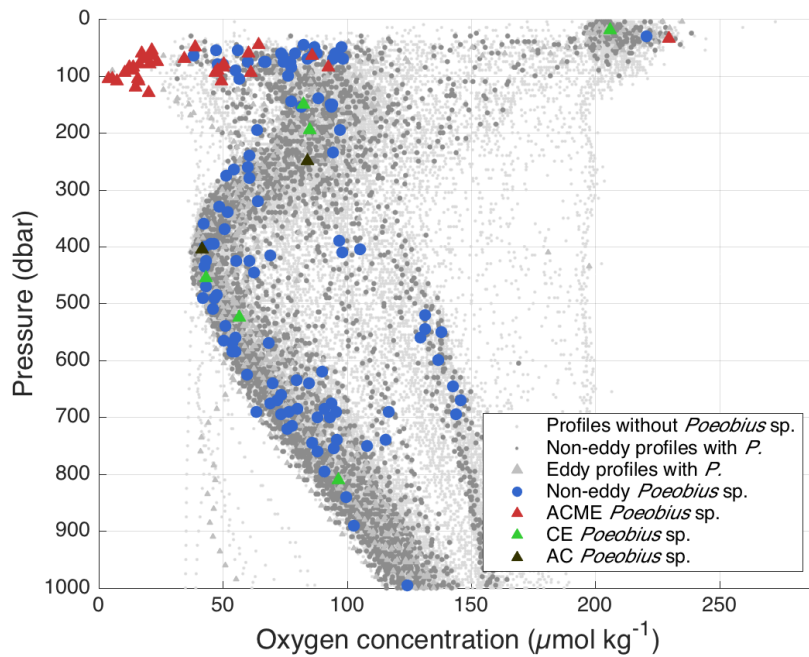
Figure 10: *Poeobius* sp. distribution in relation to oxygen and pressure. Grey circles and triangles indicate sampled conditions, the coloured symbols indicate the presence of *Poeobius* sp. in the respective conditions, differentiated between non-eddy stations and different eddy types.

*Particle concentration*

In non-eddy UVP5 profiles, all except one *Poeobius* sp. occurred in concentrations between 20 and 179 particles $L^{-1}$ (Figure 11). One individual was observed at particle concentrations of 16.9 $L^{-1}$. The range of occurrences in relation to particle concentration was compared to the median particle concentration in non-eddy profiles across the water column. No *Poeobius* sp. was observed below 1000 m, where the median particle abundance was below 20 $L^{-1}$.
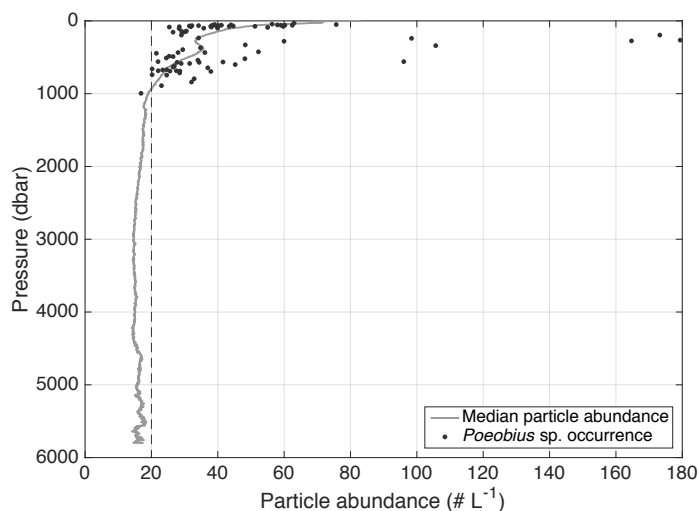


Figure 11: *Poeobius* sp. occurrence in relation to particle abundance and pressure in non-eddy vertical casts. The line represents the median particle abundance of all non-eddy UVP5 profiles; the dots indicate conditions where *Poeobius* sp. was found.

### 3.1.4 *Poeobius* sp. length

*Poeobius* sp. lengths were determined because length in combination with abundance may be an important factor for the impact of a species on its ecosystem. Additionally these data might provide insights into the so far unknown development of this species. *Poeobius sp.* with lengths between 2.7 mm and 23.5 mm were recorded with the UVP5. The median length of all observations was 7.9 mm, the mean length 9.3 mm ± 4.5 mm standard deviation. Non-eddy specimens were usually smaller than those in most eddies (KS test: p-value<0.001; Figure 12). However, the largest individual was observed in a non-eddy profile (outlier in Figure 12). The mean length of *Poeobius* sp. in the M119 eddy (16.5 ± 2.7 mm) was significantly (*Mann-Whitney* p < 0.001) larger than in the other eddies or at the non-eddy stations, where the mean length ranged from 5.2-10.3 mm. The two specimens in ACs excluded, the on average smallest specimens were found in the M116 eddy with 6.6 ± 2 mm length.
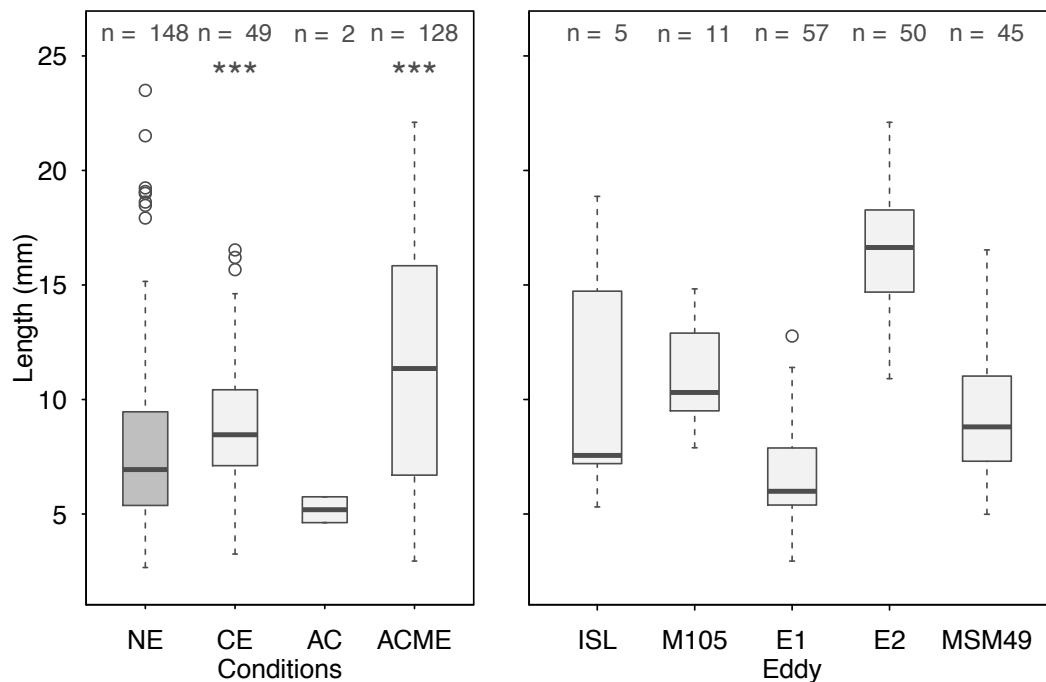


Figure 12: Boxplot of *Poeobius* sp. lengths in a) different eddy types and at non-eddy stations (NE), as well as b) in single eddies with more than 5 (or as exception 5 in ISL) individuals. The M105 eddy was the same feature as ISL, sampled about two weeks later. Significance levels (*Mann-Whitney* U test: ***: p-value<0.001) indicate similarity of means of the lengths of *Poeobius* sp. in CEs and ACMEs compared with non-eddy observations. n is the number of *Poeobius* sp. in the respective eddy. Only good quality measurements (see 2.5.2) are included.

Relations of the size of an animal with longitude, season or depth could give indications on its life cycle. A linear regression of length on longitude showed a slope significantly different from zero (linear regression: p > 0.05) indicating that larger *Poeobius* sp. were found further west (Figure 13a). The eddies with more than 5 individuals were located between 21°W and 24.5°W. No relation of the mean size within these eddies to longitude was found. In both non-eddy and eddy conditions,

sizes of *Poeobius* sp. did not change with depth (linear regression: p>0.05, Figure 13b). However, the largest individuals were found at shallow depths. *Poeobius* sp. was found with a broad range of sizes in all seasons in non-eddy profiles. Larger individuals were observed between September and December compared to March to June, but this may be a result of higher sampling effort in these months due to the horizontal tows that were conducted only in that season. In summary, the length of *Poeobius* sp. size was significantly linearly related to longitude, but no pattern with depth or season was observed when the difference between eddy and non-eddy stations was accounted for.
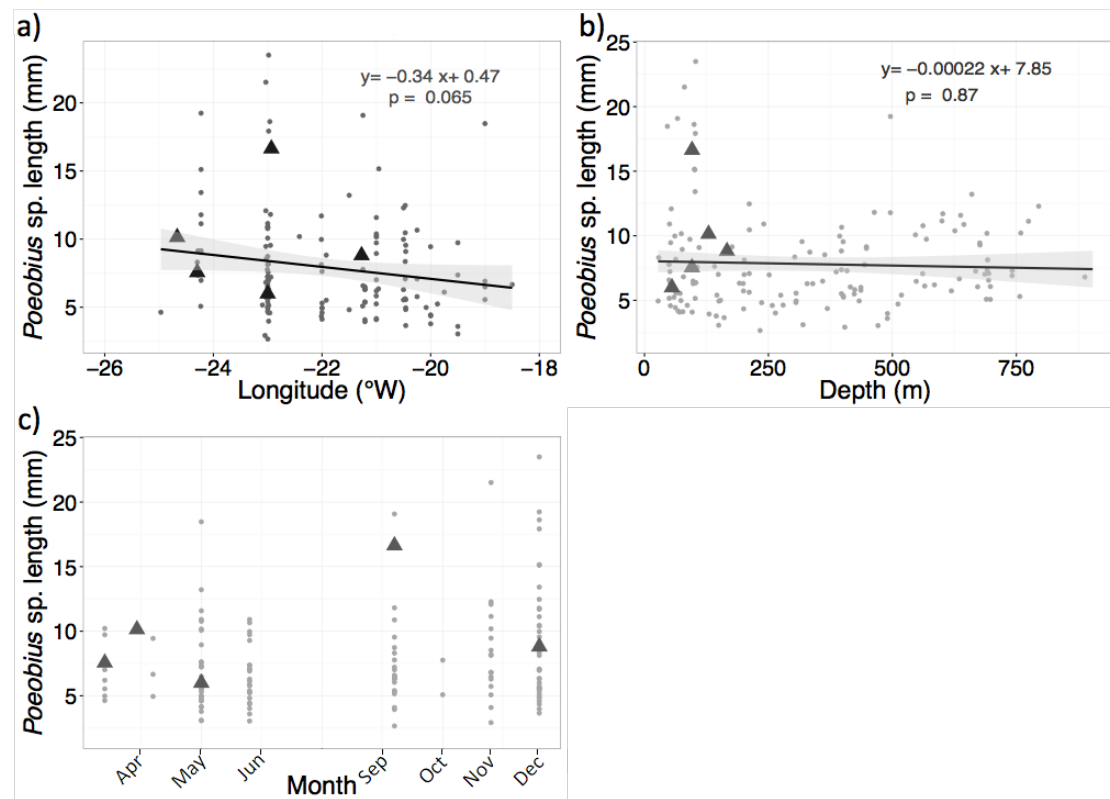


Figure 13: *Poeobius* sp. length in relation to a) longitude (restricted to longitudes east of 26°W due to low sample sizes further west), b) depth, c) season. Dots represent *Poeobius* sp. lengths in non-eddy conditions, filled triangles the median length in eddies with more than 5 individuals. The linear regressions include only non-eddy data, the regression equation is given in the figure (a and b). The grey shaded areas indicate the 95% confidence interval.

## 3.2 Implications of high *Poeobius* sp. abundances on the particle abundance and biogeochemistry of mesoscale eddies

*Poeobius* sp. is a flux-feeder, which means that it can possibly alter the abundance and flux of particles in the water column. In order to investigate this impact, feeding observations were evaluated. Distribution patterns of particle abundance and of

*Poeobius* sp. were compared and particle sizes of different depth layers analysed for changes that might be the consequence of *Poeobius* sp. feeding.

### 3.2.1 Observations of feeding behaviour

*Poeobius* sp. was observed in different feeding modes, *i.e.* not-feeding, with tentacles visible, with attached food particles or with a deployed mucus net (Figure 14). Those *Poeobius* sp. with attached particles or deployed mucus net were considered actively feeding. Active feeding was observed in up to 26.3% of individuals in eddies and in 12.6% of the individuals at non-eddy stations. The frequency of feeding observations varied between eddy stations (Table 4). In the M105/Islandia ACME, 15% were actively feeding and 26.3% in the MSM49 CE. No food particles were associated with *Poeobius* sp. in E1 and E2. The particles on the images were probably mostly retracted mucous nets with captured smaller particles. Examples of different stages of feeding are shown in Figure 14. One image shows a *Poeobius* sp. feeding on an aggregate about 2 times larger than the worm itself (Figure 14). This aggregate could also be a mucus net during retraction.
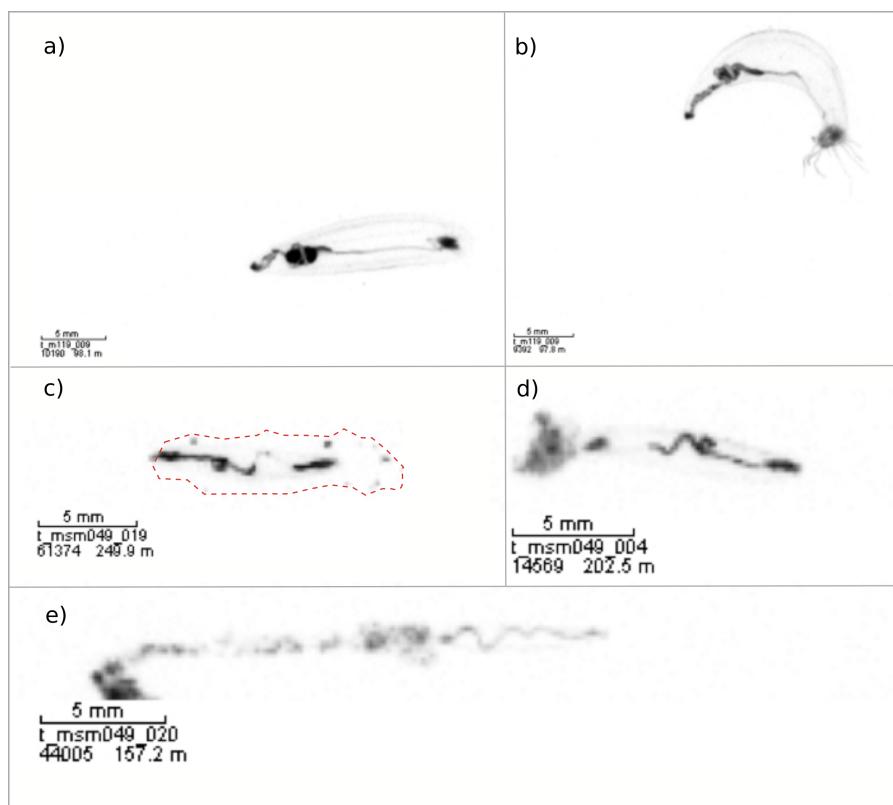


Figure 14: Examples of UVP5 images with *Poeobius* sp. in different feeding modes: a) not feeding, tentacles retracted, b) not feeding, tentacles visible, c) active feeding with mucus net deployed, net outlined in dotted line, d) active feeding of a retracted mucus net / large particle, e) individual feeding on an aggregate about 2 times its size.

Table 4: Proportion of *Poeobius* sp. observed actively feeding on UVP5 images in eddies with more than 5 recorded individuals and integrated for the non-eddy observations.

| Cruise (Eddy) | *Poeobius sp.* number | Feeding | Percentage |
|---|---|---|---|
| ISL/M105 ACME | 20 | 3 | 15% |
| E1 | 63 | 0 | 0 % |
| E2 | 107 | 0 | 0 % |
| MSM49 CE | 76 | 20 | 26.3 % |
| Non-eddy | 198 | 25 | 12.6 % |
| All | 481 | 52 | 10.8 % |

*Mucus net sizes*

The area of mucus nets of *Poeobius* sp. can be taken as an indicator of its potential particle clearing efficiency. The nets were not directly visible in the UVP5 images, however, such nets could be identified by small particles in the periphery of a few *Poeobius* sp. According to these measurements, mucus net size on UVP images was about the same size as the worm itself up to roughly 1.5 times its size, but these nets were probably in the act of being retracted. The mucus net size was also estimated from PELAGIOS frame shots (Figure 15). Mucus nets on these images showed irregular shapes with lengths about 10 times the length of the worm and approximate widths of about 1.7 times *Poeobius* sp. length. With an assumed *Poeobius* sp. length of 1 cm, the mucus nets on 5 frame shots had areas between around 7 cm$^2$ and 24 cm$^2$ with a mean area of about 12 cm$^2$ (Table 5).
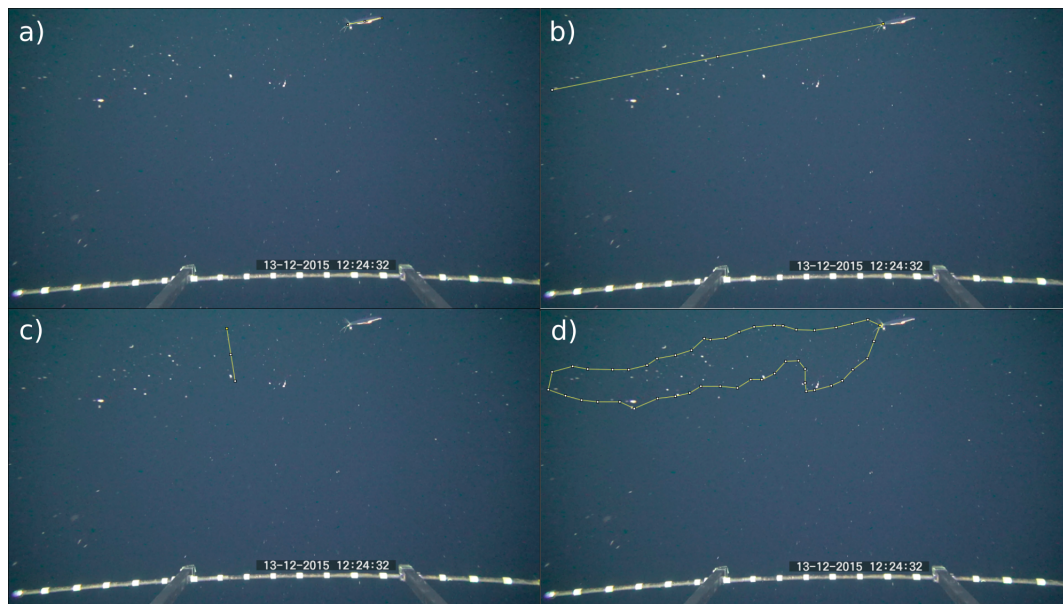


Figure 15: Measurements on an exemplary mucus net in a frame shot from PELAGIOS video. *Poeobius* sp. length (a) served as scale for the determination of relative length (b), width (c) and polygon area (d) of the mucus net.

Table 5: Mucus net sizes as determined from measurements of 5 PELAGIOS video frame shots in *ImageJ*. Sizes are relative to the respective length of *Poeobius* sp.

| Animal | Net length | Net width | Net area |
|---|---|---|---|
| 1 | 9.4 | 1.5 | 10.5 |
| 2 | 9.6 | 2.9 | 23.7 |
| 3 | 10.6 | 1.3 | 9.9 |
| 4 | 11.2 | 0.9 | 7.0 |
| 5 | 8.5 | 1.8 | 10.2 |
| Mean ± std | 9.9 ± 1.1 | 1.7 ± 0.8 | 12.3 ± 6.5 |

### 3.2.2 Implications on the biogeochemistry of eddies

Highest *Poeobius* sp. abundances were observed in the ACMEs during M116 (E1) and M119 (E2). Therefore, the analysis of the potential impact of *Poeobius* sp. on particle concentrations and fluxes concentrates on these two eddies, which were located at 8°N and 23°W. Data from further 8 cruises without eddies were available for the 23°W transect and served as a comparison of the eddy conditions in E1 and E2 with the background system.

*Particle abundances on the 23°W transect*

Particle concentrations on the 23°W transect in Figure 17 show a particle low in both E1 and E2 (located at 8°N), with particle concentrations reaching less than 20 particles $L^{-1}$ in both eddies. The particle concentrations deviated from the background concentration by more than 60%. The particle low was especially pronounced in E2, where particles were almost completely depleted (less than 10 particles $L^{-1}$) between 95 and 105 m depth in one of the two profiles at that station. In E1 the surface particle concentration was partly higher than in the background profiles, in E2 the particle depletion was visible across the whole water column (Figure 16).
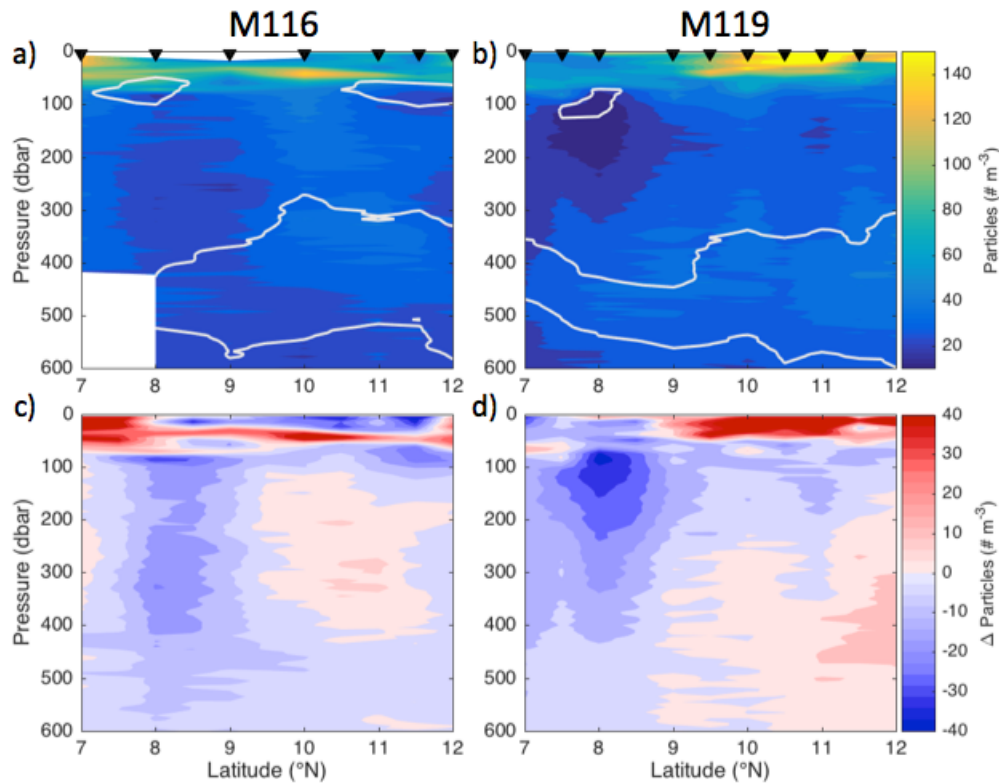
Figure 16: Particle concentrations (a and b) and deviation from the background concentration (c and d) along 23°W between 7°N and 12°N during M116 (a and c) and M119 (b and d). Stations are indicated by black triangles. Contour lines stand for the 55 μmol oxygen isoline, outlining the location of the OMZ and of the low-oxygen-eddies E1 (a and c) and E2 (b and d) at 8°N 23°W.

*Particle abundance of E1 and E2 and relation to* Poeobius *sp.*

The vertical profiles of eddy and background particle abundance were compared with *Poeobius* sp. biomass. Biomass was used instead of abundance to account for the different animal sizes in the two eddies (as determined in 3.1.4). The particle maximum was at about 40 m depth in all profiles (E1, E2 and median background), with a following decline down to about 100 m depth (Figure 17). The decline in both eddies was much stronger than in the background profiles, with the steepest slope in E1. Highest biomasses of *Poeobius* sp. were observed directly below the particle maximum, co-occurring with the decline of particles. While particle numbers in the background profiles only slightly increased between 200 and 300 m and then again decreased, a strong increase in concentration could be observed in E2 deeper than 120 m. E1 particle concentrations stayed constant below 120 m. At 600 m depth, profiles from E1 and E2 showed only slightly lower particle abundances than the median background profile.
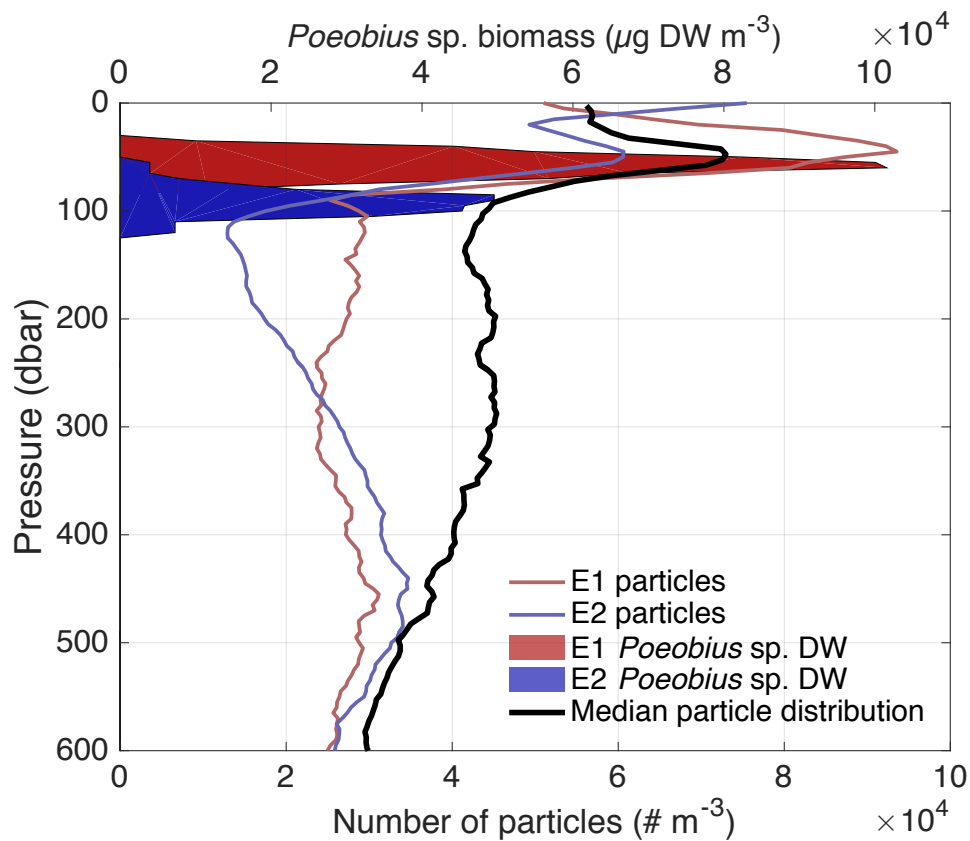
Figure 17: Particle abundance and *Poeobius* sp. biomass at 8°N 23°W as observed in E1, E2 and in the median background profile. *Poeobius* sp. abundance was subtracted from the particle abundance. The curves were smoothed by a running mean.

*Horizontal toes with* Poeobius *sp. abundance and particle concentration*

The UVP5 horizontal tows provide the possibility not only to analyse changes in zooplankton and particle concentration with depth, but also with time at constant depth. Therefore, the E2 transect cast was analysed for changes in particle concentration with increasing or decreasing in *Poeobius* sp. abundance. In E2 at 50 m depth, neither large nor medium sized particles showed a change in concentration when *Poeobius* sp. abundance rapidly increased. At 100 m depth, though, an increase in both large aggregates and medium sized particles (0.8 - 5 mm) could be observed concurrent with a decrease in *Poeobius* sp. abundance (Figure 18).

.
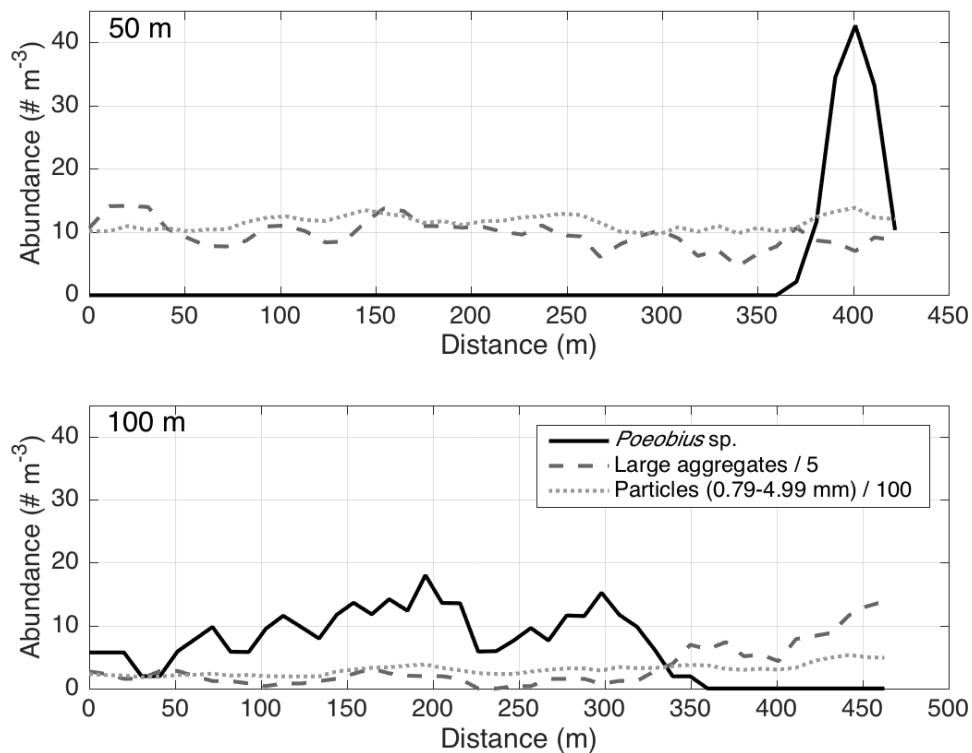
Figure 18: Results from a horizontal tow in E2. Abundance of *Poeobius* sp., large aggregates and medium sized particles over distance at discrete sampling depths a) 50 m and b) 100 m. Abundance of large aggregates was divided by 5 and abundance of medium sized particles divided by 100.

*Changes in particle size*

In order to detect the influence of *Poeobius* sp. on the size distribution of particles, the particle abundance in distinct size classes of background stations (no *Poeobius* sp.) was compared with that of E1 and E2 (high *Poeobius* sp. abundances). Depths of particle removal were identified from three distinct depth layers in E1 and E2:

In E1 the surface layer without *Poeobius* sp. was defined to be between 12.5 and 42.5 m, in E2 between 12.5 and 62.5 m. *Poeobius* sp. were observed between 42.5 and 72.5 m in E1 and 62.5 to 112.5 m in E2 (the '*Poeobius* layer'). The 'deep layer' (without *Poeobius* sp.) accordingly ranged from 72.5 to 102.5 m in E1 and from 112.5 to 162.5 m in E2.

In all layers of eddy and background conditions, particle abundance decreased with increasing particle size (Figure 19a and b), and particle volume increased (Figure 19c and d). Some differences in particle abundance of the different size classes between the surface layer and the deep layer for the two eddies and the background situation were identified:

The relation of particle abundance and total particle volume, respectively, to size was described by linear regressions on the log-log transformed data. A statistical

comparison of the linear regressions of E1 and background particle abundances between the deep and surface layers was performed with an ANCOVA (Table 6). This revealed that neither slopes nor intercepts differed significantly between the surface layer of E1 and the surface background layer. The slope of the deep background layer and the E1 surface layer were similar, but particle abundances were lower in the deep background layer. However, the slope in the deep layer of E1 was significantly different from those of the other layers (p<0.001), indicating an effect of the eddy on the particle size distribution, but not generally on particle abundance. The results of the ANCOVA for differences between volume-size spectra in E1 were the same as for the abundance-size spectra.

The ANCOVA for comparing abundance-size spectra for particles in E2 and in the background revealed a significantly (p<0.01 and p<0.05, respectively) steeper slope in the deep layer of E2 compared to the surface layer of E2 and the background surface layer. The slopes of the eddy surface layer compared to the background surface layer, as well as the background deep layer compared to all other layers, were similar (p>0.05). The surface layer abundance size spectrum was similar in E2 and background conditions, but intercepts, *i.e.* particle abundance were significantly lower in the deep layers.

In summary, a difference in particle abundance between the surface layer and the background deep layer could be statistically validated in E1 and E2. A significant difference in the slopes between the surface layer and the deep layer in E1 and in E2 indicate an effect of *Poeobius* sp. on the particle size distribution in the eddies. This indicates that mainly the small size classes were reduced in E1, and especially the large size classes in E2.
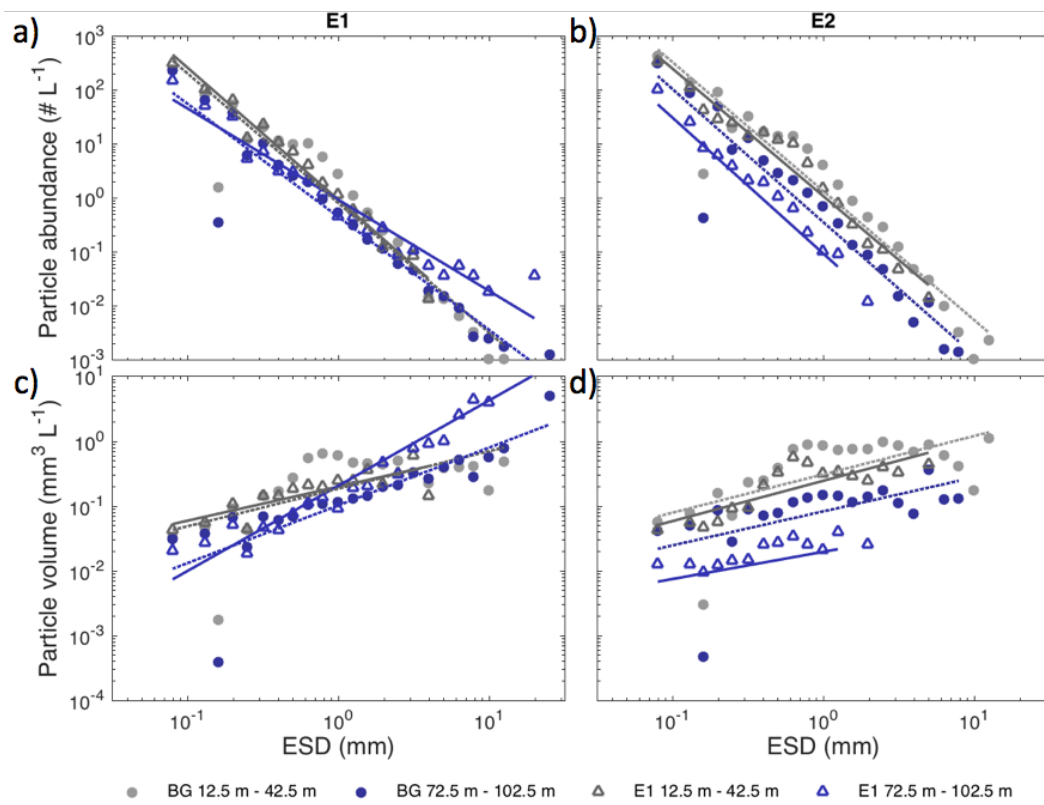
Figure 19: Particle-abundance (a and b) and particle-volume spectra (c and d) for two different depth layers in eddies E1 (a and c) and E2 (b and d), compared to background conditions.

Table 6: Results of slope comparison and ANCOVA between log-log-transformed abundance-size spectra and volume-size spectra of particles in E1 and the background, for two different depth layers. The linear regression model for each layer for abundance and volume is given below the layer description.

| E1 | | Slope comparison (ANOVA) | | | |
|---|---|---|---|---|---|
| **ANCOVA** | | **Eddy surface** | **Eddy deep** | **Non-eddy surface** | **Non-eddy deep** |
| | Abundance | y = -2.44x-0.032 | y = -2x-0.13 | y = -2.4x-0.09 | y = -2.15x-0.36 |
| | Volume | y = 0.53x-0.7 | y = 1x-0.8 | y = 0.58x-0.74 | y = 0.83x-1.01 |
| **Eddy surface** | | / | ** | n.s. | n.s. |
| **Eddy deep** | | - | / | *** | *** |
| **Non-eddy surface** | | n.s. | - | / | n.s. |
| **Non-eddy deep** | | *** | - | n.s. | / |

The upper part of the covariance matrix indicates significant differences in slopes, the lower part significant differences in intercepts. Significance levels: ***: $p<0.001$; **: $p<0.01$; *: $p<0.05$; n.s.: $p>0.05$. No intercept comparison was done when slopes were significantly different (indicated by -). The linear regression model is given as: y = slope*x+intercept.

Table 7: Results of slope comparison and ANCOVA between log-log-transformed abundance-size spectra and volume-size spectra of particles in E2 and the background, for two different depth layers. The linear regression model for each layer for abundance and volume is given below the layer description.

| E2 | Slope comparison (ANOVA) | | | |
|---|---|---|---|---|
| **ANCOVA** | **Eddy surface** | **Eddy deep** | **Non-eddy surface** | **Non-eddy deep** |
| Abundance | y = -1.9x+0.32 | y = -2.52x-1.03 | y = -2.25x+0.18 | y = -2.46x-0.45 |
| Volume | y = 1.06x-0.35 | y = 0.42x-1.7 | y = 0.74x-0.46 | y = 0.53x-1.09 |
| **Eddy surface** | / | ** | n.s. | n.s. |
| **Eddy deep** | - | / | * | n.s. |
| **Non-eddy surface** | n.s. | - | / | n.s. |
| **Non-eddy deep** | ** | ** | *** | / |

The upper part of the covariance matrix indicates significant differences in slopes, the lower part significant differences in intercepts. Significance levels: ***: $p<0.001$; **: $p<0.01$; *: $p<0.05$; n.s.: $p>0.05$. No intercept comparison was done when slopes were significantly different (indicated by -). The linear regression model is given as: y = slope*x+intercept.

*Influence on particulate matter flux to the deep sea*

The combination of particle abundances and sizes revealed the particle flux in E1, E2 and in the median background situation. All vertical flux profiles showed highest values in the upper 100 m of the water column, followed by a substantial decrease. Below 100 m, the flux was rather constant (Figure 20).

In E1, the flux was higher than the background flux at its maximum around 60 m. The values oscillated around those of the background flux below that depth. At 600 m depth, the flux in E1 was similar to the background flux. In E2, the highest flux was measured at the surface and was similar to the background. It then decreased until it was reduced to the lowest recorded flux at that site at around 150 m depth. Below 100 m, the flux in E2 was always markedly lower than the background flux. The decline of the particle flux from maximum to minimum was steepest in E1 and least steep in E2.
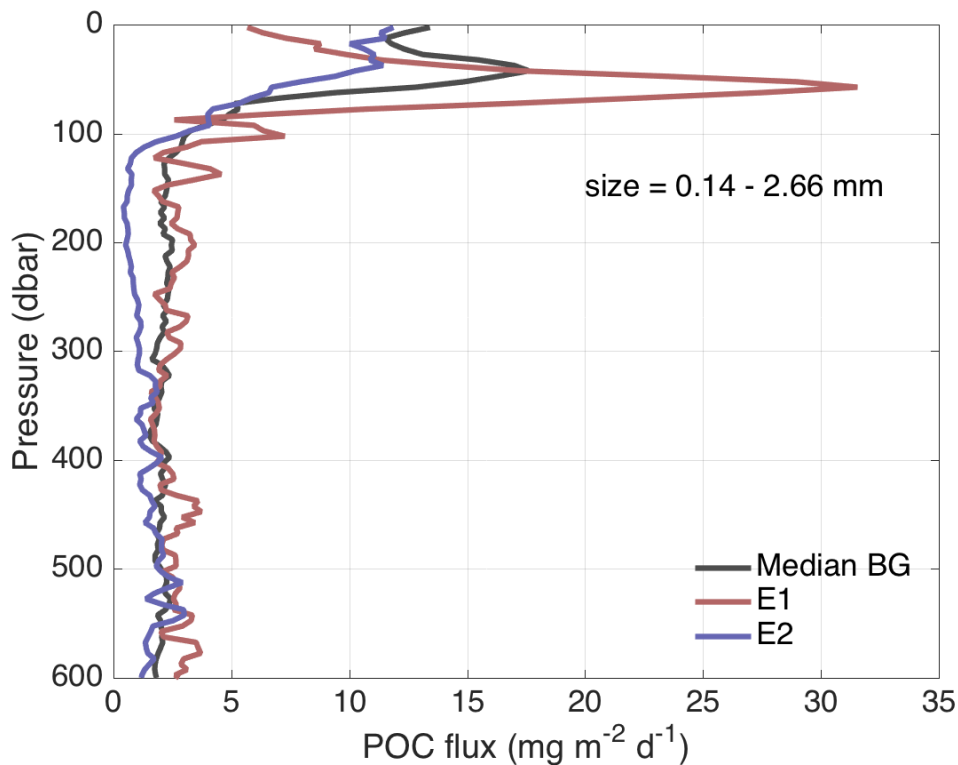
Figure 20: Integrated particle fluxes of size classes between 0.14 and 2.66 mm to the deep sea at 8°N 23°W in all available vertical UVP5 profiles. The curves are smoothed by a running mean. E1 is emphasized in red, E2 in blue. The median background flux is shown as black line.

Poeobius *sp. respiration and carbon utilisation*

*Poeobius* sp. respiration rates and carbon utilisation rates were calculated for E1 and E2. Respiration rates between 5 and 18 $\mu$mol $O_2$ $m^{-3}$ $d^{-1}$ were calculated for bins with *Poeobius* sp. in E1 and between 1 and 8 $\mu$mol $O_2$ $m^{-3}$ $d^{-1}$ in E2. Integrated for the depth layer where *Poeobius* sp. occurred this added up to 58 $\mu$mol $O_2$ $m^{-2}$ $d^{-1}$ in E1 and 18 $\mu$mol $O_2$ $m^{-2}$ $d^{-1}$ in E2.

These oxygen respiration rates resulted in carbon utilisation rates between 0.06 and 0.2 mg C $m^{-3}$ $d^{-1}$ in E1 and between 0.02 and 0.09 mg C $m^{-3}$ $d^{-1}$ in E2. Integrated carbon removal by oxygen respiration was 0.68 mg C $m^{-2}$ $d^{-1}$ in E1 and 0.21 mg C $m^{-2}$ $d^{-1}$ in E2.

### 3.2.3 Other zooplankton in E1, E2 and the background

The relative abundance and composition of the zooplankton in E1 and E2 shows the dominance of *Poeobius* sp. in relation to other zooplankton groups in certain depth layers. In E1, the integrated abundance of zooplankton was about 900 ind $m^{-3}$ at its maximum at around 70 m depth (Figure 21). *Poeobius* sp. occurred between 50 m and 80 m and made up between 23 and 53% of the zooplankton in that layer. Another highly represented group in that layer were the rhizaria (especially collodaria),

adding between 10 - 30% to the total zooplankton. Copepods were less abundant where *Poeobius* sp. occurred, making up only up 0 - 10% of the zooplankton in this layer, and 20-100% at the other depths in the upper 100 m. Below 100 m depth, abundance was generally lower with low numbers of copepods, rhizaria and other zooplankton.

In E2 the total zooplankton abundance was much lower than in E1 with a maximum abundance of about 95 ind m$^{-3}$ at about 30 m depth. *Poeobius* sp. occurred between 70 m and 110 m depth and made up between 0-100% of the zooplankton in that layer. Other than *Poeobius* sp., mainly unidentified zooplankton was observed in that layer with 50-100%. In this category, also doubtful *Poeobius* sp. identifications were located. No zooplankton was observed between 120 and 300 m, below that depth, mainly rhizarians were present, making up between 75 and 100% of the zooplankton in most depths.

In the averaged background situation, a maximum of about 90 ind m$^{-3}$ was observed at 50 m depth. No *Poeobius* sp. was observed in the background situation. The largest fraction in the upper 100 m was the unidentified zooplankton with 10 - 80%. Copepods made up between 5-60%, other identified zooplankton 7-50% and rhizaria 0-30%. All zooplankton classes were represented below 100 m depth, with low abundances between 100-400 m and increasing abundance below that depth. The rhizaria fraction below 100 m was larger than in the upper 100 m, making up between 15-100% of the zooplankton in most depths.
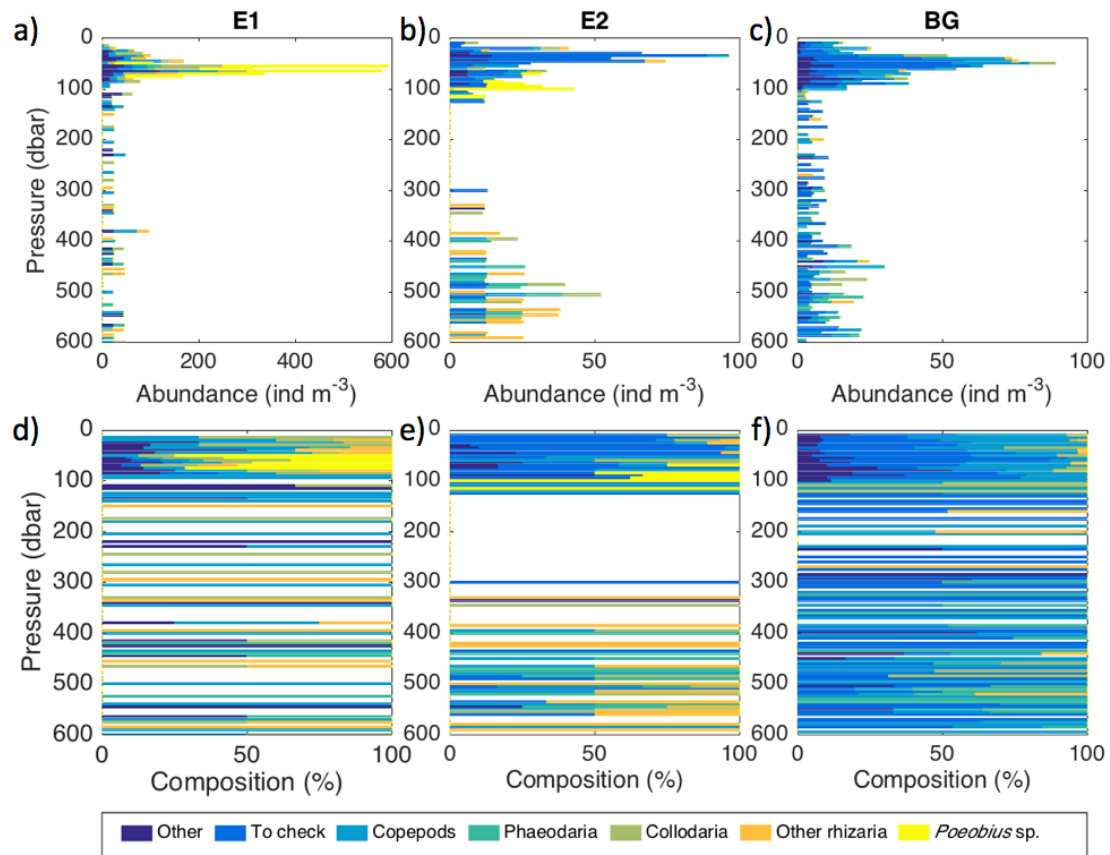
Figure 21: Zooplankton composition in E1 (a and d), E2 (b and e) and the background situation (c and f) in the upper 600 m of the water column from UVP5 vertical profiles. Stacked abundance (a, b and c) and composition in percentages (d, e and f) are shown for *Poeobius* sp., different rhizaria taxa, copepods, other zooplankton groups ('other') and unidentified zooplankton (to check). Note the difference in scales for the stacked abundances.

*Estimation of* Poeobius *sp. potential impact on particle flux*

The proportion of particle flux that is potentially removed by *Poeobius sp.* was calculated as follows: The integrated area covered by *Poeobius sp.* mucus nets ∂ was described from the abundance *Ab*, taking into account the part of the animals that were actively feeding $p_{feeding}$, and the mean net area $A_{net}$:

$$\partial = Ab * p_{feeding} * A_{net} \qquad (9)$$

The length and width of the mucus nets relative to the animal length were obtained in 3.2.1. Assuming a linear relationship between net size and animal length, these relative values were used to calculate the area of mucus nets in E1 and E2 from the respective mean size of *Poeobius* sp. Calculated individual net area $A_{net}$ was 5.8 cm$^{-2}$ in E1 and 36 cm$^{-2}$ in E2. In E1, 1131 ind m$^{-2}$ were observed within a 35 m depth range, in E2 102 ind m$^{-2}$. No active feeding was observed in E1 and E2 on the UVP5 images, but particle abundances were very low. Deployed feeding nets could be observed from PELAGIOS video clips, but they were very hard to identify due to the low particle abundance. In a careful estimation, mucus nets were visible in about 40% of

the *Poeobius* sp. on these video clips. No net shapes could be identified, only strands of mucus with attached particles that moved relative to the camera in the same way as the polychaete. Extended tentacles were visible in more than 80% of the polychaetes, indicating that the counting of mucus nets alone may underestimate the actual proportion of feeding *Poeobius* sp.

Assuming optimal horizontal alignment of mucus nets, a fraction of 40% actively feeding *Poeobius* sp. under an area of 1 m² could potentially cover an area $\partial$ of 0.26 m² in E1 and of 0.15 m² in E2. When accounting for the bad visibility of mucus nets in low particle concentrations and assuming active feeding in all individuals, this would result in a coverage $\partial$ of 0.65 m² in E1 and a $\partial$ of 0.37 m² in E2. Thus, *Poeobius* sp. could remove 65% and 37%, respectively, of the flux below 1 m² in E1 and E2.

## 3.3  Comparison between UVP5 and PELAGIOS

### 3.3.1  Relationship between counts of the different instruments

*Poeobius* sp. was well identifiable with both UVP5 and PELAGIOS and therefore was taken as model organism for comparing the two systems and identifying relationships between their results. These relationships were used to verify the applicability of the UVP5 for the description of distribution patterns of organisms of very low concentrations, such as *Poeobius* sp. The dimensions of the UVP5 field of view is 22 x 18 cm (Picheral *et al.* 2010). A continuous recording along a 10 minute (309 m with a towing speed of 1 knot = 0.5144 m s⁻¹) transect would result in a sampled volume of 12.22 m³. The actually recorded volume on a 10 minute transect, derived from the mean volume recorded per second (0.0085 m³ s⁻¹), was only 5.1 m³, though, *i.e.* the UVP5 recorded only about 40% of the volume (and the zooplankton) that was passed by the instrument. This implies, that the measured volumes has to be multiplied with a factor of 2.4 in order to calculate the total volume that was passed by the instrument.

A linear model showed a highly significant (linear regression: $p < 0.001$) relationship between the counts of the UVP5 and PELAGIOS (Figure 22). The slope of about 0.05 was used to calculate the volume of the not-quantitative PELAGIOS from the quantitative UVP5: The known volume recorded by the UVP5 (*UVP*$_{vol}$) divided by the slope of the linear regression (*slope*) results in an approximate volume sampled by PELAGIOS. PELAGIOS records continuously, therefore, the volume derived from the UVP5 volume and the slope was multiplied with a correction factor (*UVP*$_{corr}$) to account for the missed volume.

$$Pelagios\_vol = (\frac{UVP_{vol}}{slope}) * UVP\_corr \qquad (10)$$

The mean recorded volume of 0.0085 m$^3$ s$^{-1}$ by the UVP5 divided by a slope of 0.05 and multiplied with a correction factor of 2.4 resulted in an approximate volume of 0.41 m$^3$ s$^{-1}$ recorded by PELAGIOS. With a towing speed of 1 knot (= 0.5144 m s$^{-1}$), a cross-sectional view field of 0.8 m$^2$ of PELAGIOS can be expected.
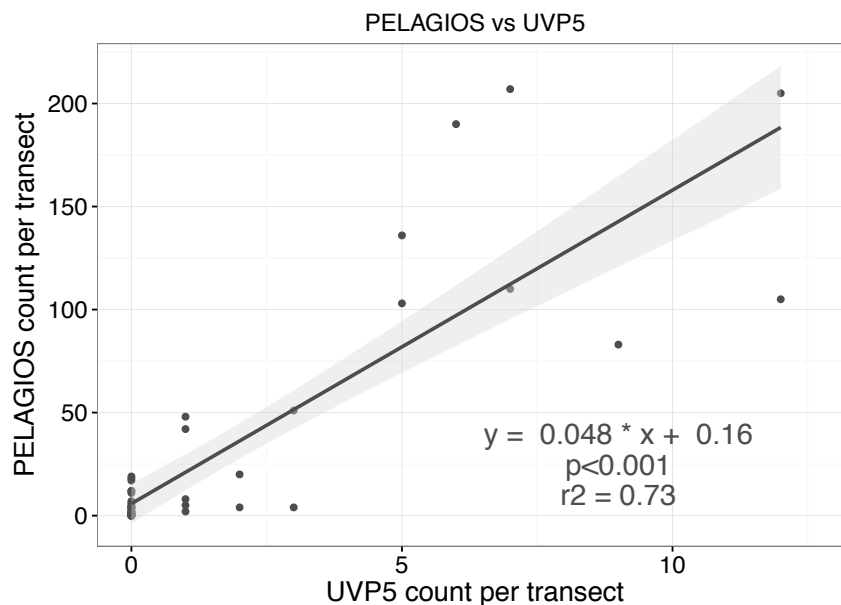


Figure 22: Counts of *Poeobius* sp. from PELAGIOS video plotted against UVP5 counts on the same transects at two stations on cruise MSM49. A linear model was fitted comparing the counts of the two instruments.

### 3.3.2 Additional observations from PELAGIOS videos

I had a look into short sequences of the video from E2, where high abundances of *Poeobius* sp. were found in co-occurrence with low particle concentrations. In contrast to the UVP5 results described above, feeding behaviour could be observed in the video: since only a few particles were stuck to them, it was difficult to identify mucus nets, but at a closer look they were present and sometimes even single strands of mucus could be seen. In some parts of the video it seemed like most particles were somehow connected to each other and to the worms. The short clipping also emphasized the dominance of *Poeobius* sp. in that layer. Other organisms, like crustaceans and other gelatinous organisms such as siphonophores and medusae were also present, but in comparably low numbers. For example, in a 50 second video clip I roughly counted 17 larger crustaceans (euphausiids, decapods and copepods), but at least 100 *Poeobius* sp. In the complete video from the 100 m transect, a total of 3600 Poeobius sp. were estimated compared to in total 120 individuals from other zooplankton taxa (H.J. Hoving, unpublished data).

# 4 Discussion

We discovered very high abundances of the holopelagic polychaete *Poeobius* sp. in a mesoscale eddy in the tropical Atlantic, in combination with the lowest recorded particle concentration for that region. This observation of an - until today - for the Atlantic undescribed species which dominated in such a specific environment was the impulse for this study. The aim was to assess the distribution of *Poeobius* sp. in the tropical Atlantic, as well as to detect a possible eddy association and evaluate implications on the biogeochemistry of mesoscale eddies. Image and particle data from the Underwater Vision Profiler (UVP5) were used, supplemented by a few observations from videos of the towed pelagic *in situ* observation system (PELAGIOS).

## 4.1 Advantages and disadvantages of the UVP5 and PELAGIOS

Conventional net sampling was shown to undersample gelatinous zooplankton (Hamner *et al.* 1975; Remsen *et al.* 2004; Robison 2004) due to destroying the fragile organisms (Robison 2004) and underestimating their biovolume due to shrinkage in formalin preserved specimens (Steedmann 1976). Net samples have the advantage that identification to species level is possible in the most cases, but this is not the case for gelatinous organisms. Advances in optical methods like the development of the Optical Plankton Counter, OPC (Herman 1992), the Shadowed Image Particle Profiling and Evaluation Recorder, SIPPER (Samson *et al.* 2001; Remsen *et al.* 2004) and the Video Plankton Recorder, VPR (Davis *et al.* 1992a) improved continuous zooplankton distribution assessment, but either recorded in a very low taxonomic resolution (OPC) or only a very small volume (SIPPER, Samson *et al.* 2001; Remsen *et al.* 2004; Broughton and Lough 2006).

The UVP5 provides quantitative data of particles and mesozooplankton (Picheral *et al.* 2010) at a high spatio-temporal resolution. Automatic image processing and semi-automatic identification by image recognition algorithms enable a quick data analysis. Nevertheless, although its scanned volume is larger than that of the VPR or SIPPER, it is still small (about 6 $m^3$ on a 600 m vertical cast) compared to most nets and due to this possibly misses rare species. The UVP5 does not record continuously, thereby missing almost 60% of the passed water volume. This is accounted for by the volume-specific abundances but has to be kept in mind when count data are used. It indicates that the distribution of *Poeobius* sp. may be underestimated by data from vertical UVP5 casts. Also, the taxonomic resolution is low (although higher than with

the OPC), and avoidance of the lights by organisms may impede quantitative zooplankton assessments.

PELAGIOS is a towed video camera that is particularly useful for observations of slowly moving gelatinous fauna. It has a larger field of view than the UVP5 and thus records a bigger volume and makes the detection of rare species more probable. It is also suitable for the observation of behaviour, for example for describing feeding, mating or escape behaviour. The comparison between the feeding information from the UVP5 with PELAGIOS video observations revealed that, especially in low particle concentrations, the UVP5 misses substantial information. PELAGIOS is not a quantitative system because the size and depth of the field of view is unknown.

The linear relationship between counts of the non-moving *Poeobius* sp. with UVP5 and PELAGIOS indicates comparability of the two different methods and that the volume recorded by PELAGIOS is about 50 times larger than that of the UVP5. It has to be kept in mind, though, that by contrast to the UVP5, PELAGIOS counts did not start directly when transect depth was reached. This was not accounted for here and might shift the results to a higher slope. So although the linear model provides an estimate of count relation, this is probably inaccurate and different methods should be applied for calibrating PELAGIOS volumes.

The combination of the two instruments provides a great opportunity to assess both the mesopelagic fauna and particles (UVP5) and larger macrozooplankton (PELAGIOS). This non-destructive tool combination is advantageous to net catches especially for fragile gelatinous animals. Fast moving, robust organisms and those that avoid the camera lights are probably better caught with nets, although net avoidance is also a known problem (Fleminger and Clutter 1965). In comparison to remotely operated vehicles (ROVs), the towed PELAGIOS/UVP5 combination has the advantage that it is silent and organisms do not get disturbed by engine noise or pumps and can be observed in their natural behaviour.

The comparability of the UVP5 and PELAGIOS suggested that the UVP5 was an appropriate tool for assessing the distribution of *Poeobius* sp. in the tropical Atlantic.

## 4.2   *Poeobius* sp. distribution in the tropical Atlantic

### 4.2.1   Horizontal and vertical distribution and relation to water masses

*Poeobius* sp. was found at sampling stations across the tropical Atlantic and at all depths between 22 m and 997 m with highest numbers of occurrence shallower than 100 m. In the present study, abundances and standing stocks of *Poeobius* sp. with

maxima of 309 ind m$^{-2}$ at non-eddy and more than 6000 ind m$^{-2}$ at eddy stations were considerably larger than those published from the Pacific Ocean. McGowan (1960) found highest standing stocks of around 4 ind m$^{-2}$. In the depth layer where Robison (2010) detected dominance of *Poeobius meseres* associated with a decrease in particle concentration, a maximum abundance of around 0.3 ind m$^{-3}$ was identified for a 100 m depth layer. In the Atlantic Ocean, the maximum abundance was 40 ind m$^{-3}$ in a 100 m depth layer with a peak abundance of 342 ind m$^{-3}$ in a 5 m depth bin. Integrated abundances over the water column were smaller than abundances of, for example, copepods (Schnack-Schiel *et al.* 2010), but locally in mesoscale eddies, the abundance was comparably high and in certain depth layers *Poeobius* sp. dominated the zooplankton composition.

The results of the general linear mixed model suggest that the depth distribution of *Poeobius* sp. was most impacted by eddy conditions and oxygen concentration, with these two factors interacting. This model might be inaccurate because the selected error distribution - although the one with the best fit - did not fit very high or low values. The application of model selection is debated (Bolker *et al.* 2009) and there are possibly ways to better evaluate this data set by the use of Akaike Information Criterion (AIC) or Markov chain Monte Carlo (MCMC) procedures (Bolker *et al.* 2009). Nevertheless, the methodology used here should provide sufficient indications on the main factors driving the depth distribution of *Poeobius* sp.

All *Poeobius* sp. occurred below the mixed layer. As the worm is a flux feeder that is feeding with a fragile mucus net (Uttal and Buck 1996), it might be avoiding the surface turbulences that could damage its net, as also hypothesized for pteropods (Mackas *et al.* 2005). No specimens were observed below 1000 m depth, although 70% of the casts were lowered to more than 1000 m depth and 25% of the casts went deeper than 2000 m. A reason for this pattern may be that *Poeobius* sp. requires a certain particle concentration - or rather flux - to survive. Only two individuals were observed at particle concentrations below 20 L$^{-1}$ in non-eddy profiles, which corresponds to the median particle abundance in the depth layer below 1000 m.

The relation of occurrences to water masses shows that *Poeobius* sp. is distributed across the North Atlantic and South Atlantic Central waters, with observations reaching into the upper limit of the Antarctic Intermediate water, but staying above a temperature of 5°C. Single *Poeobius* sp. were observed at temperatures higher than 20°C. This is in sharp contrast to what has been described for the Pacific congener *Poeobius meseres* by McGowan (1960), who found *Poeobius meseres* almost exclusively in the Pacific Subarctic water mass with temperatures below 5°C. It was noted, however, that the distribution did not necessarily reflect the physiological

boundaries of the species, but might also be a result of the higher food availability in that water mass (McGowan 1960). Specimens observed in Monterey Bay also occurred in water temperatures higher than 5°C (Robison *et al.* 2010, DSG 2016). The difference in preferred water mass properties may be an indication that the *Poeobius* sp. found in the Atlantic belong to a different species.

### 4.2.2   Reasons for the recent discovery

Despite its broad distribution, *Poeobius* sp. has never been described in the Atlantic Ocean. There are probably three reasons for this:

1. Due to the very fragile nature and small size of *Poeobius* sp., these worms probably get destroyed in net samples with high throughput and unprotected cod-ends, especially in towed nets with rather large mesh size. On cruise MSM49, at the same stations that were sampled with the UVP5, different nets were deployed (MOCNESS 1 m$^2$ with 333 $\mu$m and 2000 $\mu$m mesh size, MOCNESS 10 m$^2$ / 1500 $\mu$m, WP3 / 200 $\mu$m). While in the UVP5 images 136 animals were found throughout the cruise, only 2 specimens were caught with the WP3 and none with any of the other nets (unpublished data).

2. No one knew what to look for: Most net samples taken at sea are directly preserved and analysed back ashore. Once in formalin or ethanol, the gelatinous worms shrink (Steedmann 1976) and loose their colour. They are a hard-to-identify gelatinous mass that is also damaged in most cases (Figure 23). The identification of such samples is often reduced to categorizing them as some kind of gelatinous zooplankton. Looking back into MultiNet® (type 'midi, net opening 0.25 m$^2$, 200 $\mu$m mesh size) samples from the M105 eddy revealed that 14 specimens were caught at the core station (example in Figure 23).

3. Although *Poeobius* sp. is widely distributed in the tropical Atlantic, in most UVP5 profiles none or only one worm could be identified. If it were not for the deployment of PELAGIOS and the outstanding abundances and dominance in the mesoscale eddies on cruises M116 and M119, *Poeobius* sp. in the Atlantic would still fall into a summarising category of unidentified gelatinous zooplankton. In the Pacific Ocean, zooplankton sampling was also based on nets in the first half of the last century (McGowan 1960). Abundances were low as well, but *Poeobius* sp. was discovered there already in 1930. I cannot rule out later introduction of *Poeobius* sp. into the Atlantic, but I think that the discovery in the Pacific is merely due to a very attentive zoologist who forwarded the unknown animals to Harold Heath for identification (Heath 1930).
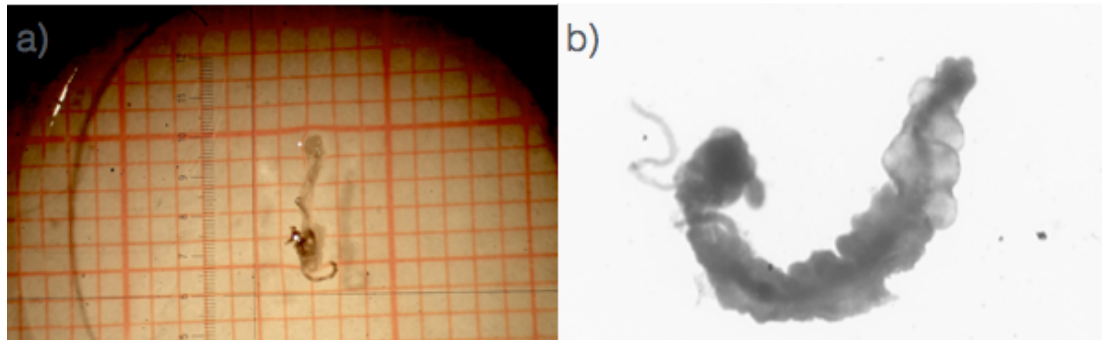
Figure 23: Examples of preserved specimens of *Poeobius* sp. a) an ethanol preserved *Poeobius meseres* caught in Monterey Bay; b) a scanned specimen of proposed Atlantic *Poeobius* sp. after formalin-fixation, caught in the M105 eddy with a 200 *μ*m MultiNet®.

## 4.3 Comparison of the Atlantic *Poeobius* sp. with *P. meseres*

The polychaete that we found in the Atlantic Ocean and that is described in this thesis was visually identified to be *Poeobius* sp. by Dr. Henk-Jan Hoving (GEOMAR), Dr. Bruce Robison (MBARI) and Dr. Karen Osborn (Smithsonian Institution), but genetic analysis was not finished at the time of this writing. Thus, the taxonomic relation to *Poeobius meseres* is not yet known. Table 8 shows a comparison of some characteristics of *Poeobius meseres* and the polychaete described in this thesis. The Atlantic *Poeobius* sp. resembles the described *Poeobius meseres* in size and morphology, as well as in the observed feeding behaviour. Nevertheless, there are also differences that indicate that we could be dealing with a different species: The depth distribution is shallower in the Atlantic (DSG 2016). The worms differ partly in posture, *Poeobius meseres* was only observed straight (Dr. B. Robison, MBARI, personal communication), whereas the Atlantic *Poeobius sp.* was often slightly bent. In the Pacific, *Poeobius meseres* was observed actively swimming (Dr. B. Robison, MBARI, personal communication), whereas in PELAGIOS videos from the Atlantic all specimens appeared passively drifting only.

Table 8: Comparison of the Atlantic *Poeobius* sp. investigated in this thesis to the Pacific *Poeobius meseres*.

| Observation | Atlantic *Poeobius* sp. | *Poeobius meseres* |
|---|---|---|
| **Size** | 2.7 - 23.5 mm [1] | 5 - 27 mm [2] |
| **Depth distribution** | 22.7 - 997.5 m [1] | 175 -3575 m [3] |
| **Feeding** | Mucus nets, tentacles [1] | Mucus nets, tentacles [4] |
| **Body posture** | Sometimes bent [1] | Always straight [5] |
| **Active swimming** | No [1] | Yes [5] |

[1] This study; [2] (Heath 1930); [3] DSG (2016); [4] (Uttal and Buck 1996); [5] Dr. B. Robison, MBARI, personal communication.

## 4.4 Eddy association of *Poeobius* sp.

### 4.4.1 *Poeobius* sp. abundance in eddies

The results show that *Poeobius* sp. abundance and depth distribution are impacted by mesoscale eddies, especially anticyclonic modewater eddies (ACMEs), in the tropical Atlantic Ocean. The comparison of data from the upper 600 m of eddy and non-eddy profiles revealed significantly higher standing stocks at ACME and cyclone (CE) stations than at those in non-eddy conditions. Only two individuals were found in anticyclones. Enhanced abundances in ACMEs and CEs can be the result of physical aggregation, increased reproduction, or a combination of both. I suggest that a combination of both is the most likely, and propose two possible mechanisms:

*Inclusion of a seed population during formation:*

Most eddies that are formed in the eastern tropical North Atlantic originate at the shelf off Cape Blanc (Mauretania), and from there propagate to the west at about 2.8 km d$^{-1}$ (Schütte *et al.* 2016a). A small seed population could get enclosed in the eddy water mass during its formation, find suitable growth and reproduction conditions and reproduce in the water mass. This fact, in combination with the theory that *Poeobius* sp. abundance are the result of a reproducing seed population, would suggest that there are more *Poeobius* sp. to be found at shelf stations than in the open ocean. This hypothesis could be rejected with the available data from the Mauritanian shelf, where no *Poeobius* sp. were found, but the sample size at shelf stations was very small. The two ACMEs with the highest *Poeobius* sp. abundance probably did not form at the shelf; The existence of these eddies does not fit the theory that no eddies are generated or can be pertained between 10°N and 10°S due to the low Coriolis force at those latitudes (Chelton *et al.* 2003). So the high abundances in these two eddies are most likely not the result of an enclosed seed population from the shelf.

*Inclusion through physical forcing*

The most probable explanation is that the animals enter the eddy due to physical forcing: Cyclones and ACMEs are characterized by an upwelling of water masses in the eddy interior (McGillicuddy *et al.* 2007; Karstensen *et al.* 2016; Schütte *et al.* 2016a). Mesopelagic fauna could be flushed into the eddy through this upwelling and kept there by the retention of the water at the surface and the isolation of the eddy core (Karstensen *et al.* 2016). These processes have already been described: Eddies are known to transport coastal species into the open ocean (Mackas and

Galbraith 2002; Mackas *et al.* 2005; Tsurumi *et al.* 2005; Waite *et al.* 2015), but also to take up open ocean fauna on the way (Mackas and Galbraith 2002).

This mechanism would increase the encounter rate for otherwise highly dispersed, rare species, and the ability for them to reproduce. The schematic in Figure 24 attempts to explain these processes. Tsurumi et al (2005) described growth of pteropods in mesoscale eddies in the Alaska gyre but did not have evidence of reproduction. Deibel *et al.* (1985) reported sexual and asexual reproduction of doliolids in Gulf Stream cold-core remnants with extremely high abundances but short duration. No size difference was detected between *Poeobius* sp. that were sampled in the same eddy about half a month apart during cruises ISL00314 and M105, but this might be due to the short time span in-between and also due to low *Poeobius* sp. numbers, *i.e.* low sample sizes at both times.
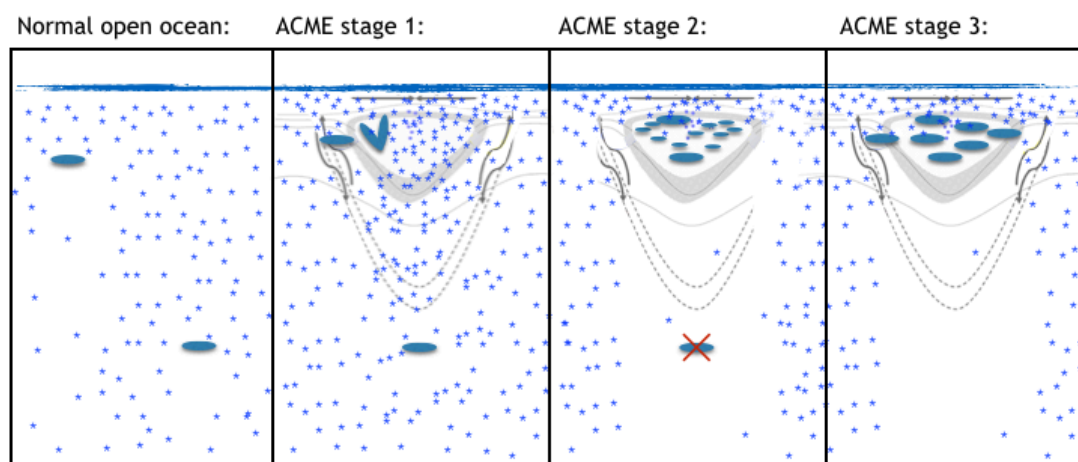


Figure 24: Schematic illustrating the potential processes in the lifetime of an ACME with the stars representing particles and the ovals representing *Poeobius* sp. a) Normal open ocean conditions: *Poeobius* sp. live anywhere in the water column in low abundances. b) *Poeobius* sp. get introduced into an ACME core by upwelling processes - particle production is enhanced due to nutrient input by the same mechanisms and by doming of the upper isopycnal. Optimal feeding conditions and higher encounter rates facilitate reproduction of the polychaete. c) Juvenile *Poeobius* sp. compete for sinking particles - they aggregate close to the mixed layer. Export flux is reduced and individuals at lower depths starve. d) Grown up *Poeobius* sp. deplete the particle flux in the ACME until the eddy dissolves. Modified from Karstensen *et al.* (2016).

We observed ACMEs at the same position on the cruises M116 (E1) and M119 (E2). It was not possible to verify that the two eddies were the same, only in different developmental stages; therefore I will treat them as independent features in the following sections. In both E1 and E2, high abundances of *Poeobius* sp. were found. In E1 the animals were significantly smaller than in E2, where some *Poeobius* sp. were observed very close together, which could probably be attributed to mating behaviour (Dr. H.J. Hoving, GEOMAR, personal communication). The high abundances in E1 could be the result of recent reproduction of the seed population at an earlier stage of the eddy. E2 might be a representative of an older eddy stage with

grown up *Poeobius* sp. Unfortunately, it was not possible to detect the age of the respective eddies or to track them on satellite images (Dr. F. Schütte, GEOMAR, personal communication).

The 'pickup' mechanism by mesoscale eddies also provides an opportunity for rare species to spread as they get released in another area of the ocean than the one they were captured from when the eddy dissolves. A linear relationship between *Poeobius* sp. length and longitude with larger individuals further west, supports this theory of eddies serving as transport vectors. Also, the largest individuals of *Poeobius* sp. were observed in shallow non-eddy waters. These may be adult *Poeobius* sp. that were released from dissolving eddies, but it was not possible to identify whether the locations where these worms were found had recently been passed by an eddy.

*Further factors supporting high* Poeobius *sp. abundance in eddies*

Cyclonic eddies and ACMEs often show increased primary productivity due to upwelling nutrients (McGillicuddy *et al.* 1998; McGillicuddy *et al.* 2007; Löscher *et al.* 2015; Romero *et al.* 2016) and enhanced particle fluxes (Waite *et al.* 2015; Fiedler *et al.* 2016; Fischer *et al.* 2016; Hauss *et al.* 2016). The increased primary production and particle production lead to increased remineralisation rates just below the mixed layer, resulting in oxygen loss and suboxic to nearly anoxic conditions (Karstensen *et al.* 2015; Fiedler *et al.* 2016; Hauss *et al.* 2016; Schütte *et al.* 2016c). Both the increased particle flux and the reduced oxygen concentrations may benefit *Poeobius* sp. and may lead to an advantage over other zooplankton and enhanced abundances in the eddy.

Pteropods are also flux feeders and should benefit from high particle flux. Pteropods were shown to be introduced into eddies in the Pacific Ocean (Tsurumi *et al.* 2005), but no pteropods were found on the images of the UVP5 in E1 and E2 and in the PELAGIOS video. A possible reason is that pteropods have a high metabolism of 28.8 - 86.4 $\mu$mol g$^{-1}$ d$^{-1}$ (Maas *et al.* 2012) compared with a respiration rate 0.068 $\mu$mol O$_2$ g$^{-1}$ d$^{-1}$ reported for *Poeobius* sp.'s congener *Poeobius meseres* (Thuesen and Childress 1993)) and are possibly affected by the low oxygen concentrations in the eddy core. A reduction of metabolism in low oxygen environments has been shown for migratory pteropod species in the Pacific ocean (Maas *et al.* 2012), but the authors concluded that this suppression revealed their inability to "meet their metabolic needs without metabolic suppression at oxygen concentrations lower than 30 $\mu$mol kg$^{-1}$". This supports the hypothesis that pteropods cannot permanently stay in the hypoxic core that was found in most ACMEs of this study.

*Poeobius* sp. occurred at the minimum oxygen concentration of 3.77 $\mu$mol kg$^{-1}$ in the eddy sampled during cruise M105. Also in the other ACMEs, *Poeobius* sp. was especially abundant in the eddy cores and dominated the zooplankton community in layers of low oxygen concentrations in at least two of those eddies. Thuesen and Childress (1993) measured very low metabolic rates for *Poeobius meseres* in contrast to other pelagic polychaetes. This seems to enable them to live in the hypoxic to nearly anoxic environment of the ACME cores. Increased abundances may also be a result of the exclusion of oxygen demanding predators. However the metabolic rates from Thuesen and Childress (1993) have to be handled with caution, because i) the measurements were done with *Poeobius meseres*, probably a different species than the Atlantic Ocean *Poeobius* sp., ii) the rates represent resting metabolism and underestimate respiration while feeding and iii) the measurements were done at 5°C - all *Poeobius* sp. observed in the Atlantic were found at warmer temperatures, suggesting higher metabolic rates.

### 4.4.2    *Poeobius* sp. depth distribution in eddies

Only one *Poeobius* sp. was found deeper than 200 m in the ACMEs of this study, whereas at the non-eddy stations and in other eddy types the polychaetes were found anywhere between the surface and 1000 m depth, with 61% of the observations below 200 m. Jackson (1993) described different feeding strategies of flux feeders and resulting clearing efficiency in the water column in dependence of their abundance: If the abundance of flux-feeders is high, the total cross-sectional area of mucus nets $\sum_{netarea}$ is also high, and the flux removal due to feeding leaves only a small fraction of the surface flux settling into deeper layers. So a high $\sum_{netarea}$ leads to a strategy where flux-feeders gather directly below their food source, *i.e.* below the particle maximum in the lower mixed layer, in order to maximise their food uptake. In contrast, when only single flux feeders are present, *i.e.* $\sum_{netarea}$ is low, the flux is more or less constant over depth, and there is no reason to compete for space in a certain depth layer. Jackson (1993) proposes that a uniform distribution over depth of a rare species might make it less vulnerable to predation.

These strategies can be an explanation for the depth distributions found in this thesis: In the ACMEs, high abundances of *Poeobius* sp. were found in combination with very low particle fluxes in the eddy core and below (see next section), especially in E1 and E2. Hence, the animals aggregate close to the mixed layer in order to increase their probability to catch particles. In the non-eddy profiles, where only one or two *Poeobius* sp. were found, the depth distribution is not restricted to the upper 200 m; competition about sinking particles is lower. Another possible mechanism is that the polychaetes are caught in the isolated eddy core and cannot escape shallow depths.

### 4.4.3    Differences between the eddy types

The data show different effects of ACMEs and cyclones or anticyclones on *Poeobius* sp. abundance and distribution. Abundances of *Poeobius* sp. higher than in non-eddy conditions were observed only in the ACMEs sampled on the cruises M97, M105/ISL, M116 (E1) and M119 (E2). Temperature and salinity anomalies are more strongly developed in ACMEs than in the other eddy types and these comparatively rare features (ACMEs make up only 9% of the eddies generated in the ETNA per year; Schütte *et al.* 2016a) have been described to be extraordinary in productivity compared to normal conditions and also to cyclones (McGillicuddy *et al.* 2007). ACMEs can maintain high productivity over long timescales, whereas cyclones have been reported to have only 'ephemeral' bloom conditions (McGillicuddy *et al.* 2007).

Mean abundances in CEs were also higher than at non-eddy stations, but the effect was only small in the UVP5 data. An extensive sampling of a CE was done with PELAGIOS during cruise MSM49. This revealed significantly higher abundances of *Poeobius* sp. in the eddy compared with the reference station (H.J. Hoving, unpublished data). These findings suggest an accumulation effect also in CEs, which is probably not visible in the vertical UVP5 casts due to the low sampled volume.

Only two specimens of *Poeobius* sp. were recorded in normal anticyclones. Due to downward bent isopycnals (*e.g.* McGillicuddy *et al.* 2007), primary productivity (and particle flux) in this eddy type is low and probably does not provide enough resources to support reproduction or the maintenance of larger standing stocks of flux-feeders in this environment.

Most cyclones and all anticyclones were detected in retrospect, in contrast to all ACMEs, which were verified by CTD and ADCP data during the cruises. As the sea surface anomaly (SLA) data, on which the algorithm for eddy identification is mainly based, have a resolution of only 30 km (Florian Schütte, personal communication), the allocation of eddies is possibly imprecise. Anticyclonic modewater eddies only have a weak surface signature and are possibly underestimated from SLA data. On the other hand, the algorithm may detect CEs and ACs that are weak in comparison with those eddies that have been identified during cruises due to their strong characteristics. A possible positive effect of eddies on *Poeobius* sp. abundance may only be visible in strongly developed features.

## 4.5    Implications on the biogeochemistry of mesoscale eddies

Mesoscale eddies can be seen as natural mesocosms as they isolate water masses for up to several months (Schütte *et al.* 2016b). Processes in these features differ from

those outside the eddy, including the biological carbon pump working at a different pace (Romero *et al.* 2016). Processes are changing over the development of the eddy: Nutrient injections through upwelling of deeper waters and following peaks in primary productivity, flux and respiration (resulting in suboxic core oxygen concentrations) can be observed especially in early-stage eddies (McGillicuddy *et al.* 2007; Buesseler *et al.* 2008), whereas later stages often have normal to low fluxes (Sweeney *et al.* 2003; McGillicuddy *et al.* 2007; Buesseler *et al.* 2008). Remineralisation (Fiedler *et al.* 2016) in combination with the isolation of the eddy core and the creation of a stability maximum around it (Karstensen *et al.* 2016) may explain the low oxygen concentrations in older eddies with no longer significantly elevated flux.

### 4.5.1 Influence of flux-feeders on particle flux

Stemman *et al.* (2004) showed that the effect of mesozooplankton on particle fluxes at depths shallower than 500 m is more important than microbial degradation; below that depth microbial processes dominate. Deibel *et al.* (1985) described that strong blooms of filter-feeding salps affected particle flux by a repackaging of small, slowly sinking particles into larger fecal pellets. Still, filter feeding is proposed not to be fast enough to remove large particles because of the high sinking speeds in large size classes (2004). Flux-feeding with mucus nets on the other hand provides the possibility to catch also fast sinking (large) particles and thus reducing their flux into the deep ocean (Jackson 1993; Iversen *et al.* 2010). Flux-feeding might be an explanation for the change in particle flux of mesoscale eddies (Buesseler *et al.* 2008).

The role of gelatinous zooplankton other than salps as mediator in particle fluxes is poorly understood. Uttal and Buck (1996) were the first to investigate the diet of the gelatinous midwater species *Poeobius meseres*, and calculated that a single organism of this species can consume up to 0.002% of the daily primary production under 1 m² in Monterey Bay. The same species has been shown to significantly reduce the particle concentration in the deep sea of Monterey Bay (Robison *et al.* 2010). In one of the ACME profiles in the tropical Atlantic, *Poeobius* sp. coincided with strongly reduced fluxes into the deep ocean. This suggests an impact of *Poeobius* sp. on particle flux in these features similar to the observations in the Pacific.

### 4.5.2 Patterns in eddies with high *Poeobius* sp. abundances

Standing stocks of *Poeobius* sp. in the Atlantic Ocean obtained from the UVP5 data were generally low and even in most eddy profiles the numbers were not high enough for statistical analysis. For this reason, the results dealing with the biogeochemical impact of *Poeobius* sp. concentrate on the ACMEs on M116 (E1) and

M119 (E2), where comparatively high numbers of the animal could be obtained. Another advantage of these eddies for the analysis was that a good background dataset of the 23°W transect was available due to regular sampling (at least once a year) since 2012.

*Strong reduction of particle abundance*

Particle abundance was markedly reduced in E1 and E2, compared to the background situation at the 8°N 23°W site and to the 23°W transect between 7°N and 12°N. In E2, particle abundance was reduced to one of the lowest recorded in that region. The particle low was less pronounced in E1. A reason for the difference between the particle signatures of the two eddies may be different developmental stages of the features, but no data were available for the identification of the eddy age. *Poeobius* sp. sizes were significantly different in the two features suggesting that E1 was older than E2. The difference in particle reduction may be a result of *Poeobius* sp. standing stocks and the different sizes of the polychaetes.

*Change of particle size distribution*

The general pattern of particle abundance-size and particle volume-size spectra was comparable to those observed by Iversen *et al.* (2010) off Cape Blanc, Mauritania with higher numbers of small particles but higher integrated volume of large particles. Deibel *et al.* (1985) reported a decrease in slope of the particle-volume spectrum as a consequence of a doliolid bloom in the Sargasso Sea, *i.e.* a stronger decrease of small particles by the filter feeders. In my data, the particle size distributions differed between the eddies and the respective background conditions, but the difference was not always significant. In E1, small particles were more strongly reduced, in E2 large particles. In E2, particles of sizes larger than 1.1 mm were completely depleted in the layer below which *Poeobius* sp. were observed. As larger particles (according to Stokes Law) have a higher sinking speed and thus higher flux, this may explain why fluxes in the deeper layers of E2 were very low, but similar to the background in E1. However, surface fluxes were also different in the two eddies (lower than median background in E2, higher than median background in E1).

The small size of *Poeobius* sp. in E1 could explain their effect on the size of the exported particles: The mean size of particles was higher than in the background, possibly because small *Poeobius* sp. - although capable of catching those particles - are either not able to consume very large particles (above their own size) or they need more time for this process and thus utilize only a fraction of the large particles.

In E2, the abundance of particles in all size classes was reduced. The slope of the particle abundance-spectrum was significantly different between the eddy surface layer and the depth layer where *Poeobius* sp. occurred, indicating a stronger reduction of larger particles. This fits to the theory that the impact of flux-feeders is larger on big than on small particles, because the latter have a lower sinking speed and can get replenished more easily by horizontal advection (McCAVE 1975). Advection might also explain the increase of total particle concentrations and fluxes below 200 m in E1 and E2.

*Reduction of particle flux*

Fiedler *et al.* (2016) reported fluxes of 0.19-0.23 g C m$^{-2}$ d$^{-1}$ at 100 m depth in the ACME that was sampled during M105 and ISL00314. My calculations for the same eddy resulted in a difference by a factor of about 10 (Appendix). This may be due to different methodology as Fiedler *et al.* (2016) used apparent oxygen utilisation rates (aOUR). I used particles between 0.14 and 2.66 mm for the flux calculations. The inclusion of larger particles could increase the calculated value. Although I could not find any mistakes in my calculations this should be checked again for a resulting publication.

The deviation in absolute values from the literature has no impact on the observed signal, which showed a strong flux reduction by more than 90% from the particle maxima in E1 and E2. Very high fluxes were observed in the upper 100 m in E1, whereas in E2 the flux was below the background flux at any depth shallower than 500 m. Flux was reduced to the lowest recorded values of the dataset used in this thesis in E2.

*Impact on remineralisation and oxygen consumption*

A strong flux reduction is an indicator for high remineralisation in the respective layer, *i.e.* that only a small part of the incoming material is exported. This remineralisation can occur through microbial remineralisation and by particle grazing animals, such as *Poeobius* sp. High remineralisation also means high respiration. Decreases of particle flux were strongest in E1, compared to E2 and the background signal at 8°N 23°W. The oxygen concentration in E1 was one of the lowest measured in that region (Dr. S. Schmidtko, GEOMAR, personal communication). High *Poeobius* sp. abundances indicate that these polychaetes may have played a substantial role in the particle remineralisation and the resulting flux reduction and oxygen depletion. However, it may also be possible that *Poeobius* sp. actually rather repackaged the particles into very dense, large fecal pellets that might

not be well resolved with the UVP5. This would lead to increased carbon export and thus lower oxygen consumption. We have no evidence for this since no data are available on *Poeobius* sp. fecal pellet production.

### 4.5.3    Relation of *Poeobius* sp. to the observed particle patterns

The flux reduction occurred just below the mixed layer. There, other zooplankton and microbes may also contribute strongly to the consumption of particles. Here I show different approaches to relate the observed patterns to *Poeobius* sp. abundance.

*Changes in* Poeobius *sp. abundance and particle concentration from horizontal tows*

The horizontal tows of the UVP5 provide a possibility to analyse the *Poeobius* sp.-particle relation without any depth interference. In the M119 eddy (E2), a marked increase in particles with decreasing *Poeobius* sp. numbers could be identified at around 100 m depth where the most significant drop in particles could be seen also in the vertical profile. In PELAGIOS video of the same transect, *Poeobius* sp. made up more than 90% of the total zooplankton (H.J. Hoving, unpublished data). On the other hand, a transect at 50 m depth in the same eddy revealed no impact of increasing *Poeobius* sp. abundance on particle concentration, but this may be due to the fact that this was directly below the particle maximum and therefore the supply of particles was high. The horizontal change in particle concentration and *Poeobius* sp. abundance also points out the patchiness of the distribution of this polychaete. This indicates that also the flux reduction may be a small-scale process, dependent on the patchiness of *Poeobius* sp. abundance, which should not be directly extrapolated on the total area of an eddy.

*Other particle-feeders*

*Poeobius* sp. is not the only zooplankton species feeding on particles and if we assume that the high *Poeobius* sp. abundances are the results of physical transport into the eddy by upwelling, this mechanism should also work with other planktonic species. However, *Poeobius* sp. contributed up to more than 50% to the total zooplankton in E1, and in E2 even up to 100% at the depth where particle concentrations decreased. Some components of the zooplankton, such as copepods, may be underestimated here, because these avoid the camera lights (Dr. R. Kiko, GEOMAR, personal communication). In the PELAGIOS video, *Poeobius* sp. also made up more than 90% of the zooplankton in E2 (Dr. H.J. Hoving, GEOMAR, unpublished data). For this reason I suggest *Poeobius* sp. as one main factor for particle removal in these two eddies. Rhizaria are another group that might play a major role in particle

consumption. These unicellular protists are well resolved with the UVP5 and made up a considerable (yet smaller than *Poeobius* sp.*)* fraction of the zooplankton in E1. A detailed analysis of these organisms should be included in the assessment of zooplankton communities that are influenced by eddy conditions.

The UVP5 recorded not a single animal between about 120 and 300 m in the day and night vertical casts performed in E2 in about 50 km distance. This proposes that the layers below *Poeobius* sp. were not only depleted of particles but also depleted of life, which could indicate that the strong removal of particle flux also has an impact on other parts of the zooplankton community in depths below 120 m. However this lack of zooplankton could also be seen in several other UVP5 profiles in day and night profiles in non-eddy conditions and in different eddies. So the particle depletion by *Poeobius* sp. might play a role in the creation of this 'dead zone', but it might also be a result of generally low zooplankton abundances at those depths and the small volume recorded by the UVP5.

*Carbon utilisation from respiration rates*

Carbon utilisation rates of *Poeobius* sp. were smaller than the observed particle flux reduction by a factor of almost 50 (E1) and 70 (E2). The calculation included several uncertainties and approximations that may explain this deviation:

1. Carbon utilisation rate was directly converted from oxygen respiration rates. This only includes the amount of carbon that was actually respired, but not the total amount of carbon that was taken up. Nothing is known about the metabolic efficiency of *Poeobius* sp. - it is possible that most of the carbon that is taken up is excreted unused. Bailey *et al.* (1995) used assimilation efficiencies of 70% in different ctenophore and medusa species. The use of the same value for C assimilation in *Poeobius* sp. would lead to an increase in carbon uptake of 30%, but this is still far from being comparable to the observed flux reduction.

2. Thuesen and Childress (1993) reported respiration rates from animals with wet weights between 0.1 and 1.2 g. *Poeobius* sp. in E1 were substantially lighter than this and possibly in growth, so the respiration rates may have been higher.

3. Feeding activity may increase respiration rates, which was not accounted for in Thuesen and Childress (1993).

Poeobius *sp. flux-feeding observations and implications*

Neither in E1 nor in E2, *Poeobius* sp. on the UVP5 images was recorded feeding - by contrast to the other investigated eddies and to the background field. This can probably be explained by the limited visibility of the mucus nets on the UVP5

images, where the presence of mucus nets can only be inferred from the particles that are stuck to them. In low particle concentrations, mucus nets may be deployed but barely visible. On PELAGIOS videos mucus nets were directly visible, and footage from E2 showed that mucus nets were actually deployed in this eddy. Most of the particles that were left in the water column seemed somehow to be stuck to one of these mucus nets (personal observation). This observation could mean that the already very low calculated flux in the layer where *Poeobius* sp. was abundant may be an overestimation, since the particles recorded by the UVP5 were not sinking independently, but were already caught by *Poeobius* sp.

*Quantification of particle flux reduction by* Poeobius *sp.*

An attempt was made to quantify the potential impact of *Poeobius* sp. on particle flux from abundances of the worm and observations of mucus net size. These calculations are based on several assumptions and uncertainties. For example, the mucus net area was determined relative to *Poeobius* sp. length and a linear relation between the animal length and the net size was assumed. Further measurements with an absolute scale are needed to verify this relation. Also, the mucus nets have a three dimensional structure, which could not be considered in the area determination. The nets were only identified from the particles that were stuck to them and may have been underestimated in low particle concentrations. This would imply that the net areas are possibly even larger. No data and no publications about *Poeobius* sp. ingestion rates and fecal pellet production are available. Therefore, it is not known what fraction of the particles captured is actually utilised and what is further processed and excreted as faeces that may re-join particle flux.

However, a conservative estimation of the proportion of flux that was removed by *Poeobius* sp. was possible and highlights the potential impact of this zooplankton species on particle flux. Assuming a mean *Poeobius* sp. length of about 1 cm, a mucus net would have an area of about 12 cm$^2$. A single worm with such a net could remove about 0.1% of the particle flux. In locations of high *Poeobius* sp. abundances this can have a considerable impact on fluxes. If only 40% of the animals were feeding, *i.e.* had their mucus nets deployed at any time, the more than 1000 animals in a depth range of 35 m in E1 would remove about 25% of the peak particle flux (8.4 mg POC m$^{-2}$ d$^{-1}$). The estimation of 40% feeding does not consider that empty nets were probably not identified; thus, the proportion of feeding animals may be larger. If all animals had their mucus net deployed, the small worms in E1 could capture more than 65% of the total particle flux under 1 m$^2$. This would amount to up to more than 20 mg POC m$^{-2}$ d$^{-1}$ that could be removed from the peak particle flux by *Poeobius* sp. alone.

# 5 Conclusion and outlook

In this thesis I investigated the distribution and role of the holopelagic polychaete *Poeobius* sp. in the tropical Atlantic. I evaluated particle data and almost two million images of zooplankton and detritus recorded with the UVP5 on 13 cruises to come to the following main conclusions and answers to my research questions:

1. *Poeobius* sp. is broadly distributed in the tropical Atlantic Ocean, both horizontally and vertically, although mostly in low abundance. The distribution is mostly influenced by eddy conditions.

2. Anticyclonic mode water eddies (ACMEs) significantly increase the abundance of *Poeobius* sp. Higher abundances were also identified in cyclonic eddies (CEs), whereas anticyclonic eddies (ACs) did not have an effect. I suggest an accumulation effect of rare zooplankton species by physical processes in ACMEs and CEs and subsequent improved conditions for growth, reproduction and dispersal. *Poeobius* sp. may benefit from enhanced particle fluxes in ACMEs and CEs and from the exclusion of competitors and predators in low oxygen concentrations.

3. ACMEs reduce *Poeobius* sp. depth distribution to a narrow depth range close to the surface mixed layer. This is probably a result of both the competition of the flux-feeding animals for sinking particles and the physical isolation of the eddy core.

4. Very low particle concentrations and fluxes were measured below layers with high *Poeobius* sp. abundances. The flux-feeder has the potential to substantially reduce particle flux. This flux reduction by remineralisation may be accompanied with increased oxygen consumption.

These conclusions emphasize the importance to study the role of fragile organisms in the marine ecosystem, which can best be done with optical methods. The results highlight that mesoscale eddies may play an important role in the reproduction and dispersal of rare species and that these, in turn, may change the environment in the eddy. An accumulation of particle feeding zooplankton in mesoscale eddies may explain the often observed change in particle flux in ageing eddies. Time series with a combination of autonomous and ship based sampling of an eddy are needed to assess the change of biological communities and particle fluxes in mesoscale eddies over time. This thesis presents one example of a so far undescribed species, *Poeobius* sp., that benefits from eddy conditions and that may play a significant role in structuring the biogeochemistry of these specific environments.

# 6 Acknowledgements

# 7 References

## 7.1 Literature

Alldredge A (1998) The carbon, nitrogen and mass content of marine snow as a function of aggregate size. Deep Sea Research Part I: Oceanographic Research Papers 45:529–541. doi: 10.1016/s0967-0637(97)00048-4

Antia AN, Koeve W, Fischer G, Blanz T (2001) Basin wide particulate carbon flux in the Atlantic Ocean: Regional export patterns and potential for atmospheric CO2 sequestration. Global Biogeochem Cycles 15:845–862. doi: 10.1029/2000gb001376

Bailey TG, Youngbluth MJ, Owen GP (1995) Chemical composition and metabolic rates of gelatinous zooplankton from midwater and benthic boundary layer environments off Cape Hatteras, North Carolina, USA. Mar Ecol Prog Ser 122:121–134. doi: 10.3354/meps122121

Banse K (1995) Zooplankton: Pivotal role in the control of ocean production I. Biomass and production. ICES Journal of Marine Science 52:265–277. doi: 10.1016/1054-3139(95)80043-3

Biard T, Picheral M, Mayot N, et al (2016) In situ imaging reveals the biomass of giant protists in the global ocean. Nature 532:504–507. doi: 10.1038/nature17652

Boehlert GW, Genin A (1987) A review of the effects of seamounts on biological processes. Geophysical Monograph Series 43:319–334. doi: 10.1029/gm043p0319

Bolker BM, Brooks ME, Clark CJ, et al (2009) Generalized linear mixed models: a practical guide for ecology and evolution. Trends in Ecology & Evolution 24:127–135. doi: 10.1016/j.tree.2008.10.008

Bollmann M, Bosch T, Colijn F, et al (2010) World ocean review 2010: living with the oceans.

Broughton EA, Lough RG (2006) A direct comparison of MOCNESS and Video Plankton Recorder zooplankton abundance estimates: Possible applications for augmenting net sampling with video systems. Deep Sea Research Part II: Topical Studies in Oceanography 53:2789–2807. doi: 10.1016/j.dsr2.2006.08.013

Buesseler KO, Lamborg C, Cai P, et al (2008) Particle fluxes associated with mesoscale eddies in the Sargasso Sea. Deep Sea Research Part II: Topical Studies in Oceanography 55:1426–1444. doi: 10.1016/j.dsr2.2008.02.007

Burnette AB, Struck TH, Halanych KM (2005) Holopelagic *Poeobius meseres* ("Poeobiidae," Annelida) is derived from benthic flabelligerid worms. The Biological Bulletin 208:213. doi: 10.2307/3593153

Chelton DB, Schlax MG, Lyman JM, Johnson GC (2003) Equatorially trapped Rossby waves in the presence of meridionally sheared baroclinic flow in the Pacific Ocean. Progress in Oceanography 56:323–380. doi: 10.1016/S0079-6611(03)00008-9

Davis CS, Gallager SM, Berman MS (1992a) The video plankton recorder (VPR):

design and initial results. Arch Hydrobiol.: 36:67-81, doi: 0071-1128/92/0036-0067

Davis CS, Gallager SM, Solow AR (1992b) Microaggregations of Oceanic Plankton Observed by Towed Video Microscopy. Science 257:230–232. doi: 10.1126/science.257.5067.230

de Boyer Montégut C (2004) Mixed layer depth over the global ocean: An examination of profile data and a profile-based climatology. J Geophys Res. doi: 10.1029/2004jc002378

Deibel D (1985) Blooms of the pelagic tunicate, *Dolioletta gegenbauri*: Are they associated with Gulf Stream frontal eddies? Journal of Marine Research 43:211–236. doi: 10.1357/002224085788437307

Denda A, Christiansen B (2013) Zooplankton distribution patterns at two seamounts in the subtropical and tropical NE Atlantic. Mar Ecol 35:159–179. doi: 10.1111/maec.12065

DK S, MW S, CH P (1997) Role of mesopelagic zooplankton in the community metabolism of giant larvacean house detritus in Monterey Bay, California, USA. Mar Ecol Prog Ser 147:167–179. doi: 10.3354/meps147167

Durkin CA, Estapa ML, Buesseler KO (2015) Observations of carbon export by small sinking particles in the upper mesopelagic. Marine Chemistry 175:72–81. doi: 10.1016/j.marchem.2015.02.011

Fernández E, Pingree RD (1996) Coupling between physical and biological fields in the North Atlantic subtropical front southeast of the Azores. Deep Sea Research Part I: Oceanographic Research Papers 43:1369–1393. doi: 10.1016/s0967-0637(96)00065-9

Fiedler B, Grundle DS, Schütte F, et al (2016) Oxygen utilization and downward carbon flux in an oxygen-depleted eddy in the eastern tropical North Atlantic. Biogeosciences 13:5633–5647. doi: 10.5194/bg-13-5633-2016

Fischer G, Karstensen J, Romero O, et al (2016) Bathypelagic particle flux signatures from a suboxic eddy in the oligotrophic tropical North Atlantic: production, sedimentation and preservation. Biogeosciences 13:3203–3223. doi: 10.5194/bg-13-3203-2016

Fleminger A, Clutter RI (1965) Avoidance of towed nets by zooplankton. Limnol. Oceanogr 10/1:96-104 doi: 10.4319/lo.1965.10.1.0096

Folt CL, Burns CW (1999) Biological drivers of zooplankton patchiness. Trends in Ecology & Evolution 14:300–305. doi: 10.1016/s0169-5347(99)01616-x

Gasol JM, del Giorgio PA, Duarte CM (1997) Biomass distribution in marine planktonic communities. Limnology and Oceanography 42:1353–1363. doi: 10.4319/lo.1997.42.6.1353

Gilmer RW (1974) Some aspects of feeding in thecosomatous pteropod molluscs. Journal of Experimental Marine Biology and Ecology 15:127–144. doi: 10.1016/0022-0981(74)90039-2

Godø OR, Samuelsen A, Macaulay GJ, et al (2012) Mesoscale Eddies Are Oases for Higher Trophic Marine Life. PLoS ONE 7:e30161–9. doi:

10.1371/journal.pone.0030161

Gorsky G, Ohman MD, Picheral M, et al (2010) Digital zooplankton image analysis using the ZooScan integrated system. Journal of Plankton Research 32:285–303. doi: 10.1093/plankt/fbp124

Hamner WM, Madin LP, Alldredge AL, et al (1975) Underwater observations of gelatinous zooplankton: Sampling problems, feeding biology, and behavior. Limnology and Oceanography 20:907–917. doi: 10.4319/lo.1975.20.6.0907

Hauss H, Christiansen S, Schütte F, et al (2016) Dead zone or oasis in the open ocean? Zooplankton distribution and migration in low-oxygen modewater eddies. Biogeosciences 13:1977–1989. doi: 10.5194/bg-13-1977-2016

Heath H (1930) A connecting link between the Annelida and the Echiuroidea (*Gephyrea armata*). Journal of Morphology 49:223–249. doi: 10.1002/jmor.1050490106

Herman AW (1992) Design and calibration of a new optical plankton counter capable of sizing small zooplankton. Deep Sea Research Part A Oceanographic Research Papers 39:395–415. doi: 10.1016/0198-0149(92)90080-d

IOC *et al.* (2010) The international thermodynamic equation of seawater-2010: Calculation and use of thermodynamic properties, Intergovernmental Oceanographic Commission, Manual and Guides No. 56, UNESCO (English), 196 pp. doi: 10.1149/1.3502443

Iversen MH, Nowald N, Ploug H, et al (2010) High resolution profiles of vertical particulate organic matter export off Cape Blanc, Mauritania Degradation processes and ballasting effects. Deep-Sea Research Part I 57:771–784. doi: 10.1016/j.dsr.2010.03.007

Jackson GA (1993) Flux feeding as a mechanism for zooplankton grazing and its implications for vertical particulate flux. Limnology and Oceanography 38:1328–1331. doi: 10.4319/lo.1993.38.6.1328

Jackson GA, Checkley DM (2011) Particle size distributions in the upper 100m water column and their implications for animal feeding in the plankton. Deep-Sea Research Part I 58:283–297. doi: 10.1016/j.dsr.2010.12.008

Karakaş G, Nowald N, Schäfer-Neth C, et al (2009) Impact of particle aggregation on vertical fluxes of organic matter. Progress in Oceanography 83:331–341. doi: 10.1016/j.pocean.2009.07.047

Karstensen J, Fiedler B, Schütte F, et al (2015) Open ocean dead zones in the tropical North Atlantic Ocean. Biogeosciences 12:2597–2605. doi: 10.5194/bg-12-2597-2015

Karstensen J, Schütte F, Pietri A, et al (2016) Upwelling and isolation in oxygen-depleted anticyclonic modewater eddies and implications for nitrate cycling. Biogeosciences Discuss 1–25. doi: 10.5194/bg-2016-34

Kiørboe T (2000) Colonization of marine snow aggregates by invertebrate zooplankton: Abundance, scaling, and possible role. Limnology and Oceanography 45:479–484. doi: 10.4319/lo.2000.45.2.0479

Kriest I (2002) Different parameterizations of marine snow in a 1D-model and their influence on representation of marine snow, nitrogen budget and sedimentation.

Deep Sea Research Part I: Oceanographic Research Papers 49:2133–2162. doi: 10.1016/s0967-0637(02)00127-9

Lehette P, Hernández-León S (2009) Zooplankton biomass estimation from digitized images: a comparison between subtropical and Antarctic organisms. Limnol Oceangr Methods 7:304–308. doi: 10.4319/lom.2009.7.304

Longhurst AR, Harrison WG (1989) The biological pump: profiles of plankton production and consumption in the upper ocean. Progress in Oceanography 22:47–123. doi: 10.1016/0079-6611(89)90010-4

Löscher CR, Fischer MA, Neulinger SC, et al (2015) Hidden biosphere in an oxygen-deficient Atlantic open-ocean eddy: future implications of ocean deoxygenation on primary production in the eastern tropical North Atlantic. Biogeosciences 12:7467–7482. doi: 10.5194/bg-12-7467-2015

Maas AE, Wishner KF, Seibel BA (2012) Metabolic suppression in thecosomatous pteropods as an effect of low temperature and hypoxia in the eastern tropical North Pacific. Marine Biology 159:1955–1967. doi: 10.1007/s00227-012-1982-x

Mackas DL, Galbraith MD (2002) Zooplankton Distribution and Dynamics in a North Pacific Eddy of Coastal Origin: I. Transport and Loss of Continental Margin Species. Journal of Oceanography 58:725–738. doi: 10.1023/A:1022802625242

Mackas DL, Tsurumi M, Galbraith MD, Yelland DR (2005) Zooplankton distribution and dynamics in a North Pacific Eddy of coastal origin: II. Mechanisms of eddy colonization by and retention of offshore species. Deep Sea Research Part II: Topical Studies in Oceanography 52:1011–1035. doi: 10.1016/j.dsr2.2005.02.008

Martin AP (2003) Phytoplankton patchiness: the role of lateral stirring and mixing. Progress in Oceanography 57:125–174. doi: 10.1016/S0079-6611(03)00085-5

Martin JH, Knauer GA, Karl DM (1987) VERTEX: carbon cycling in the northeast Pacific. Deep Sea Research Part I. 34/2:267-285, doi: 10.1016/0198-0149(87)90086-0

McCave IN (1975) Vertical flux of particles in the ocean. Deep Sea Research and Oceanographic Abstracts 22:491–502. doi: 10.1016/0011-7471(75)90022-4

McGillicuddy DJ, Anderson LA, Bates NR, et al (2007) Eddy/Wind Interactions Stimulate Extraordinary Mid-Ocean Plankton Blooms. Science 316:1021–1026. doi: 10.1126/science.1136256

McGillicuddy DJ, Robinson AR, Siegel DA (1998) Influence of mesoscale eddies on new production in the Sargasso Sea. Nature 394:263–266. doi: 10.1038/28367

McGowan JA (1960) The relationship of the distribution of the planktonic worm, *Poeobius meseres* Heath, to the water masses of the North Pacific. Deep Sea Research (1953) 6:125–139. doi: 10.1016/0146-6313(59)90064-4

Moloney CL, Field JG (1989) General allometric equations for rates of nutrient uptake, ingestion, and respiration in plankton organisms. Limnology and Oceanography 34:1290–1299. doi: 10.4319/lo.1989.34.7.1290

Oschlies A (2002) Can eddies make ocean deserts bloom? Global Biogeochem Cycles 16:53–1–53–11. doi: 10.1029/2001GB001830

Picheral M, Guidi L, Stemmann L, et al (2010) The Underwater Vision Profiler 5: An advanced instrument for high spatial resolution studies of particle size spectra and zooplankton. Limnol Oceangr Methods 8:462–473. doi: 10.4319/lom.2010.8.462

Prants SV, Budyansky MV, Uleysky MY (2014) Identifying Lagrangian fronts with favourable fishery conditions. Deep-Sea Research Part I 90:27–35. doi: 10.1016/j.dsr.2014.04.012

Quéré CL, Harrison SP, Colin Prentice I, et al (2005) Ecosystem dynamics based on plankton functional types for global ocean biogeochemistry models. Glob Change Biol 11:2016–2040. doi: 10.1111/j.1365-2486.2005.1004.x

Ramirez-Llodra E, Brandt A, Danovaro R, et al (2010) Deep, diverse and definitely different: unique attributes of the world's largest ecosystem. Biogeosciences 7:2851–2899. doi: 10.5194/bg-7-2851-2010

Redfield AC, Ketchum BH, Richards FA (1963) The influence of organisms on the composition of sea-water. In: Hill MN, editor. The Sea, vol. II. pp. 26–77. John Wiley, New York.

Remsen A, Hopkins TL, Samson S (2004) What you see is not what you catch: a comparison of concurrently collected net, Optical Plankton Counter, and Shadowed Image Particle Profiling Evaluation Recorder data from the northeast Gulf of Mexico. Deep Sea Research Part I: Oceanographic Research Papers 51:129–151. doi: 10.1016/j.dsr.2003.09.008

Ring G (1981) Gulf stream cold-core rings: their physics, chemistry, and biology. Science (New York 212:1091–1100. doi: 10.1126/science.212.4499.1091

Robison BH (2004) Deep pelagic biology. Journal of Experimental Marine Biology and Ecology 300:253–272. doi: 10.1016/j.jembe.2004.01.012

Robison BH, Reisenbichler KR, Sherlock RE (2005) Giant Larvacean Houses: Rapid Carbon Transport to the Deep Sea Floor . Science 308:1609–1611. doi: 10.1126/science.1109104

Robison BH, Sherlock RE, Reisenbichler KR (2010) The bathypelagic community of Monterey Canyon. Deep Sea Research Part II: Topical Studies in Oceanography 57:1551–1556. doi: 10.1016/j.dsr2.2010.02.021

Romero OE, Fischer G, Karstensen J, Cermeño P (2016) Eddies as trigger for diatom productivity in the open-ocean Northeast Atlantic. PROGRESS IN OCEANOGRAPHY 147:38–48. doi: 10.1016/j.pocean.2016.07.011

Samson S, Hopkins T, Remsen A (2001) A system for high-resolution zooplankton imaging. IEEE Journal of Oceanic Engineering. 26:671 - 676, doi: 10.1109/48.972110

Schnack-Schiel SB, Mizdalski E, Cornils A (2010) Copepod abundance and species composition in the Eastern subtropical/tropical Atlantic. Deep-Sea Research Part II 57:2064–2075. doi: 10.1016/j.dsr2.2010.09.010

Schütte F, Brandt P, Karstensen J (2016a) Occurrence and characteristics of mesoscale eddies in the tropical northeastern Atlantic Ocean. Ocean Sci 12:663–685. doi: 10.5194/os-12-663-2016

Schütte F, Brandt P, Karstensen J (2016b) Occurrence and characteristics of mesoscale eddies in the tropical northeastern Atlantic Ocean. Ocean Sci 12:663–685. doi: 10.5194/os-12-663-2016

Schütte F, Karstensen J, Krahmann G, et al (2016c) Characterization of "dead-zone" eddies in the tropical Northeast Atlantic Ocean. Biogeosciences Discuss 1–25. doi: 10.5194/bg-2016-33

Seki MP, Lumpkin R, Flament P (2002) Hawaii Cyclonic Eddies and Blue Marlin Catches: The Case Study of the 1995 Hawaiian International Billfish Tournament. Journal of Oceanography 58:739–745. doi: 10.1023/A:1022854609312

Spalding MD, Fox HE, Allen GR, et al (2007) Marine Ecoregions of the World: A Bioregionalization of Coastal and Shelf Areas. BioScience 57:573–583. doi: 10.1641/B570707

Steedmann, H. F. [Ed.] 1976. Zooplankton fixation and preservation. Monogr. Oceanogr. Methodol. 4. UNESCO Press, Paris. 350 p.

Stemmann L, Hosia A, Youngbluth MJ, et al (2008) Vertical distribution (0–1000m) of macrozooplankton, estimated using the Underwater Video Profiler, in different hydrographic regimes along the northern portion of the Mid-Atlantic Ridge. Deep Sea Research Part II: Topical Studies in Oceanography 55:94–105. doi: 10.1016/j.dsr2.2007.09.019

Stemmann L, Jackson GA, Gorsky G (2004) A vertical model of particle size distributions and fluxes in the midwater column that includes biological and physical processes—Part II: application to a three year survey in the NW Mediterranean Sea. Deep Sea Research Part I: Oceanographic Research Papers 51:885–908. doi: 10.1016/j.dsr.2004.03.002

Stramma L, Bange HW, Czeschel R, et al (2013) On the role of mesoscale eddies for the biological productivity and biogeochemistry in the eastern tropical Pacific Ocean off Peru. Biogeosciences 10:7293–7306. doi: 10.5194/bg-10-7293-2013

Sweeney EN, McGillicuddy DJ Jr., Buesseler KO (2003) Biogeochemical impacts due to mesoscale eddy activity in the Sargasso Sea as measured at the Bermuda Atlantic Time-series Study (BATS). Deep Sea Research Part II: Topical Studies in Oceanography 50:3017–3039. doi: 10.1016/j.dsr2.2003.07.008

Thuesen EV, Childress JJ (1993) Metabolic rates, enzyme activities and chemical compositions of some deep-sea pelagic worms, particularly *Nectonemertes mirabilis* (Nemertea; Hoplonemertinea) and *Poeobius meseres* (Annelida; Polychaeta) Deep Sea Research Part I: Oceanographic Research Papers 40:937–951. doi: 10.1016/0967-0637(93)90082-e

Tsurumi M, Mackas DL, Whitney FA, et al (2005) Pteropods, eddies, carbon flux, and climate variability in the Alaska Gyre. Deep Sea Research Part II: Topical Studies in Oceanography 52:1037–1053. doi: 10.1016/j.dsr2.2005.02.005

Turner JT (2015) Zooplankton fecal pellets, marine snow, phytodetritus and the ocean's biological pump. Progress in Oceanography 130:205–248. doi: 10.1016/j.pocean.2014.08.005

Uttal L, Buck KR (1996) Dietary study of the midwater polychaete *Poeobius meseres* in Monterey Bay, California. Marine Biology 125:333–343. doi: 10.1007/BF00346314

Waite AM, Beckley LE, Guidi L, et al (2015) Cross-shelf transport, oxygen depletion, and nitrate release within a forming mesoscale eddy in the eastern Indian Ocean. Limnology and Oceanography 61:103–121. doi: 10.1002/lno.10218

Whitney F, Robert M (2002) Structure of Haida eddies and their transport of nutrient from coastal margins into the NE Pacific Ocean.

Wilson SE, Ruhl HA, Smith KL Jr (2013) Zooplankton fecal pellet flux in the abyssal northeast Pacific: A 15 year time-series study. Limnology and Oceanography 58:881–892. doi: 10.4319/lo.2013.58.3.0881

## 7.2 Web pages

DSG (2016). *Poeobius meseres* (Heath, 1930) Deep-Sea Guide (DSG) at http://dsg/mbari.org/dsg/artifact/uuid/900f4ecc-75c8-4077-b421-d3ffd5f2b42f. Monterey Bay Aquarium Research Institute (MBARI). Consulted on 2016-09-27

Read, G. (2015). *Poeobius* Heath, 1930. In: Read, G.; Fauchald, K. (Ed.) (2015) World Polychaeta database. Accessed at http://marinespecies.org/polychaeta/aphia.php?p=taxdetails&id=324619 on 2016-09-28

## 7.3 Images

[1] http://www.geomar.de/typo3temp/pics/geomar_logo_eng_4c-large_69d0527d84.jpg

[2] http://www.wissenschafftzukunft-kiel.de/fileadmin/user_upload/wissenschaftsstandort_kiel/logo_cau.jpg

# Appendix

## Supplement 1:

### Particle flux in the ACME sampled during ISL00314 and M105
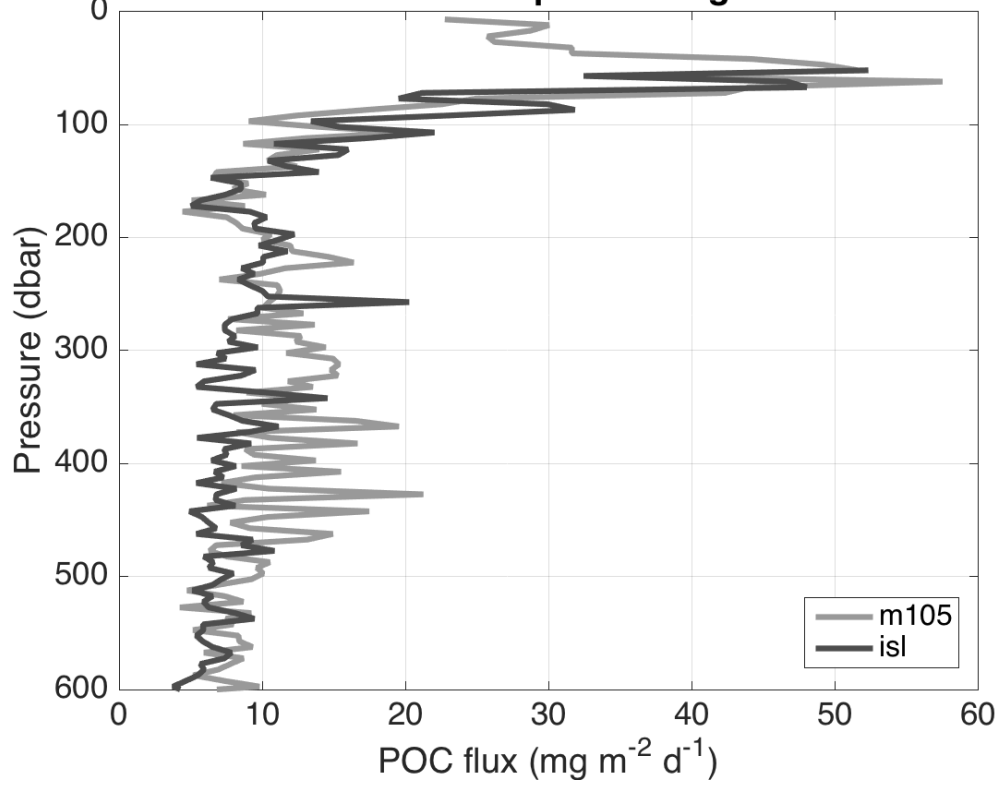


Figure 25: Particle flux calculated from abundance and sizes of particles between 0.14 and 2.66 mm ESD in the ACME sampled during ISL00314 and M105.

## Supplement 2:

Table 9: Raw data of individual *Poeobius* sp. qf stands for quality flag with 0: good measurement, 1: less accuracy and 2: no measurement possible. Lat and lon are latitude and longitude, respectively. Eddy characterisation is given as 0: non-eddy, 1: ACME, 2: AC, -1: CE. Method = 0 means that the observation was made during a vertical cast, method = 1 stands for observations in horizontal tows.

| Image name | Length | qf | feeding | depth | Lat | Lon | Month | Eddy | Method |
|---|---|---|---|---|---|---|---|---|---|
| 5676371_c_msm22_094_3799.jpg | 6,5 | 0 | 0 | 721,9 | 18,0 | -19,7 | 11 | 1 | 0 |
| 5694903_c_msm22_086_499.jpg | 8,2 | 0 | 0 | 63 | 13,0 | -23,0 | 11 | 0 | 0 |
| 5697770_c_msm22_008_1207.jpg | 8,0 | 0 | 0 | 84,2 | 12,8 | -21,0 | 10 | 1 | 0 |
| 5705327_c_msm22_076_508.jpg | 3,3 | 0 | 0 | 456,9 | 10,0 | -23,0 | 11 | -1 | 0 |
| 5718210_c_msm22_009_772.jpg | 5,7 | 1 | 1 | 65,7 | 11,0 | -21,3 | 10 | 0 | 0 |
| 5718656_c_msm22_009_1218.jpg | 5,1 | 0 | 1 | 689,6 | 11,0 | -21,3 | 10 | 0 | 0 |
| 5737445_c_msm22_070_501.jpg | 2,9 | 0 | 0 | 404 | 0,2 | -23,1 | 11 | 0 | 0 |
| 5743812_c_msm22_096_1553.jpg | 6,3 | 0 | 0 | 328,1 | 18,0 | -20,5 | 11 | 0 | 0 |
| 5744420_c_msm22_096_2161.jpg | 12,3 | 0 | 0 | 795,1 | 18,0 | -20,5 | 11 | 0 | 0 |
| 5744475_c_msm22_096_2216.jpg | NaN | 2 | 0 | 842 | 18,0 | -20,5 | 11 | 0 | 0 |
| 5747769_c_msm22_089_2490.jpg | 8,1 | 0 | 0 | 692,1 | 14,5 | -23,0 | 11 | 0 | 0 |
| 5747951_c_msm22_089_2672.jpg | 6,8 | 0 | 0 | 888,2 | 14,5 | -23,0 | 11 | 0 | 0 |
| 5754724_c_msm22_028_1793.jpg | 10,2 | 0 | 0 | 690,6 | 4,5 | -22,4 | 11 | 0 | 0 |
| 5768364_c_msm22_016_1041.jpg | 7,8 | 0 | 0 | 443,8 | 7,0 | -23,0 | 10 | 0 | 0 |
| 5788126_c_msm22_044_849.jpg | 6,5 | 0 | 0 | 548,1 | 0,7 | -23,0 | 11 | 0 | 0 |
| 5826544_c_msm22_104_837.jpg | 5,1 | 0 | 0 | 697,6 | 17,6 | -24,2 | 11 | 0 | 0 |
| 6183341_c_msm23_064_986.jpg | 5,4 | 0 | 0 | 518,3 | 0,0 | -23,0 | 12 | 0 | 0 |
| 6209219_c_msm23_022_503.jpg | 10,4 | 0 | 0 | 626 | 10,6 | -21,0 | 12 | 0 | 0 |
| 6223478_c_msm23_015_874.jpg | 4,1 | 0 | 0 | 70,9 | 11,5 | -21,0 | 11 | 0 | 0 |
| 9451617_m97_c_014_928.jpg | NaN | 2 | 0 | 683,3 | 10,5 | -22,5 | 5 | 0 | 0 |
| 9452156_m97_c_090_1526.jpg | 3,6 | 0 | 0 | 489,9 | 11,0 | -19,5 | 6 | 0 | 0 |
| 9455878_m97_c_074_1235.jpg | 6,9 | 0 | 0 | 741,5 | 9,5 | -19,0 | 6 | 0 | 0 |
| 9457087_m97_c_084_671.jpg | 9,7 | 0 | 0 | 568,6 | 12,0 | -19,5 | 6 | 0 | 0 |
| 9458983_m97_c_096_1574.jpg | 4,6 | 0 | 0 | 404,9 | 10,3 | -21,3 | 6 | 2 | 0 |
| 9459813_m97_c_021_418.jpg | 7,2 | 1 | 0 | 486,4 | 11,5 | -21,2 | 5 | 0 | 0 |
| 9460061_m97_c_013_487.jpg | 5,0 | 0 | 1 | 153,4 | 10,5 | -23,0 | 5 | 0 | 0 |
| 9462116_m97_c_066_1186.jpg | 3,0 | 0 | 0 | 471 | 10,5 | -19,5 | 6 | 0 | 0 |
| 9467336_m97_c_150_2132.jpg | 5,8 | 0 | 0 | 436,5 | 9,5 | -20,3 | 6 | 0 | 0 |
| 9506256_m97_c_008_445.jpg | 7,6 | 0 | 0 | 141,3 | 12,0 | -22,0 | 5 | 0 | 0 |
| 9528108_m97_c_147_1002.jpg | NaN | 2 | 0 | 571,9 | 9,5 | -21,3 | 6 | 0 | 0 |
| 9532540_m97_c_027_202.jpg | NaN | 2 | 0 | 21,8 | 11,3 | -20,0 | 6 | -1 | 0 |
| 9704187_m098_c_054_473.jpg | NaN | 2 | 0 | 471,2 | 0,0 | 0,0 | 0 | 0 | 0 |
| 9705304_m97_c_118_512.jpg | 8,8 | 1 | 0 | 538,5 | 9,7 | -20,0 | 6 | 0 | 0 |
| 9706091_m97_c_067_1142.jpg | 7,4 | 0 | 1 | 397,3 | 10,0 | -19,5 | 6 | 0 | 0 |
| 9708243_m97_c_064_745.jpg | 10,7 | 0 | 0 | 397,7 | 10,5 | -20,3 | 6 | 0 | 0 |
| 9710322_m97_c_120_478.jpg | 4,4 | 0 | 0 | 368,8 | 9,9 | -20,0 | 6 | 0 | 0 |
| 9710998_m97_c_157_1368.jpg | 11,6 | 0 | 0 | 70,9 | 9,0 | -21,0 | 6 | 1 | 0 |
| 9711175_m97_c_015_916.jpg | 8,1 | 0 | 0 | 810,5 | 11,0 | -22,5 | 5 | -1 | 0 |
| 9711441_m97_c_121_457.jpg | 5,2 | 0 | 0 | 59,4 | 9,7 | -19,9 | 6 | 0 | 0 |
| 9711619_m97_c_020_697.jpg | 13,2 | 0 | 0 | 660,2 | 11,5 | -21,5 | 5 | 0 | 0 |
| 9711953_m97_c_024_973.jpg | NaN | 2 | 0 | 997,3 | 11,5 | -20,5 | 5 | 0 | 0 |
| 9712873_m97_c_148_1100.jpg | 5,2 | 0 | 1 | 401,4 | 9,5 | -21,0 | 6 | 0 | 0 |
| 9713931_m97_c_047_379.jpg | 9,3 | 1 | 0 | 51 | 10,7 | -20,3 | 6 | 0 | 0 |
| 9714200_m97_c_036_359.jpg | NaN | 2 | 0 | 195,2 | 11,0 | -22,0 | 6 | -1 | 0 |
| 9714552_m97_c_064_1053.jpg | 7,1 | 0 | 0 | 694,6 | 10,5 | -20,3 | 6 | 0 | 0 |
| 9715555_m97_c_022_386.jpg | 10,2 | 0 | 0 | 74,3 | 11,5 | -21,0 | 5 | 0 | 0 |
| 9715931_m97_c_049_183.jpg | 10,0 | 0 | 1 | 61,3 | 10,7 | -20,5 | 6 | 0 | 0 |
| 9778132_m97_c_009_658.jpg | 4,5 | 1 | 0 | 155,9 | 12,0 | -22,5 | 5 | 0 | 0 |
| 9793130_m97_c_097_1472.jpg | 4,8 | 0 | 0 | 236,3 | 10,3 | -21,5 | 6 | 0 | 0 |
| 9816665_m97_c_046_369.jpg | 4,4 | 0 | 0 | 62,2 | 10,7 | -20,0 | 6 | 0 | 0 |
| 9819686_m97_c_157_1283.jpg | 7,3 | 0 | 1 | 61 | 9,0 | -21,0 | 6 | 1 | 0 |
| 9848874_m97_c_170_1324.jpg | 5,8 | 0 | 0 | 423,9 | 8,5 | -21,0 | 6 | 0 | 0 |
| 9876882_m97_c_157_1243.jpg | 4,5 | 0 | 0 | 57,6 | 9,0 | -21,0 | 6 | 1 | 0 |
| 9878984_m97_c_061_826.jpg | NaN | 2 | 0 | 641 | 10,5 | -21,0 | 6 | 0 | 0 |
| 9884433_m97_c_010_695.jpg | 4,7 | 0 | 0 | 511,3 | 12,0 | -23,0 | 5 | 0 | 0 |
| 9909844_m97_c_157_1280.jpg | 5,3 | 1 | 0 | 60,7 | 9,0 | -21,0 | 6 | 1 | 0 |

| | | | | | | | | | |
|---|---|---|---|---|---|---|---|---|---|
| 9914227_m97_c_153_1254.jpg | 6,1 | 0 | 0 | 565,2 | 9,0 | -19,7 | 6 | 0 | 0 |
| 9944408_m97_c_157_1301.jpg | 14,3 | 0 | 0 | 62,2 | 9,0 | -21,0 | 6 | 1 | 0 |
| 9945408_m97_c_008_104.jpg | 4,9 | 0 | 0 | 27,6 | 12,0 | -22,0 | 5 | 0 | 0 |
| 11173180_c_msm049_014_492.jpg | 6,7 | 1 | 0 | 426,2 | 18,5 | -21,9 | 12 | 0 | 0 |
| 11175544_c_msm049_018_693.jpg | NaN | 2 | 0 | 149,4 | 16,3 | -21,2 | 12 | -1 | 0 |
| 11175545_c_msm049_018_694.jpg | NaN | 2 | 0 | 149,5 | 16,3 | -21,2 | 12 | -1 | 0 |
| 11179073_c_msm049_020_1046.jpg | NaN | 2 | 0 | 207,4 | 16,2 | -21,3 | 12 | -1 | 0 |
| 11238855_043_506.jpg | 5,5 | 0 | 0 | 71,9 | 10,0 | -20,5 | 3 | 0 | 0 |
| 11243059_023_1516.jpg | NaN | 2 | 0 | 743,6 | 12,5 | -21,0 | 3 | 0 | 0 |
| 11243060_023_1517.jpg | NaN | 2 | 0 | 743,6 | 12,5 | -21,0 | 3 | 0 | 0 |
| 11246473_032_2462.jpg | 7,0 | 0 | 0 | 686,4 | 8,0 | -21,0 | 3 | 0 | 0 |
| 11263227_048_651.jpg | 11,5 | 1 | 0 | 58,6 | 11,5 | -20,5 | 3 | 0 | 0 |
| 11264689_022_463.jpg | 9,7 | 0 | 1 | 91,6 | 13,0 | -21,0 | 3 | 0 | 0 |
| 11276219_135_360.jpg | NaN | 2 | 0 | 193,7 | 9,0 | -25,0 | 4 | 0 | 0 |
| 11301707_049_1205.jpg | NaN | 2 | 0 | 713,4 | 12,0 | -20,5 | 3 | 0 | 0 |
| 11308736_017_720.jpg | 5,0 | 0 | 0 | 73,6 | 16,6 | -20,1 | 3 | 0 | 0 |
| 11315606_025_1563.jpg | 6,2 | 0 | 0 | 584,8 | 11,5 | -21,0 | 3 | 0 | 0 |
| 11331676_074_1328.jpg | 6,7 | 0 | 0 | 635,1 | 9,0 | -18,5 | 4 | 0 | 0 |
| 11374014_009_1371.jpg | 8,1 | 1 | 0 | 83,4 | 19,0 | -24,8 | 3 | 1 | 0 |
| 11374230_009_1587.jpg | 10,0 | 0 | 0 | 104,6 | 19,0 | -24,8 | 3 | 1 | 0 |
| 11378319_110_383.jpg | NaN | 2 | 0 | 74,5 | 12,0 | -22,0 | 4 | 0 | 0 |
| 11386145_013_638.jpg | 4,6 | 0 | 0 | 279,6 | 18,8 | -25,0 | 3 | 0 | 0 |
| 11400298_021_824.jpg | 10,2 | 0 | 0 | 759 | 13,5 | -21,0 | 3 | 0 | 0 |
| 11403268_079_1153.jpg | 9,4 | 0 | 0 | 676,2 | 8,0 | -20,0 | 4 | 0 | 0 |
| 11405587_011_509.jpg | 9,9 | 0 | 0 | 82,9 | 19,0 | -24,8 | 3 | 1 | 0 |
| 11405656_011_578.jpg | 8,7 | 0 | 0 | 91,1 | 19,0 | -24,8 | 3 | 1 | 0 |
| 11405730_011_652.jpg | 10,3 | 0 | 0 | 97,5 | 19,0 | -24,8 | 3 | 1 | 0 |
| 11405838_011_760.jpg | NaN | 2 | 0 | 106 | 19,0 | -24,8 | 3 | 1 | 0 |
| 11405878_011_800.jpg | 7,9 | 0 | 0 | 111 | 19,0 | -24,8 | 3 | 1 | 0 |
| 11405894_011_816.jpg | 11,0 | 0 | 0 | 111,7 | 19,0 | -24,8 | 3 | 1 | 0 |
| 11405946_011_868.jpg | 13,9 | 0 | 0 | 118 | 19,0 | -24,8 | 3 | 1 | 0 |
| 11405947_011_869.jpg | 14,8 | 0 | 0 | 118 | 19,0 | -24,8 | 3 | 1 | 0 |
| 11406055_011_977.jpg | NaN | 2 | 0 | 130,5 | 19,0 | -24,8 | 3 | 1 | 0 |
| 11406600_011_1522.jpg | 13,4 | 0 | 1 | 200,3 | 19,0 | -24,8 | 3 | 1 | 0 |
| 11412937_010_1100.jpg | 9,1 | 0 | 0 | 71,2 | 19,0 | -24,8 | 3 | 1 | 0 |
| 11413118_010_1281.jpg | 12,4 | 0 | 0 | 80,8 | 19,0 | -24,8 | 3 | 1 | 0 |
| 11509293_c_m107_066_2525.jpg | 4,0 | 0 | 0 | 264,1 | 19,9 | -17,6 | 6 | 0 | 0 |
| 11509332_c_m107_066_2564.jpg | 5,4 | 0 | 0 | 274,9 | 19,9 | -17,6 | 6 | 0 | 0 |
| 11559073_c_m107_012_1909.jpg | NaN | 2 | 0 | 193,4 | 18,1 | -16,9 | 6 | 0 | 0 |
| 11569799_c_m107_042_4070.jpg | 9,3 | 0 | 0 | 676,6 | 18,2 | -16,8 | 6 | 0 | 0 |
| 11576985_c_m107_013_5562.jpg | 7,1 | 0 | 0 | 561 | 18,2 | -16,8 | 6 | 0 | 0 |
| 11590577_c_m107_008_3208.jpg | 10,9 | 0 | 1 | 240,7 | 18,0 | -17,2 | 6 | 0 | 0 |
| 11681106_c_m107_011_4339.jpg | 6,3 | 0 | 0 | 339,4 | 18,2 | -16,8 | 6 | 0 | 0 |
| 11721105_c_ps88b_014_1318.jpg | 21,5 | 0 | 0 | 80,6 | 10,0 | -23,0 | 11 | 0 | 0 |
| 11727933_t_msm049_024_10180.jpg | 6,4 | 0 | 0 | 51,7 | 12,0 | -21,0 | 12 | 0 | 1 |
| 11734520_t_msm049_024_13357.jpg | 6,5 | 1 | 0 | 284 | 12,0 | -21,0 | 12 | 0 | 1 |
| 11737654_t_msm049_024_14881.jpg | NaN | 2 | 0 | 436,6 | 12,0 | -21,0 | 12 | 0 | 1 |
| 11746261_t_msm049_025_2761.jpg | 7,2 | 1 | 0 | 52,3 | 12,0 | -23,0 | 12 | 0 | 1 |
| 11747716_t_msm049_025_3468.jpg | 5,2 | 0 | 1 | 102,4 | 12,0 | -23,0 | 12 | 0 | 1 |
| 11747739_t_msm049_025_3478.jpg | 17,9 | 0 | 1 | 102,6 | 12,0 | -23,0 | 12 | 0 | 1 |
| 11747940_t_msm049_025_3575.jpg | 23,5 | 0 | 1 | 103,3 | 12,0 | -23,0 | 12 | 0 | 1 |
| 11749365_t_msm049_025_4271.jpg | 7,9 | 1 | 0 | 200,4 | 12,0 | -23,0 | 12 | 0 | 1 |
| 11749401_t_msm049_025_4288.jpg | 7,0 | 0 | 1 | 201 | 12,0 | -23,0 | 12 | 0 | 1 |
| 11749619_t_msm049_025_4392.jpg | 5,7 | 0 | 0 | 199,7 | 12,0 | -23,0 | 12 | 0 | 1 |
| 11749784_t_msm049_025_4472.jpg | 6,3 | 0 | 1 | 199,1 | 12,0 | -23,0 | 12 | 0 | 1 |
| 11751888_t_msm049_025_5501.jpg | 4,4 | 1 | 1 | 306,1 | 12,0 | -23,0 | 12 | 0 | 1 |
| 11753115_c_ps88b_040_1139.jpg | 11,1 | 0 | 0 | 600 | -0,7 | -23,0 | 11 | 0 | 0 |
| 11757882_t_msm049_025_8421.jpg | 4,0 | 0 | 0 | 490,1 | 12,0 | -23,0 | 12 | 0 | 1 |
| 11762458_t_msm049_025_10665.jpg | 7,5 | 1 | 0 | 904 | 12,0 | -23,0 | 12 | 0 | 1 |
| 11774967_t_msm049_026_6096.jpg | 4,6 | 0 | 0 | 52,4 | 12,0 | -23,0 | 12 | 0 | 1 |
| 11778215_t_msm049_026_7699.jpg | NaN | 2 | 0 | 53 | 12,0 | -23,0 | 12 | 0 | 1 |
| 11778818_t_msm049_026_7997.jpg | NaN | 2 | 0 | 100,4 | 12,0 | -23,0 | 12 | 0 | 1 |
| 11779148_t_msm049_026_8155.jpg | 18,6 | 0 | 0 | 100,1 | 12,0 | -23,0 | 12 | 0 | 1 |
| 11781536_t_msm049_026_9345.jpg | 5,4 | 1 | 0 | 302,7 | 12,0 | -23,0 | 12 | 0 | 1 |
| 11785857_t_msm049_026_11479.jpg | 6,0 | 0 | 0 | 436,5 | 12,0 | -23,0 | 12 | 0 | 1 |
| 11792054_c_ps88b_013_995.jpg | 9,5 | 0 | 1 | 52,8 | 10,5 | -23,0 | 11 | 0 | 0 |
| 11792082_c_ps88b_013_1009.jpg | 12,1 | 0 | 0 | 54 | 10,5 | -23,0 | 11 | 0 | 0 |

| | | | | | | | | | |
|---|---|---|---|---|---|---|---|---|---|
| 11792321_c_ps88b_013_1128.jpg | 6,8 | 0 | 0 | 78,6 | 10,5 | -23,0 | 11 | 0 | 0 |
| 11794832_c_ps88b_018_505.jpg | 5,7 | 0 | 0 | 619 | 8,0 | -23,0 | 11 | 0 | 0 |
| 11797098_c_ps88b_008_1026.jpg | 8,5 | 0 | 0 | 363,6 | 13,0 | -23,0 | 11 | 0 | 0 |
| 11808216_t_msm049_022_8257.jpg | 9,1 | 0 | 1 | 110,2 | 15,0 | -20,5 | 12 | 0 | 1 |
| 11811651_t_msm049_022_9948.jpg | 3,7 | 0 | 0 | 160,7 | 15,0 | -20,5 | 12 | 0 | 1 |
| 11818013_t_msm049_022_13075.jpg | 4,8 | 0 | 0 | 305,4 | 15,0 | -20,5 | 12 | 0 | 1 |
| 11818296_t_msm049_022_13217.jpg | 5,0 | 0 | 0 | 305,9 | 15,0 | -20,5 | 12 | 0 | 1 |
| 11818358_t_msm049_022_13246.jpg | 5,6 | 0 | 1 | 305,8 | 15,0 | -20,5 | 12 | 0 | 1 |
| 11818839_t_msm049_022_13484.jpg | 9,5 | 0 | 0 | 317,8 | 15,0 | -20,5 | 12 | 0 | 1 |
| 11842611_t_msm049_009_1557.jpg | 4,3 | 0 | 0 | 200 | 17,2 | -22,0 | 12 | 0 | 1 |
| 11851904_t_msm049_020_3802.jpg | 7,6 | 0 | 1 | 86,2 | 16,2 | -21,3 | 12 | -1 | 1 |
| 11852214_t_msm049_020_4112.jpg | 13,7 | 1 | 0 | 110,5 | 16,2 | -21,3 | 12 | -1 | 1 |
| 11852488_t_msm049_020_4386.jpg | 6,8 | 1 | 0 | 111,2 | 16,2 | -21,3 | 12 | -1 | 1 |
| 11852576_t_msm049_020_4474.jpg | 13,0 | 0 | 0 | 110,7 | 16,2 | -21,3 | 12 | -1 | 1 |
| 11852671_t_msm049_020_4569.jpg | NaN | 2 | 0 | 111,4 | 16,2 | -21,3 | 12 | -1 | 1 |
| 11852697_t_msm049_020_4595.jpg | 10,1 | 0 | 0 | 110,8 | 16,2 | -21,3 | 12 | -1 | 1 |
| 11853027_t_msm049_020_4925.jpg | NaN | 2 | 0 | 110,8 | 16,2 | -21,3 | 12 | -1 | 1 |
| 11853301_t_msm049_020_5199.jpg | 10,4 | 0 | 0 | 134 | 16,2 | -21,3 | 12 | -1 | 1 |
| 11853635_t_msm049_020_5533.jpg | NaN | 2 | 0 | 134,3 | 16,2 | -21,3 | 12 | -1 | 1 |
| 11853752_t_msm049_020_5650.jpg | 12,9 | 0 | 1 | 134,3 | 16,2 | -21,3 | 12 | -1 | 1 |
| 11853864_t_msm049_020_5762.jpg | 6,6 | 0 | 0 | 134,4 | 16,2 | -21,3 | 12 | -1 | 1 |
| 11853868_t_msm049_020_5766.jpg | 15,7 | 0 | 1 | 134,9 | 16,2 | -21,3 | 12 | -1 | 1 |
| 11854355_t_msm049_020_6253.jpg | NaN | 2 | 1 | 159,7 | 16,2 | -21,3 | 12 | -1 | 1 |
| 11854401_t_msm049_020_6299.jpg | 8,4 | 0 | 1 | 159,9 | 16,2 | -21,3 | 12 | -1 | 1 |
| 11854490_t_msm049_020_6388.jpg | 7,1 | 0 | 0 | 160,5 | 16,2 | -21,3 | 12 | -1 | 1 |
| 11854615_t_msm049_020_6513.jpg | NaN | 2 | 0 | 160,1 | 16,2 | -21,3 | 12 | -1 | 1 |
| 11854680_t_msm049_020_6578.jpg | 5,6 | 0 | 1 | 158,8 | 16,2 | -21,3 | 12 | -1 | 1 |
| 11854739_t_msm049_020_6637.jpg | 8,8 | 0 | 0 | 157,7 | 16,2 | -21,3 | 12 | -1 | 1 |
| 11854911_t_msm049_020_6809.jpg | 16,2 | 0 | 1 | 156,7 | 16,2 | -21,3 | 12 | -1 | 1 |
| 11855046_t_msm049_020_6944.jpg | 14,2 | 0 | 0 | 156,5 | 16,2 | -21,3 | 12 | -1 | 1 |
| 11855065_t_msm049_020_6963.jpg | 6,4 | 0 | 1 | 157,2 | 16,2 | -21,3 | 12 | -1 | 1 |
| 11855398_t_msm049_020_7296.jpg | 11,5 | 0 | 1 | 207,6 | 16,2 | -21,3 | 12 | -1 | 1 |
| 11855439_t_msm049_020_7337.jpg | 10,4 | 0 | 1 | 207,1 | 16,2 | -21,3 | 12 | -1 | 1 |
| 11855502_t_msm049_020_7400.jpg | 7,1 | 0 | 0 | 206,3 | 16,2 | -21,3 | 12 | -1 | 1 |
| 11855830_t_msm049_020_7728.jpg | 8,3 | 0 | 1 | 208,5 | 16,2 | -21,3 | 12 | -1 | 1 |
| 11855835_t_msm049_020_7733.jpg | 8,4 | 0 | 1 | 208,9 | 16,2 | -21,3 | 12 | -1 | 1 |
| 11855954_t_msm049_020_7852.jpg | NaN | 2 | 0 | 210,8 | 16,2 | -21,3 | 12 | -1 | 1 |
| 11856159_t_msm049_020_8057.jpg | 7,6 | 0 | 0 | 210,5 | 16,2 | -21,3 | 12 | -1 | 1 |
| 11856225_t_msm049_020_8123.jpg | 9,3 | 0 | 1 | 209,4 | 16,2 | -21,3 | 12 | -1 | 1 |
| 11856296_t_msm049_020_8194.jpg | 7,3 | 0 | 1 | 210,1 | 16,2 | -21,3 | 12 | -1 | 1 |
| 11856366_t_msm049_020_8264.jpg | 6,9 | 0 | 1 | 209,5 | 16,2 | -21,3 | 12 | -1 | 1 |
| 11856518_t_msm049_020_8416.jpg | 9,6 | 1 | 1 | 208,8 | 16,2 | -21,3 | 12 | -1 | 1 |
| 11856573_t_msm049_020_8471.jpg | 9,7 | 0 | 1 | 208,7 | 16,2 | -21,3 | 12 | -1 | 1 |
| 11857167_t_msm049_020_9065.jpg | 6,5 | 0 | 1 | 247,7 | 16,2 | -21,3 | 12 | -1 | 1 |
| 11867173_t_msm049_003_4737.jpg | 10,6 | 1 | 0 | 101,1 | 17,7 | -24,2 | 12 | 0 | 1 |
| 11867280_t_msm049_003_4844.jpg | 13,4 | 0 | 0 | 102,2 | 17,7 | -24,2 | 12 | 0 | 1 |
| 11867677_t_msm049_003_5241.jpg | 15,1 | 0 | 0 | 101,5 | 17,7 | -24,2 | 12 | 0 | 1 |
| 11868834_t_msm049_003_6398.jpg | 7,0 | 0 | 1 | 251,5 | 17,7 | -24,2 | 12 | 0 | 1 |
| 11870758_t_msm049_003_8322.jpg | 9,1 | 0 | 0 | 447,7 | 17,7 | -24,2 | 12 | 0 | 1 |
| 11870760_t_msm049_003_8324.jpg | 9,0 | 0 | 0 | 447,7 | 17,7 | -24,2 | 12 | 0 | 1 |
| 11871084_t_msm049_003_8648.jpg | 11,8 | 0 | 0 | 496,1 | 17,7 | -24,2 | 12 | 0 | 1 |
| 11871085_t_msm049_003_8649.jpg | 19,2 | 0 | 0 | 496,1 | 17,7 | -24,2 | 12 | 0 | 1 |
| 11873436_t_msm049_003_11000.jpg | 11,1 | 0 | 0 | 774,5 | 17,7 | -24,2 | 12 | 0 | 1 |
| 11893913_t_msm049_021_7672.jpg | NaN | 2 | 0 | 82 | 15,0 | -20,5 | 12 | 0 | 1 |
| 11896087_t_msm049_021_9846.jpg | NaN | 2 | 0 | 136,4 | 15,0 | -20,5 | 12 | 0 | 1 |
| 11897123_t_msm049_021_10882.jpg | 7,1 | 0 | 0 | 211,3 | 15,0 | -20,5 | 12 | 0 | 1 |
| 11897251_t_msm049_021_11010.jpg | 5,6 | 0 | 1 | 211,2 | 15,0 | -20,5 | 12 | 0 | 1 |
| 11897273_t_msm049_021_11032.jpg | 10,5 | 0 | 0 | 211,6 | 15,0 | -20,5 | 12 | 0 | 1 |
| 11897790_t_msm049_021_11549.jpg | 12,5 | 0 | 1 | 211,3 | 15,0 | -20,5 | 12 | 0 | 1 |
| 11898282_t_msm049_021_12041.jpg | 5,1 | 1 | 0 | 252,8 | 15,0 | -20,5 | 12 | 0 | 1 |
| 11899326_t_msm049_021_13085.jpg | NaN | 2 | 0 | 305,2 | 15,0 | -20,5 | 12 | 0 | 1 |
| 11900036_t_msm049_021_13795.jpg | 8,4 | 0 | 0 | 303 | 15,0 | -20,5 | 12 | 0 | 1 |
| 11906021_t_msm049_000_2846.jpg | 9,1 | 0 | 1 | 176,6 | 17,6 | -24,3 | 12 | 0 | 1 |
| 11914405_t_msm049_023_7997.jpg | 15,2 | 0 | 0 | 100,8 | 12,0 | -21,0 | 12 | 0 | 1 |
| 11914569_t_msm049_023_8161.jpg | 13,3 | 1 | 0 | 101,6 | 12,0 | -21,0 | 12 | 0 | 1 |
| 11919256_t_msm049_023_12848.jpg | NaN | 2 | 0 | 802,3 | 12,0 | -21,0 | 12 | 0 | 1 |
| 11924214_t_msm049_010_4367.jpg | 8,1 | 0 | 0 | 201,3 | 17,2 | -22,0 | 12 | 0 | 1 |

| | | | | | | | | | |
|---|---|---|---|---|---|---|---|---|---|
| 11928072_t_msm049_010_8225.jpg | 10,0 | 0 | 0 | 393,7 | 17,2 | -22,0 | 12 | 0 | 1 |
| 11930086_t_msm049_010_10239.jpg | 11,4 | 1 | 0 | 578,9 | 17,2 | -22,0 | 12 | 0 | 1 |
| 11930188_t_msm049_010_10341.jpg | 11,7 | 0 | 0 | 601,7 | 17,2 | -22,0 | 12 | 0 | 1 |
| 11930281_t_msm049_010_10434.jpg | NaN | 2 | 0 | 599,2 | 17,2 | -22,0 | 12 | 0 | 1 |
| 11930892_t_msm049_010_11045.jpg | NaN | 2 | 0 | 596,3 | 17,2 | -22,0 | 12 | 0 | 1 |
| 11948071_t_msm049_019_8544.jpg | 7,4 | 0 | 1 | 87,3 | 16,2 | -21,3 | 12 | -1 | 1 |
| 11948922_t_msm049_019_9395.jpg | 5,0 | 0 | 0 | 86,8 | 16,2 | -21,3 | 12 | -1 | 1 |
| 11949180_t_msm049_019_9653.jpg | 16,5 | 0 | 0 | 110,5 | 16,2 | -21,3 | 12 | -1 | 1 |
| 11949233_t_msm049_019_9706.jpg | 9,3 | 0 | 0 | 110,7 | 16,2 | -21,3 | 12 | -1 | 1 |
| 11949616_t_msm049_019_10089.jpg | 10,8 | 0 | 0 | 110,2 | 16,2 | -21,3 | 12 | -1 | 1 |
| 11949696_t_msm049_019_10169.jpg | 5,8 | 1 | 0 | 109,7 | 16,2 | -21,3 | 12 | -1 | 1 |
| 11949728_t_msm049_019_10201.jpg | 11,7 | 0 | 0 | 110,3 | 16,2 | -21,3 | 12 | -1 | 1 |
| 11949903_t_msm049_019_10376.jpg | 11,0 | 0 | 0 | 110,1 | 16,2 | -21,3 | 12 | -1 | 1 |
| 11950104_t_msm049_019_10577.jpg | 13,8 | 0 | 0 | 117,4 | 16,2 | -21,3 | 12 | -1 | 1 |
| 11950536_t_msm049_019_11009.jpg | NaN | 2 | 0 | 134,3 | 16,2 | -21,3 | 12 | -1 | 1 |
| 11950903_t_msm049_019_11376.jpg | NaN | 2 | 0 | 135,7 | 16,2 | -21,3 | 12 | -1 | 1 |
| 11950916_t_msm049_019_11389.jpg | 14,6 | 0 | 0 | 135,9 | 16,2 | -21,3 | 12 | -1 | 1 |
| 11950940_t_msm049_019_11413.jpg | 9,4 | 0 | 0 | 135,6 | 16,2 | -21,3 | 12 | -1 | 1 |
| 11951055_t_msm049_019_11528.jpg | 11,9 | 1 | 0 | 136,6 | 16,2 | -21,3 | 12 | -1 | 1 |
| 11951480_t_msm049_019_11953.jpg | 11,2 | 0 | 0 | 158,4 | 16,2 | -21,3 | 12 | -1 | 1 |
| 11951572_t_msm049_019_12045.jpg | NaN | 2 | 0 | 159,9 | 16,2 | -21,3 | 12 | -1 | 1 |
| 11951641_t_msm049_019_12114.jpg | NaN | 2 | 0 | 159,9 | 16,2 | -21,3 | 12 | -1 | 1 |
| 11951844_t_msm049_019_12317.jpg | 7,4 | 1 | 0 | 160,2 | 16,2 | -21,3 | 12 | -1 | 1 |
| 11951856_t_msm049_019_12329.jpg | 9,6 | 0 | 0 | 160,2 | 16,2 | -21,3 | 12 | -1 | 1 |
| 11952221_t_msm049_019_12694.jpg | 8,2 | 1 | 0 | 175,7 | 16,2 | -21,3 | 12 | -1 | 1 |
| 11952232_t_msm049_019_12705.jpg | 9,7 | 1 | 0 | 180,5 | 16,2 | -21,3 | 12 | -1 | 1 |
| 11952295_t_msm049_019_12768.jpg | 8,4 | 0 | 0 | 206,7 | 16,2 | -21,3 | 12 | -1 | 1 |
| 11952475_t_msm049_019_12948.jpg | 6,3 | 0 | 0 | 208,7 | 16,2 | -21,3 | 12 | -1 | 1 |
| 11952484_t_msm049_019_12957.jpg | 8,9 | 1 | 0 | 209,4 | 16,2 | -21,3 | 12 | -1 | 1 |
| 11952553_t_msm049_019_13026.jpg | NaN | 2 | 0 | 207,1 | 16,2 | -21,3 | 12 | -1 | 1 |
| 11952629_t_msm049_019_13102.jpg | 6,9 | 1 | 0 | 207,6 | 16,2 | -21,3 | 12 | -1 | 1 |
| 11952646_t_msm049_019_13119.jpg | 9,5 | 0 | 0 | 207,6 | 16,2 | -21,3 | 12 | -1 | 1 |
| 11952687_t_msm049_019_13160.jpg | 7,8 | 0 | 0 | 207,4 | 16,2 | -21,3 | 12 | -1 | 1 |
| 11952855_t_msm049_019_13328.jpg | 7,3 | 1 | 0 | 207,7 | 16,2 | -21,3 | 12 | -1 | 1 |
| 11952884_t_msm049_019_13357.jpg | NaN | 2 | 0 | 207,1 | 16,2 | -21,3 | 12 | -1 | 1 |
| 11953040_t_msm049_019_13513.jpg | 6,8 | 1 | 0 | 204,8 | 16,2 | -21,3 | 12 | -1 | 1 |
| 11953398_t_msm049_019_13871.jpg | 5,9 | 0 | 0 | 207,6 | 16,2 | -21,3 | 12 | -1 | 1 |
| 11953437_t_msm049_019_13910.jpg | NaN | 2 | 0 | 207,2 | 16,2 | -21,3 | 12 | -1 | 1 |
| 11953509_t_msm049_019_13982.jpg | NaN | 2 | 0 | 207,7 | 16,2 | -21,3 | 12 | -1 | 1 |
| 11953580_t_msm049_019_14053.jpg | 6,9 | 0 | 1 | 232,5 | 16,2 | -21,3 | 12 | -1 | 1 |
| 11953618_t_msm049_019_14091.jpg | 8,5 | 1 | 0 | 249,8 | 16,2 | -21,3 | 12 | -1 | 1 |
| 11954034_t_msm049_019_14507.jpg | 8,1 | 0 | 0 | 248,5 | 16,2 | -21,3 | 12 | -1 | 1 |
| 11954231_t_msm049_019_14704.jpg | 6,6 | 1 | 0 | 250,5 | 16,2 | -21,3 | 12 | -1 | 1 |
| 11954379_t_msm049_019_14852.jpg | 8,6 | 0 | 0 | 249,9 | 16,2 | -21,3 | 12 | -1 | 1 |
| 11974052_t_msm049_016_7895.jpg | 8,8 | 0 | 0 | 397,2 | 17,2 | -21,9 | 12 | 0 | 1 |
| 11974152_t_msm049_016_7995.jpg | 5,5 | 0 | 0 | 397,2 | 17,2 | -21,9 | 12 | 0 | 1 |
| 11980854_t_msm049_004_5136.jpg | 8,9 | 1 | 1 | 103,7 | 17,6 | -24,3 | 12 | -1 | 1 |
| 11980998_t_msm049_004_5280.jpg | 6,3 | 1 | 0 | 103,7 | 17,6 | -24,3 | 12 | -1 | 1 |
| 11981267_t_msm049_004_5549.jpg | NaN | 2 | 0 | 201,6 | 17,6 | -24,3 | 12 | -1 | 1 |
| 11981348_t_msm049_004_5630.jpg | 8,6 | 0 | 1 | 202,5 | 17,6 | -24,3 | 12 | -1 | 1 |
| 13118254_m119_036_443.jpg | 6,6 | 0 | 0 | 694 | 1,3 | -23,0 | 9 | 0 | 0 |
| 13122110_m119_021_459.jpg | 15,5 | 1 | 0 | 93,5 | 7,5 | -22,9 | 9 | 1 | 0 |
| 13122112_m119_021_461.jpg | 11,3 | 1 | 0 | 93,9 | 7,5 | -22,9 | 9 | 1 | 0 |
| 13122113_m119_021_462.jpg | 13,4 | 0 | 0 | 93,9 | 7,5 | -22,9 | 9 | 1 | 0 |
| 13122115_m119_021_464.jpg | 18,3 | 0 | 0 | 94,8 | 7,5 | -22,9 | 9 | 1 | 0 |
| 13122121_m119_021_470.jpg | 16,7 | 0 | 0 | 96,6 | 7,5 | -22,9 | 9 | 1 | 0 |
| 13122148_m119_021_497.jpg | 5,5 | 1 | 0 | 108 | 7,5 | -22,9 | 9 | 1 | 0 |
| 13127144_m119_051_336.jpg | 10,9 | 0 | 0 | 644,2 | -3,5 | -23,0 | 9 | 0 | 0 |
| 13136589_m119_020_393.jpg | 14,3 | 0 | 0 | 65,3 | 8,0 | -22,9 | 9 | 1 | 0 |
| 13136633_m119_020_437.jpg | 16,9 | 1 | 0 | 78 | 8,0 | -22,9 | 9 | 1 | 0 |
| 13136638_m119_020_442.jpg | 15,1 | 0 | 0 | 82,9 | 8,0 | -22,9 | 9 | 1 | 0 |
| 13136645_m119_020_449.jpg | 14,4 | 1 | 0 | 87,4 | 8,0 | -22,9 | 9 | 1 | 0 |
| 13136650_m119_020_454.jpg | 18,7 | 1 | 0 | 88 | 8,0 | -22,9 | 9 | 1 | 0 |
| 13136654_m119_020_458.jpg | NaN | 2 | 0 | 88,5 | 8,0 | -22,9 | 9 | 1 | 0 |
| 13136658_m119_020_462.jpg | 10,9 | 0 | 0 | 90,5 | 8,0 | -22,9 | 9 | 1 | 0 |
| 13136667_m119_020_471.jpg | 11,5 | 0 | 0 | 94,7 | 8,0 | -22,9 | 9 | 1 | 0 |
| 13171720_m119_006_1369.jpg | 6,0 | 0 | 0 | 671,9 | 14,0 | -23,0 | 9 | 0 | 0 |

| | | | | | | | | | |
|---|---|---|---|---|---|---|---|---|---|
| 13206980_m116_046_391.jpg | 10,9 | 0 | 0 | 50,5 | 11,0 | -23,0 | 5 | 0 | 0 |
| 13207015_m116_046_402.jpg | 7,2 | 0 | 0 | 51,3 | 11,0 | -23,0 | 5 | 0 | 0 |
| 13207035_m116_046_409.jpg | 5,9 | 0 | 0 | 52,1 | 11,0 | -23,0 | 5 | 0 | 0 |
| 13210559_t_m119_005_1528.jpg | 7,8 | 0 | 0 | 49,7 | 11,0 | -21,2 | 9 | 0 | 1 |
| 13212085_t_m119_005_2104.jpg | 6,6 | 0 | 0 | 49,7 | 11,0 | -21,2 | 9 | 0 | 1 |
| 13212675_t_m119_005_2326.jpg | 9,2 | 1 | 0 | 49,9 | 11,0 | -21,2 | 9 | 0 | 1 |
| 13215164_t_m119_005_3267.jpg | 19,1 | 0 | 0 | 66,7 | 11,0 | -21,2 | 9 | 0 | 1 |
| 13232686_t_m119_004_2287.jpg | 19,0 | 1 | 0 | 72,6 | 12,0 | -23,0 | 9 | 0 | 1 |
| 13235843_t_m119_004_3474.jpg | 7,0 | 0 | 0 | 149 | 12,0 | -23,0 | 9 | 0 | 1 |
| 13244258_t_m119_003_708.jpg | 9,5 | 1 | 0 | 50,8 | 13,0 | -23,0 | 9 | 0 | 1 |
| 13244261_t_m119_003_709.jpg | 8,8 | 1 | 0 | 50,9 | 13,0 | -23,0 | 9 | 0 | 1 |
| 13248353_m116_025_969.jpg | 5,8 | 0 | 0 | 248,7 | 11,0 | -34,0 | 5 | 2 | 0 |
| 13256250_t_m119_003_5036.jpg | 8,7 | 0 | 0 | 333,6 | 13,0 | -23,0 | 9 | 0 | 1 |
| 13263608_m116_052_550.jpg | 5,3 | 0 | 0 | 757 | 9,0 | -22,0 | 5 | 0 | 0 |
| 13273129_m116_028_756.jpg | 5,5 | 0 | 0 | 423,2 | 11,0 | -31,0 | 5 | 0 | 0 |
| 13294318_t_m119_009_2310.jpg | 18,8 | 0 | 0 | 72 | 8,0 | -22,9 | 9 | 1 | 1 |
| 13294407_t_m119_009_2341.jpg | NaN | 2 | 0 | 79,8 | 8,0 | -22,9 | 9 | 1 | 1 |
| 13294422_t_m119_009_2346.jpg | NaN | 2 | 0 | 79,9 | 8,0 | -22,9 | 9 | 1 | 1 |
| 13294439_t_m119_009_2351.jpg | 11,0 | 0 | 0 | 81,3 | 8,0 | -22,9 | 9 | 1 | 1 |
| 13294444_t_m119_009_2353.jpg | 18,7 | 0 | 0 | 81,9 | 8,0 | -22,9 | 9 | 1 | 1 |
| 13294461_t_m119_009_2359.jpg | 17,8 | 1 | 0 | 85,1 | 8,0 | -22,9 | 9 | 1 | 1 |
| 13294489_t_m119_009_2370.jpg | NaN | 2 | 0 | 87,4 | 8,0 | -22,9 | 9 | 1 | 1 |
| 13294508_t_m119_009_2376.jpg | NaN | 2 | 0 | 89 | 8,0 | -22,9 | 9 | 1 | 1 |
| 13294520_t_m119_009_2381.jpg | NaN | 2 | 0 | 92,3 | 8,0 | -22,9 | 9 | 1 | 1 |
| 13294537_t_m119_009_2387.jpg | 15,5 | 1 | 0 | 93,1 | 8,0 | -22,9 | 9 | 1 | 1 |
| 13294552_t_m119_009_2392.jpg | 15,0 | 0 | 0 | 93,9 | 8,0 | -22,9 | 9 | 1 | 1 |
| 13294577_t_m119_009_2400.jpg | NaN | 2 | 0 | 94,9 | 8,0 | -22,9 | 9 | 1 | 1 |
| 13294588_t_m119_009_2404.jpg | 20,2 | 0 | 0 | 95,8 | 8,0 | -22,9 | 9 | 1 | 1 |
| 13294646_t_m119_009_2427.jpg | NaN | 2 | 0 | 97,9 | 8,0 | -22,9 | 9 | 1 | 1 |
| 13294677_t_m119_009_2438.jpg | 15,5 | 0 | 0 | 98,1 | 8,0 | -22,9 | 9 | 1 | 1 |
| 13294684_t_m119_009_2440.jpg | 19,0 | 0 | 0 | 98 | 8,0 | -22,9 | 9 | 1 | 1 |
| 13294717_t_m119_009_2452.jpg | 18,8 | 1 | 0 | 97,8 | 8,0 | -22,9 | 9 | 1 | 1 |
| 13294742_t_m119_009_2461.jpg | 17,9 | 0 | 0 | 97,7 | 8,0 | -22,9 | 9 | 1 | 1 |
| 13294876_t_m119_009_2512.jpg | 17,8 | 0 | 0 | 98,1 | 8,0 | -22,9 | 9 | 1 | 1 |
| 13294914_m116_009_591.jpg | 7,3 | 0 | 0 | 408,5 | 11,0 | -42,0 | 5 | 0 | 0 |
| 13294958_t_m119_009_2543.jpg | NaN | 2 | 0 | 98,4 | 8,0 | -22,9 | 9 | 1 | 1 |
| 13294980_t_m119_009_2551.jpg | 17,9 | 0 | 0 | 98,2 | 8,0 | -22,9 | 9 | 1 | 1 |
| 13294987_t_m119_009_2554.jpg | 13,6 | 0 | 0 | 98,2 | 8,0 | -22,9 | 9 | 1 | 1 |
| 13295000_t_m119_009_2559.jpg | 18,3 | 0 | 0 | 98 | 8,0 | -22,9 | 9 | 1 | 1 |
| 13295073_t_m119_009_2585.jpg | 13,9 | 0 | 0 | 98,4 | 8,0 | -22,9 | 9 | 1 | 1 |
| 13295118_t_m119_009_2602.jpg | 15,8 | 0 | 0 | 99 | 8,0 | -22,9 | 9 | 1 | 1 |
| 13295128_t_m119_009_2606.jpg | 19,3 | 0 | 0 | 99,1 | 8,0 | -22,9 | 9 | 1 | 1 |
| 13295163_t_m119_009_2620.jpg | 14,7 | 0 | 0 | 99,1 | 8,0 | -22,9 | 9 | 1 | 1 |
| 13295174_t_m119_009_2624.jpg | 15,8 | 0 | 0 | 99 | 8,0 | -22,9 | 9 | 1 | 1 |
| 13295187_t_m119_009_2629.jpg | NaN | 2 | 0 | 98,8 | 8,0 | -22,9 | 9 | 1 | 1 |
| 13295206_t_m119_009_2636.jpg | NaN | 2 | 0 | 98,7 | 8,0 | -22,9 | 9 | 1 | 1 |
| 13295207_t_m119_009_2637.jpg | 18,8 | 0 | 0 | 98,7 | 8,0 | -22,9 | 9 | 1 | 1 |
| 13295286_t_m119_009_2667.jpg | NaN | 2 | 0 | 98,7 | 8,0 | -22,9 | 9 | 1 | 1 |
| 13295306_t_m119_009_2674.jpg | 14,7 | 0 | 0 | 98,6 | 8,0 | -22,9 | 9 | 1 | 1 |
| 13295310_t_m119_009_2675.jpg | 14,0 | 1 | 0 | 98,6 | 8,0 | -22,9 | 9 | 1 | 1 |
| 13295360_t_m119_009_2694.jpg | 22,0 | 0 | 0 | 99,2 | 8,0 | -22,9 | 9 | 1 | 1 |
| 13295399_t_m119_009_2708.jpg | 16,2 | 0 | 0 | 99,2 | 8,0 | -22,9 | 9 | 1 | 1 |
| 13295464_t_m119_009_2733.jpg | 16,6 | 0 | 0 | 98,3 | 8,0 | -22,9 | 9 | 1 | 1 |
| 13295467_t_m119_009_2734.jpg | 15,7 | 1 | 0 | 98,3 | 8,0 | -22,9 | 9 | 1 | 1 |
| 13295537_t_m119_009_2761.jpg | 14,6 | 1 | 0 | 98,3 | 8,0 | -22,9 | 9 | 1 | 1 |
| 13295552_t_m119_009_2766.jpg | 16,7 | 0 | 0 | 98,2 | 8,0 | -22,9 | 9 | 1 | 1 |
| 13295563_t_m119_009_2771.jpg | 16,5 | 0 | 0 | 98,6 | 8,0 | -22,9 | 9 | 1 | 1 |
| 13295654_t_m119_009_2805.jpg | NaN | 2 | 0 | 97,9 | 8,0 | -22,9 | 9 | 1 | 1 |
| 13295759_t_m119_009_2844.jpg | 15,5 | 0 | 0 | 98,3 | 8,0 | -22,9 | 9 | 1 | 1 |
| 13295762_t_m119_009_2845.jpg | NaN | 2 | 0 | 98,3 | 8,0 | -22,9 | 9 | 1 | 1 |
| 13295786_t_m119_009_2854.jpg | NaN | 2 | 0 | 98,4 | 8,0 | -22,9 | 9 | 1 | 1 |
| 13295805_t_m119_009_2860.jpg | NaN | 2 | 0 | 98,4 | 8,0 | -22,9 | 9 | 1 | 1 |
| 13295837_t_m119_009_2870.jpg | 16,7 | 1 | 0 | 98,3 | 8,0 | -22,9 | 9 | 1 | 1 |
| 13295901_t_m119_009_2894.jpg | NaN | 2 | 0 | 98,3 | 8,0 | -22,9 | 9 | 1 | 1 |
| 13295914_t_m119_009_2899.jpg | 14,1 | 0 | 0 | 98,3 | 8,0 | -22,9 | 9 | 1 | 1 |
| 13295929_t_m119_009_2905.jpg | 13,7 | 1 | 0 | 98,3 | 8,0 | -22,9 | 9 | 1 | 1 |
| 13295963_t_m119_009_2918.jpg | 18,6 | 0 | 0 | 98 | 8,0 | -22,9 | 9 | 1 | 1 |

| | | | | | | | | | |
|---|---|---|---|---|---|---|---|---|---|
| 13295978_t_m119_009_2922.jpg | 17,8 | 0 | 0 | 98 | 8,0 | -22,9 | 9 | 1 | 1 |
| 13296018_t_m119_009_2937.jpg | NaN | 2 | 0 | 98,1 | 8,0 | -22,9 | 9 | 1 | 1 |
| 13296058_t_m119_009_2950.jpg | 13,7 | 1 | 0 | 98,1 | 8,0 | -22,9 | 9 | 1 | 1 |
| 13296082_t_m119_009_2960.jpg | 12,1 | 1 | 0 | 98,1 | 8,0 | -22,9 | 9 | 1 | 1 |
| 13296122_t_m119_009_2974.jpg | 14,8 | 1 | 0 | 98,2 | 8,0 | -22,9 | 9 | 1 | 1 |
| 13296128_t_m119_009_2976.jpg | 14,3 | 1 | 0 | 98,3 | 8,0 | -22,9 | 9 | 1 | 1 |
| 13296149_t_m119_009_2984.jpg | 18,7 | 0 | 0 | 98,3 | 8,0 | -22,9 | 9 | 1 | 1 |
| 13296149_t_m119_009_2984.jpg | 22,1 | 0 | 0 | 98,3 | 8,0 | -22,9 | 9 | 1 | 1 |
| 13296169_t_m119_009_2992.jpg | NaN | 2 | 0 | 98,1 | 8,0 | -22,9 | 9 | 1 | 1 |
| 13296221_t_m119_009_3010.jpg | 14,2 | 1 | 0 | 98,1 | 8,0 | -22,9 | 9 | 1 | 1 |
| 13296227_t_m119_009_3013.jpg | NaN | 2 | 0 | 98,2 | 8,0 | -22,9 | 9 | 1 | 1 |
| 13296258_t_m119_009_3024.jpg | 17,9 | 1 | 0 | 98,2 | 8,0 | -22,9 | 9 | 1 | 1 |
| 13296337_t_m119_009_3051.jpg | 11,1 | 0 | 0 | 98 | 8,0 | -22,9 | 9 | 1 | 1 |
| 13296344_t_m119_009_3053.jpg | 16,0 | 0 | 0 | 98 | 8,0 | -22,9 | 9 | 1 | 1 |
| 13296377_t_m119_009_3066.jpg | 17,6 | 0 | 0 | 98,2 | 8,0 | -22,9 | 9 | 1 | 1 |
| 13296393_t_m119_009_3072.jpg | NaN | 2 | 0 | 98,4 | 8,0 | -22,9 | 9 | 1 | 1 |
| 13296429_t_m119_009_3084.jpg | NaN | 2 | 0 | 97,6 | 8,0 | -22,9 | 9 | 1 | 1 |
| 13296496_t_m119_009_3109.jpg | 18,1 | 0 | 0 | 97,9 | 8,0 | -22,9 | 9 | 1 | 1 |
| 13296518_t_m119_009_3118.jpg | NaN | 2 | 0 | 97,8 | 8,0 | -22,9 | 9 | 1 | 1 |
| 13296536_t_m119_009_3125.jpg | 15,7 | 0 | 0 | 97,8 | 8,0 | -22,9 | 9 | 1 | 1 |
| 13296572_t_m119_009_3137.jpg | NaN | 2 | 0 | 97,8 | 8,0 | -22,9 | 9 | 1 | 1 |
| 13296602_t_m119_009_3149.jpg | NaN | 2 | 0 | 97,8 | 8,0 | -22,9 | 9 | 1 | 1 |
| 13296663_t_m119_009_3173.jpg | NaN | 2 | 0 | 97,6 | 8,0 | -22,9 | 9 | 1 | 1 |
| 13296680_t_m119_009_3179.jpg | 17,8 | 0 | 0 | 97,9 | 8,0 | -22,9 | 9 | 1 | 1 |
| 13296723_t_m119_009_3194.jpg | 17,2 | 0 | 0 | 98,1 | 8,0 | -22,9 | 9 | 1 | 1 |
| 13296750_t_m119_009_3205.jpg | 17,1 | 0 | 0 | 97,8 | 8,0 | -22,9 | 9 | 1 | 1 |
| 13296786_t_m119_009_3217.jpg | 14,4 | 0 | 0 | 98 | 8,0 | -22,9 | 9 | 1 | 1 |
| 13296797_t_m119_009_3222.jpg | 12,7 | 0 | 0 | 98 | 8,0 | -22,9 | 9 | 1 | 1 |
| 13296843_t_m119_009_3239.jpg | 14,9 | 1 | 0 | 98,1 | 8,0 | -22,9 | 9 | 1 | 1 |
| 13296955_t_m119_009_3282.jpg | NaN | 2 | 0 | 98,3 | 8,0 | -22,9 | 9 | 1 | 1 |
| 13296974_t_m119_009_3288.jpg | 16,6 | 0 | 0 | 98,4 | 8,0 | -22,9 | 9 | 1 | 1 |
| 13296980_t_m119_009_3290.jpg | NaN | 2 | 0 | 98,4 | 8,0 | -22,9 | 9 | 1 | 1 |
| 13297000_t_m119_009_3297.jpg | NaN | 2 | 0 | 98,3 | 8,0 | -22,9 | 9 | 1 | 1 |
| 13297013_t_m119_009_3302.jpg | 18,1 | 0 | 0 | 98,3 | 8,0 | -22,9 | 9 | 1 | 1 |
| 13297057_t_m119_009_3317.jpg | NaN | 2 | 0 | 98,1 | 8,0 | -22,9 | 9 | 1 | 1 |
| 13297082_t_m119_009_3327.jpg | 14,7 | 1 | 0 | 98,1 | 8,0 | -22,9 | 9 | 1 | 1 |
| 13297122_t_m119_009_3339.jpg | NaN | 2 | 0 | 97,8 | 8,0 | -22,9 | 9 | 1 | 1 |
| 13297147_t_m119_009_3349.jpg | 19,0 | 1 | 0 | 97,9 | 8,0 | -22,9 | 9 | 1 | 1 |
| 13297184_t_m119_009_3362.jpg | NaN | 2 | 0 | 100,2 | 8,0 | -22,9 | 9 | 1 | 1 |
| 13297200_t_m119_009_3367.jpg | NaN | 2 | 0 | 101,1 | 8,0 | -22,9 | 9 | 1 | 1 |
| 13297367_t_m119_009_3428.jpg | 22,0 | 0 | 0 | 117 | 8,0 | -22,9 | 9 | 1 | 1 |
| 13300270_t_m119_009_4505.jpg | NaN | 2 | 0 | 402 | 8,0 | -22,9 | 9 | 1 | 1 |
| 13302170_m116_050_1954.jpg | 6,0 | 0 | 0 | 415,2 | 7,0 | -23,0 | 5 | 0 | 0 |
| 13325086_m116_026_1114.jpg | 3,1 | 0 | 0 | 319,7 | 11,0 | -33,0 | 5 | 0 | 0 |
| 13327810_m116_077_580.jpg | 4,2 | 0 | 0 | 67,9 | 13,0 | -21,0 | 5 | 0 | 0 |
| 13362125_t_m119_012_8251.jpg | 2,7 | 0 | 0 | 233,2 | 5,0 | -23,0 | 9 | 0 | 1 |
| 13364835_m116_074_1442.jpg | 3,8 | 0 | 0 | 144,8 | 11,0 | -20,0 | 5 | 0 | 0 |
| 13371376_m116_056_956.jpg | 4,6 | 0 | 0 | 257,7 | 12,0 | -22,0 | 5 | 0 | 0 |
| 13383206_t_m119_006_7496.jpg | 6,3 | 0 | 0 | 98,2 | 11,0 | -21,2 | 9 | 0 | 1 |
| 13383220_t_m119_006_7500.jpg | 6,5 | 0 | 0 | 98,2 | 11,0 | -21,2 | 9 | 0 | 1 |
| 13383547_t_m119_006_7628.jpg | NaN | 2 | 0 | 97,2 | 11,0 | -21,2 | 9 | 0 | 1 |
| 13384438_t_m119_006_7964.jpg | 4,1 | 0 | 0 | 96,2 | 11,0 | -21,2 | 9 | 0 | 1 |
| 13385660_t_m119_006_8422.jpg | 6,4 | 0 | 0 | 103,7 | 11,0 | -21,2 | 9 | 0 | 1 |
| 13385875_t_m119_006_8502.jpg | 3,9 | 0 | 0 | 130,4 | 11,0 | -21,2 | 9 | 0 | 1 |
| 13386392_t_m119_006_8693.jpg | 5,4 | 0 | 1 | 146,1 | 11,0 | -21,2 | 9 | 0 | 1 |
| 13389566_t_m119_006_9896.jpg | 6,3 | 0 | 1 | 191,5 | 11,0 | -21,2 | 9 | 0 | 1 |
| 13401091_t_m119_006_14238.jpg | 5,4 | 0 | 1 | 400,8 | 11,0 | -21,2 | 9 | 0 | 1 |
| 13408222_m116_054_681.jpg | 4,1 | 0 | 0 | 77,4 | 11,0 | -22,0 | 5 | 0 | 0 |
| 13410381_t_m119_010_3128.jpg | 7,2 | 0 | 0 | 386,7 | 7,0 | -22,9 | 9 | 0 | 1 |
| 13411616_t_m119_010_3592.jpg | 6,6 | 1 | 0 | 519,9 | 7,0 | -22,9 | 9 | 0 | 1 |
| 13421452_t_m119_013_3461.jpg | 5,2 | 0 | 0 | 49,9 | 0,0 | -23,1 | 9 | 0 | 1 |
| 13443255_m116_061_717.jpg | 8,9 | 0 | 0 | 76,1 | 8,0 | -21,0 | 5 | 0 | 0 |
| 13456625_t_m119_001_5168.jpg | 8,3 | 0 | 0 | 28,8 | 17,6 | -24,3 | 9 | 0 | 1 |
| 13464925_m116_049_199.jpg | 4,7 | 0 | 0 | 44 | 8,0 | -23,0 | 5 | 1 | 0 |
| 13464934_m116_049_202.jpg | 12,8 | 0 | 0 | 44,8 | 8,0 | -23,0 | 5 | 1 | 0 |
| 13464955_m116_049_210.jpg | 8,5 | 0 | 0 | 46,7 | 8,0 | -23,0 | 5 | 1 | 0 |
| 13464958_m116_049_211.jpg | 5,2 | 0 | 0 | 47 | 8,0 | -23,0 | 5 | 1 | 0 |

| | | | | | | | | | |
|---|---|---|---|---|---|---|---|---|---|
| 13464961_m116_049_212.jpg | 7,1 | 0 | 0 | 47,1 | 8,0 | -23,0 | 5 | 1 | 0 |
| 13464974_m116_049_215.jpg | 5,4 | 0 | 0 | 47,3 | 8,0 | -23,0 | 5 | 1 | 0 |
| 13464985_m116_049_219.jpg | 6,5 | 0 | 0 | 47,4 | 8,0 | -23,0 | 5 | 1 | 0 |
| 13465016_m116_049_230.jpg | 3,7 | 0 | 0 | 48,3 | 8,0 | -23,0 | 5 | 1 | 0 |
| 13465026_m116_049_233.jpg | 8,0 | 0 | 0 | 48,6 | 8,0 | -23,0 | 5 | 1 | 0 |
| 13465030_m116_049_235.jpg | 10,2 | 0 | 0 | 48,7 | 8,0 | -23,0 | 5 | 1 | 0 |
| 13465049_m116_049_240.jpg | 4,9 | 0 | 0 | 48,8 | 8,0 | -23,0 | 5 | 1 | 0 |
| 13465077_m116_049_250.jpg | 5,6 | 0 | 0 | 49,4 | 8,0 | -23,0 | 5 | 1 | 0 |
| 13465082_m116_049_252.jpg | 5,5 | 0 | 0 | 49,5 | 8,0 | -23,0 | 5 | 1 | 0 |
| 13465086_m116_049_254.jpg | 9,2 | 0 | 0 | 49,7 | 8,0 | -23,0 | 5 | 1 | 0 |
| 13465089_m116_049_255.jpg | 5,3 | 0 | 0 | 49,9 | 8,0 | -23,0 | 5 | 1 | 0 |
| 13465098_m116_049_259.jpg | 5,2 | 0 | 0 | 50 | 8,0 | -23,0 | 5 | 1 | 0 |
| 13465107_m116_049_262.jpg | 5,0 | 0 | 0 | 50,4 | 8,0 | -23,0 | 5 | 1 | 0 |
| 13465130_m116_049_268.jpg | 9,2 | 0 | 0 | 50,8 | 8,0 | -23,0 | 5 | 1 | 0 |
| 13465133_m116_049_269.jpg | 5,9 | 0 | 0 | 50,8 | 8,0 | -23,0 | 5 | 1 | 0 |
| 13465141_m116_049_272.jpg | 7,3 | 0 | 0 | 50,8 | 8,0 | -23,0 | 5 | 1 | 0 |
| 13465146_m116_049_274.jpg | 5,9 | 0 | 0 | 50,9 | 8,0 | -23,0 | 5 | 1 | 0 |
| 13465151_m116_049_276.jpg | 7,9 | 0 | 0 | 50,9 | 8,0 | -23,0 | 5 | 1 | 0 |
| 13465158_m116_049_278.jpg | 4,9 | 0 | 0 | 51 | 8,0 | -23,0 | 5 | 1 | 0 |
| 13465167_m116_049_282.jpg | 7,4 | 0 | 0 | 51,1 | 8,0 | -23,0 | 5 | 1 | 0 |
| 13465193_m116_049_291.jpg | 9,0 | 1 | 0 | 51,8 | 8,0 | -23,0 | 5 | 1 | 0 |
| 13465215_m116_049_300.jpg | 7,6 | 0 | 0 | 52,3 | 8,0 | -23,0 | 5 | 1 | 0 |
| 13465226_m116_049_304.jpg | 5,7 | 0 | 0 | 52,4 | 8,0 | -23,0 | 5 | 1 | 0 |
| 13465234_m116_049_307.jpg | 4,3 | 0 | 0 | 52,5 | 8,0 | -23,0 | 5 | 1 | 0 |
| 13465242_m116_049_311.jpg | 4,8 | 1 | 0 | 52,5 | 8,0 | -23,0 | 5 | 1 | 0 |
| 13465247_m116_049_313.jpg | 2,9 | 0 | 0 | 52,7 | 8,0 | -23,0 | 5 | 1 | 0 |
| 13465302_m116_049_331.jpg | 9,7 | 0 | 0 | 54,4 | 8,0 | -23,0 | 5 | 1 | 0 |
| 13465341_m116_049_343.jpg | 7,8 | 0 | 0 | 55,4 | 8,0 | -23,0 | 5 | 1 | 0 |
| 13465349_m116_049_345.jpg | 7,4 | 0 | 0 | 55,4 | 8,0 | -23,0 | 5 | 1 | 0 |
| 13465358_m116_049_348.jpg | 6,1 | 0 | 0 | 55,8 | 8,0 | -23,0 | 5 | 1 | 0 |
| 13465377_m116_049_355.jpg | 6,2 | 0 | 0 | 56,4 | 8,0 | -23,0 | 5 | 1 | 0 |
| 13465399_m116_049_363.jpg | 6,3 | 0 | 0 | 57 | 8,0 | -23,0 | 5 | 1 | 0 |
| 13465422_m116_049_368.jpg | 5,7 | 0 | 0 | 57,6 | 8,0 | -23,0 | 5 | 1 | 0 |
| 13465426_m116_049_369.jpg | 7,9 | 0 | 0 | 57,6 | 8,0 | -23,0 | 5 | 1 | 0 |
| 13465431_m116_049_371.jpg | 10,0 | 0 | 0 | 57,7 | 8,0 | -23,0 | 5 | 1 | 0 |
| 13465434_m116_049_372.jpg | 6,2 | 0 | 0 | 57,7 | 8,0 | -23,0 | 5 | 1 | 0 |
| 13465450_m116_049_377.jpg | 4,0 | 0 | 0 | 58 | 8,0 | -23,0 | 5 | 1 | 0 |
| 13465457_m116_049_379.jpg | NaN | 2 | 0 | 58,1 | 8,0 | -23,0 | 5 | 1 | 0 |
| 13465469_m116_049_383.jpg | 5,5 | 0 | 0 | 58,1 | 8,0 | -23,0 | 5 | 1 | 0 |
| 13465472_m116_049_384.jpg | 5,1 | 0 | 0 | 58,1 | 8,0 | -23,0 | 5 | 1 | 0 |
| 13465490_m116_049_390.jpg | 11,4 | 0 | 0 | 58,9 | 8,0 | -23,0 | 5 | 1 | 0 |
| 13465514_m116_049_396.jpg | 6,0 | 0 | 0 | 59,3 | 8,0 | -23,0 | 5 | 1 | 0 |
| 13465518_m116_049_397.jpg | 7,9 | 0 | 0 | 59,4 | 8,0 | -23,0 | 5 | 1 | 0 |
| 13465570_m116_049_414.jpg | 6,9 | 0 | 0 | 60,8 | 8,0 | -23,0 | 5 | 1 | 0 |
| 13465609_m116_049_426.jpg | 5,5 | 0 | 0 | 61,8 | 8,0 | -23,0 | 5 | 1 | 0 |
| 13465619_m116_049_429.jpg | 8,8 | 0 | 0 | 62 | 8,0 | -23,0 | 5 | 1 | 0 |
| 13465653_m116_049_440.jpg | NaN | 2 | 0 | 62,9 | 8,0 | -23,0 | 5 | 1 | 0 |
| 13465693_m116_049_451.jpg | 5,5 | 0 | 0 | 65,5 | 8,0 | -23,0 | 5 | 1 | 0 |
| 13465699_m116_049_453.jpg | 5,8 | 0 | 0 | 65,7 | 8,0 | -23,0 | 5 | 1 | 0 |
| 13465708_m116_049_456.jpg | 5,3 | 0 | 0 | 65,8 | 8,0 | -23,0 | 5 | 1 | 0 |
| 13465732_m116_049_464.jpg | 5,7 | 0 | 0 | 66,4 | 8,0 | -23,0 | 5 | 1 | 0 |
| 13465752_m116_049_471.jpg | 5,8 | 0 | 0 | 67 | 8,0 | -23,0 | 5 | 1 | 0 |
| 13465763_m116_049_473.jpg | 5,0 | 0 | 0 | 67,2 | 8,0 | -23,0 | 5 | 1 | 0 |
| 13465766_m116_049_474.jpg | NaN | 2 | 0 | 67,2 | 8,0 | -23,0 | 5 | 1 | 0 |
| 13465806_m116_049_487.jpg | 8,4 | 0 | 0 | 67,9 | 8,0 | -23,0 | 5 | 1 | 0 |
| 13465811_m116_049_489.jpg | 5,4 | 0 | 0 | 68,7 | 8,0 | -23,0 | 5 | 1 | 0 |
| 13465852_m116_049_503.jpg | 10,0 | 0 | 0 | 71 | 8,0 | -23,0 | 5 | 1 | 0 |
| 13465863_m116_049_507.jpg | 7,2 | 0 | 0 | 71,4 | 8,0 | -23,0 | 5 | 1 | 0 |
| 13465884_m116_049_515.jpg | NaN | 2 | 0 | 72,3 | 8,0 | -23,0 | 5 | 1 | 0 |
| 13483768_m116_020_1545.jpg | 9,3 | 1 | 0 | 84,5 | 7,5 | -35,0 | 5 | 0 | 0 |
| 13493153_m116_011_443.jpg | 7,3 | 0 | 0 | 741,7 | 7,7 | -40,8 | 5 | 0 | 0 |
| 13497157_t_m119_011_5782.jpg | 9,5 | 0 | 1 | 400,7 | 5,0 | -22,9 | 9 | 0 | 1 |
| 13497823_t_m119_011_6031.jpg | NaN | 2 | 0 | 463,5 | 5,0 | -22,9 | 9 | 0 | 1 |
| 13498024_t_m119_011_6107.jpg | 11,8 | 0 | 0 | 463,5 | 5,0 | -22,9 | 9 | 0 | 1 |
| 13499533_m116_064_905.jpg | 8,2 | 1 | 0 | 749,1 | 5,0 | -21,0 | 5 | 0 | 0 |
| 13503214_m116_062_1699.jpg | 11,6 | 0 | 0 | 637,6 | 7,0 | -21,0 | 5 | 0 | 0 |
| 13504934_m116_034_725.jpg | 6,1 | 0 | 0 | 697,7 | 9,0 | -28,0 | 5 | 0 | 0 |

| | | | | | | | | | |
|---|---|---|---|---|---|---|---|---|---|
| 13509638_m116_081_611.jpg | 7,4 | 0 | 0 | 691,1 | 17,6 | -24,3 | 6 | 0 | 0 |
| 13527901_m116_027_815.jpg | 3,1 | 0 | 0 | 149,7 | 11,0 | -32,0 | 5 | 0 | 0 |
| 13538913_m116_072_699.jpg | 18,5 | 0 | 0 | 46,3 | 11,0 | -19,0 | 5 | 0 | 0 |
| 13546502_m116_057_1367.jpg | 4,9 | 1 | 0 | 490,8 | 12,0 | -21,0 | 5 | 0 | 0 |
| 13549943_m116_066_1040.jpg | 5,8 | 1 | 0 | 61,7 | 8,0 | -19,0 | 5 | 0 | 0 |
| 13549959_m116_066_1048.jpg | 5,6 | 0 | 0 | 64 | 8,0 | -19,0 | 5 | 0 | 0 |
| 13550676_m116_066_1416.jpg | 6,5 | 0 | 0 | 359,3 | 8,0 | -19,0 | 5 | 0 | 0 |
| 13554638_m116_044_290.jpg | 5,7 | 0 | 0 | 62,9 | 11,5 | -23,0 | 5 | 0 | 0 |
| 13554785_m116_044_369.jpg | 4,6 | 0 | 0 | 86,3 | 11,5 | -23,0 | 5 | 0 | 0 |
| 13554810_m116_044_382.jpg | 7,6 | 0 | 0 | 106,3 | 11,5 | -23,0 | 5 | 0 | 0 |
| 13558496_m116_053_658.jpg | NaN | 2 | 0 | 101,9 | 10,0 | -22,0 | 5 | 0 | 0 |
| 13558593_m116_053_711.jpg | 4,9 | 0 | 0 | 150,2 | 10,0 | -22,0 | 5 | 0 | 0 |
| 13567835_m116_042_527.jpg | 13,5 | 0 | 1 | 523,4 | 11,0 | -25,0 | 5 | -1 | 0 |
| 13838109_m106_070_561.jpg | 10,8 | 0 | 0 | 561,7 | -5,0 | -23,0 | 5 | 0 | 0 |
| 13849819_m106_060_1553.jpg | 10,1 | 0 | 0 | 546,5 | -1,7 | -23,0 | 5 | 0 | 0 |
| 13865059_m106_014_558.jpg | 5,0 | 0 | 0 | 433,1 | 10,5 | -23,0 | 4 | 0 | 0 |
| 13955336_m106_062_970.jpg | 7,3 | 0 | 0 | 668 | -2,3 | -23,0 | 5 | 0 | 0 |
| 14925622_isl_003_286.jpg | 5,3 | 0 | 0 | 70,1 | 19,1 | -24,3 | 3 | 1 | 0 |
| 14925671_isl_003_335.jpg | 9,8 | 1 | 0 | 77,3 | 19,1 | -24,3 | 3 | 1 | 0 |
| 14925822_isl_003_486.jpg | 14,7 | 0 | 1 | 97,7 | 19,1 | -24,3 | 3 | 1 | 0 |
| 14925841_isl_003_505.jpg | 18,9 | 0 | 1 | 100,4 | 19,1 | -24,3 | 3 | 1 | 0 |
| 14925856_isl_003_520.jpg | 7,6 | 0 | 0 | 102,9 | 19,1 | -24,3 | 3 | 1 | 0 |
| 14925881_isl_003_545.jpg | 7,2 | 0 | 0 | 107,4 | 19,1 | -24,3 | 3 | 1 | 0 |
| | | | | | | | | | |